THE MOMENTUM FLUX IN TWO-PHASE FLOW

by

GERRY B. ANDEEN
B.S. (M.E.) University of Michigan (1962)
S.M. (M.E.) Massachusetts Institute of Technology (1963)

SUBMITTED IN PARTIAL FULFILLMENT
OF THE REQUIREMENTS FOR THE
DEGREE OF DOCTOR OF SCIENCE

at the

MASSACHUSETTS INSTITUTE OF TECHNOLOGY

October, 1965

Signature of Author .....
Department of Mechanical Engineering

Certified by .....
Thesis Supervisor

Accepted by .....
Chairman, Departmental Committee on Graduate Students

THE MOMENTUM FLUX IN TWO-PHASE FLOW

by

Gerry B. Andeen

Submitted to the Department of Mechanical Engineering in October, 1965, in partial fulfillment of the requirements for the degree of Doctor of Science

ABSTRACT

The average momentum flux at a section of a pipe with two-phase upflow has been measured by the impulse technique. Steam-water and air-water mixtures were tested in one-inch and one-half inch nominal pipes. Homogeneous velocities ranging from 150 to 1200 ft/sec. and qualities from 5% to 85% were tested.

The results are compared to the results of models currently in practice for predicting pressure drop and critical flow. The influence of the void fraction, the velocity profile, phase distribution and fluctuations upon the momentum flux are discussed.

Thesis Supervisor: Peter Griffith

Title: Associate Professor of Mechanical Engineering

BIOGRAPHICAL SKETCH

I was born in Chicago in 1940, of little importance to me since we didn't live there long enough for me to remember it. I went to grade school in Minneapolis and caught gophers. You see, gophers always have two entrances to their burrows. If you pour water down one entrance, a wet gopher will come up into an old pan over the other.

I attended high school in Connecticut as the family moved there, and I learned that I never really learned to spell. The problem is that spelling is hardly ever phonetic. Take "nite," for example, neither kind is spelled the way they both sound. You can see why I studied engineering at the University of Michigan. The only prehistoric characteristic of engineering is akward units, and no student pays attention to units anyway.

In 1962 I graduated from Michigan and came to MIT where I have been since. In fact, with the exception of summer industrial jobs, and an NROTC cruise, I have been in school continuously. For this, I owe thanks to the Scott Paper Company Foundation as an undergraduate and to the National Science Foundation as a graduate student. I have been elected to several honorary societies and, of course, am a student member of the ASME.

ACKNOWLEDGMENTS

The author wishes to thank Professor Peter Griffith and the other members of the committee, Professor J. L. Smith, Jr., and Professor S. W. Gouse, Jr., for their guidance throughout the project. Special thanks are also due to Professors Rohsenow, Brown, Bergles, Suo, and Richardson for their thoughtful and constructive suggestions.

Appreciation is expressed to the Engineering Project Laboratory Staff for their efforts in assembling the experimental apparatus.

Financial support for the project was provided by the U.S. Atomic Energy Commission, AEC Contract AT(30-1) - 3496.

The MIT Computation Center provided computer time for data reduction.

TABLE OF CONTENTS

TABLE OF CONTENTS
(continued)

TABLE OF CONTENTS
(continued)

LIST OF FIGURES

NOMENCLATURE

A	Area
B	Body force
^{o}C	Degrees Centigrade
C_1	Constant in equation (2-22)
C_2	Constant in equation (2-22)
C_3	Constant in equation (2-28)
C_4	Constant in equation (2-28)
C_5	Constant in equation (2-45)
C_6	Constant in equation (2-46)
C.S.	Control Surface
C.V.	Control Volume
F	Force
F_s	Surface force
F_τ	Shear force
G	Mass velocity
H_1	Defined, equation (2-5)
H_2	Defined, equation (2-10)
K	Orifice Coefficient (C-4)
M	Momentum Flux
MM	Momentum Multiplier
P	Pressure

R	Potentiometer Reading (C-2)
Re	Reynolds Number
T	Length of Time
V	Velocity
V'	Fluctuating Velocity with Zero Mean
X	Quality
YK	Defined equation (4-6)
ZK	Defined equation (4-7)
a	Location or position in area
b	Magnitude of sinusoidal perturbation, equation (2-34)
c	Coefficient of Damping
c'	Coefficient of Damping
d	Indicates differential
e	Voltage
f	Subscript indicates liquid
g	Gravitational acceleration
g	Subscript indicates gas
g_c	Gravitational constant
h	Width of arriving flow, equation (3-1)
i	Subscript indicates i^{th} term
k	Spring constant
k'	Spring constant
l	Length
m	Mass

m'	Mass
$\dot{m}$	Mass flow rate
n	Exponent in equation (4-3)
r	Radius
r_o	Outside radius
t	Time
v	Specific volume ($1/\rho$)
x	Displacement
y	Displacement
z	Displacement

Greek Letters

α	Void fraction
β	Decay constant
γ	Mean liquid fraction deviation equation (2-52)
δ	Calculus of variations differential
ϵ	Entrainment, equation (2-29)
ξ_1	Constant defined in equation (2-3a)
ξ_2	Constant defined in equation (2-4a)
ξ_3	Constant defined in equation (2-9a)
η_f	Local liquid mass flow fraction
η_g	Local gas mass flow fraction
θ	Thom's constant, equation (2-21)
λ_1	Constant, see 2.2.2
λ_2	Constant, see 2.2.2

λ_3	Constant, see 2.2.3
μ	Coefficient of viscosity
π	Ratio of circle circumference to radius
ρ	Density
ϕ	Bankoff's constant, equation (2-20a)
ω	Sinusoidal frequency, equation (2-34)

Other symbols

∂	Partial differential
f	Indicates function of the variables following
$\mathcal{V}$	Volume
$\vec{\ }$	Indicates vector quantity
$\bar{\ }$	Indicates averaged quantity

CHAPTER I

INTRODUCTION

The two-phase momentum flux has come to attention primarily through its relationship to pressure changes in systems involving phase change, water tube boilers, nuclear reactors, refrigerating evaporators and condensers, rockets, condensing ejectors, and the like. In addition to being of direct application, knowledge of the momentum flux would also result in additional basic knowledge and understanding of the nature of two-phase flows and the applicability of various models. This basic understanding of the momentum flux is, among other applications, particularly relevant to the critical flow phenomena.

1.1 Pressure Drop in a Pipe

The ability to predict two-phase pressure change to nearly the same degree of accuracy as is possible with single-phase flow has eluded investigators. This is fascinating from a motivational point of view as accurate determination of the two-phase pressures are of fundamental importance in the design of evaporators, condensers, and particularly nuclear reactors. That the technological need has not brought about a dependable solution is sufficient testimony to the difficulty of the problem.

The two-phase pressure change, like the single-phase change, can be considered to be composed of several, individual contributing terms. A development of the general momentum equation (see Appendix A) shows these contributing terms to be a frictional pressure drop, an hydrostatic pressure change, a momentum flux change, and an acceleration transient. Each of the terms is considerably more difficult to evaluate in the two-phase case than for a single phase. In particular, the hydrostatic pressure change is elementary for the single phase while it requires a knowledge of phase distribution for the two-phase phenomena. In single phase, fully developed, incompressible flows, the difference is easily computed assuming a similarity of velocity profiles. Further, the momentum pressure change is only significant in proportion to the frictional pressure change at high Mach numbers. It is seen that for general use the pressure change in a single phase flow, neglecting transient terms, is due primarily to one difficult term, the frictional term.

The relative simplicity of the single phase flow may well be one of the important reasons for the retarded development of two-phase technology. In the single phase, a simple pressure difference measurement is easily related to the one term needing correlation, the frictional term. This is simply not so for the two-phase system, but it did serve as a starting point for two-phase study. Certain holdovers unfortunately serve as mental blocks, and time after time

the hydrostatic and momentum flux terms were simply estimated and subtracted out in investigating the two-phase friction term. It was not considered important to consider these terms more carefully, even though they often served as the largest portion of the pressure change. Through careless consideration of the overall equation, only a half-way job can be done on the frictional correlation.

A second reason for the retarded development of two-phase technology, also due to the single phase study influence, is the tendency to consider the flow on the average. This is acceptable in the single phase as there are no natural deviations from the average steady flow, except in a careful consideration of turbulent flow. Averaging is not generally acceptable in two-phase flow because of the non-linear nature of the momentum flux and the occurrence of slugs, waves, and other natural fluctuations. As with turbulent flow, the first level of complication is a recognition and treatment of the natural fluctuations.

1.2 Momentum Flux Models

A model is a proposal giving the phase and velocity distribution as a function of space and time. For the purposes here, it is information from which one may calculate a momentum flux. A model may, of course, include several experimental parameters, in the limit being an actual photograph of the phenomena, or it may be a

highly simplified approximation. Several models have been proposed by investigators of two-phase flow pressure change in order to reduce their data for friction correlation. It should be noted that all are steady or averaged in time models.

The most simple model is the homogeneous. It merely assumes that the phases are mixed in the ratio of the flowing quality at a single velocity. The assumption is popular in that it is simple to deal with. Unfortunately, it assumes that the average velocity of the liquid and the gas are the same. Through measurement of the void fraction, the percentage of gas-occupied area at a section, this has been shown to be a gross error; the average gas velocity is often many times the average liquid velocity. Incidentally, the original purpose of the void fraction measurement was to establish the hydrostatic term.

Introduction of the void fraction as an experimental parameter, leading to a calculation of a velocity for the liquid and another for the gas, gives the two-velocity or slip model. Martinelli (1)* made a moderately successful two-phase pressure change correlation in which he calculated the momentum flux by the slip model. He presented an empirical chart of void fraction versus quality. Even recent investigation (2), apparently inspired by Martinelli's relative success, retains the two-velocity model for the momentum flux calculation.

---

* Numbers in parentheses refer to references at end of report.

They differ only in that Thom, the recent investigator, presents a mathematical relationship between void fraction in quality. The two velocity model is by far the most popular model, perhaps because it is the most simple model which manages to avoid obvious errors such as discrepancy in the void fraction.

At higher qualities and gas velocities, much of the liquid flow seems to become entrained as droplets in the gas stream. Thus was developed the entrainment model. An entrainment factor, of empirical origin, denotes the fraction of the liquid flow which is traveling at the gas velocity. The entrainment model also establishes the velocities to preserve the empirical void fraction. Magiros and Duckler (3) essentially adopt the entrainment model when they recommend that momentum be neglected in the liquid film and calculated on the basis of entrainment in the gas core.

Bankoff (4) demonstrated additional sophistication by proposing that the density and velocity profiles need not, and in fact do not, take step changes across a section. He proposed a profile for the density and another for the velocity and proceeded to show that slip between the average velocities was indeed the result. Bankoff investigated the low quality, bubbly flow, region. The power law profiles he suggested were essentially guesses based on satisfying the void fraction data.

Anderson and Mantzoranis (5) did essentially the same thing

as Bankoff in the annular flow region. Their results were highly tailored to fit empirical data and the profiles they suggest are suspect on the basis of physical reasoning. Silvestri (6) has made measurements of both the density and velocity profiles in the entrained liquid gas region. He was unsuccessful in integrating the values to predict reasonable momentum flux differences. The difficulties with complete profile specification are to find the profiles, or enough empirical data to reasonably specify them, and to deal with the problem of non-linear averaging.

1.3 Differences between Models

The selection of a model is not critical when the difference between them for the purposes for which they are to be used is small. Unfortunately, the difference in momentum predicted by the models is large. Figure 1a shows a plot of momentum pressure change versus quality as predicted by the homogeneous and by the two-velocity model, void fraction as given by Martinelli. The two models predict significantly different results at the lower qualities. Figure 1b shows the ratio of the homogeneous to the two-velocity model. Thus it can be seen that in cases where momentum flux differences play any significant role, as in rapid heating or cooling, the accurate determination of the correct model, the correct momentum flux, is of vital importance.

1.4 Direct Measurement

Four experiments are described in the literature which directly measure the momentum flux. All used the turning tee method used by this experimenter. Linning (7) first made the measurement and reduced his data to slip ratio data according to the two-velocity model. Semenov (8) did essentially the same thing, followed by Vance (9) who reproduced Linning's experiment. Semenov and Vance, both patterned their data reduction after Linning, using the two-velocity model to predict slip. As will be emphasized later, the momentum flux is more than a function of the slip ratio, and the momentum flux cannot be returned to a slip ratio which is representative of the true void fraction data. The experimenters mentioned had steady force measuring devices and were not equipped to consider fluctuating forces.

The other investigation is that of Rose (10) who attempted to evaluate each of the pressure drop terms by independent measurement in the bubbly flow regime. Rose measured the void fraction and compared his momentum flux data with that predicted by his measured void fraction in the two-velocity model and with that predicted by the homogeneous model. Although one does not necessarily expect the two-velocity model to hold as well in bubbly flow as it does in annular flow, (the two-velocity model is often called the "annular model"), the data does point out that the slip model does violate

experimental data. Rose's data is shown in Figures 29 and 30 and will be discussed in more detail.

Outside of the bubbly flow regime, the total number of experimental points is about fifty, mostly due to Vance. Considerably more direct measurement discussed in relation to the flow models is awaited.

1.5 Fluctuation

As has been mentioned, the time unsteadiness is of vital importance in two-phase flow as waves and slugs occur naturally. Some attempts have been made to correlate these natural fluctuations (8), and many investigators have presented some of their fluctuating data in its raw form. Silvestri (6) among others is able to recognize flow regimes by the fluctuating nature of some quantity. Although virtually all researchers have observed the unsteady nature, as has been mentioned, every effort has been made to neglect it through averaging. Even systematic investigations as with limited data reduction such as that of Semenov (8) are rare.

The void fraction and the momentum flux are excellent variables for the investigation of fluctuations as they can be measured at a section.

1.6 Critical Flow

Critical flow of two-phase mixtures have been predicted on the

basis of the homogeneous and two-velocity models (11). Fauske (11) claims, without giving his reasoning, that critical flow is bounded by the predictions based on these models. At the critical flow, the momentum flux change is of greatest importance. The investigation of the momentum flux should then lend some information to the validity of the critical flow modeling and the critical flow itself.

CHAPTER II

ANALYTICAL CONSIDERATIONS

2.1 The Momentum Multiplier

The momentum flux can be reduced with respect to the flow rate by the consideration of a momentum multiplier defined as

$$MM = \frac{A \iint \rho V^2 \, dA}{g_c \left(\iint \rho V \, dA \right)^2} = \frac{Force}{G^2 A} \qquad (2\text{-}1)$$

This is the same momentum multiplier defined and presented by Martinelli (1). It is important to note that the momentum multiplier is not a dimensionless quantity and that the dimensions used by Martinelli are not the same as those presented in this paper.

The consideration of the momentum flux at a particular flow rate is the same as the consideration of the momentum multiplier at the same flow rate. With this fact in mind, the terms will be used interchangeably.

2.2 Possible Bounds on the Momentum Multiplier Value

In any investigation it is of interest to know of any limits that bound the values of inquiry. The knowledge of bounds is helpful in evaluating the validity of the empirical data and in forming models or parameters by which the data may be correlated and understood.

2.2.1 Martinelli's Bounds Martinelli suspected that the actual momentum multiplier lay between those predicted by the homogeneous and two-velocity models. The given reasoning was that "the water-vapor mixture ... will be partially in the form of fog and partially separated liquid and vapor." To be more exact, the reasoning is that the two models represent idealization from which deviations always occur toward the other. Homogeneous flow is always moderated by slip, so that the average gas velocity exceeds the average liquid velocity. The two-velocity model cannot exist either, if only for the step velocity gradient between the phases and the resulting deviation will be toward the homogeneous. Apparently Fauske (11) would hold to a similar argument as he predicts that the two models give bounds to critical flow values.

That the two-velocity model gives a minimum momentum multiplier value is valid as will be shown shortly. It is impossible to conceive of a model whereby a smaller momentum multiplier value may be achieved. That the homogeneous model represents an upper bound is not similarly true, but represents only the opinion of the investigators as to the nature of the phenomena. If one conceives of the flow of one of the phases in a smaller and smaller area, the momentum multiplier grows larger without bound. As the investigators have given no physical reasoning as to why all deviations should be lower in value than the homogeneous, it does not seem reasonable to accept this as a real bound.

2.2.2 Requirements for Minimum Possible Momentum Flux The density, ρ, and the velocity, V, are allowed to be unknown functions of the position, a, in the cross sectional area, A, and of time, t. We wish to find the requirements on these functions such that the minimum possible average momentum flux is given as a result.

$$M = \lim_{T\to\infty} \frac{1}{T}\int_0^T \iint_A \rho(a,t)\, V^2(a,t)\, da\, dt \qquad (2\text{-}2)$$

The only constraint to be considered is that of average continuity of each phase.

$$\frac{\dot{m}_f}{\varsigma_1} = \lim_{T\to\infty} \frac{1}{T}\int_0^T \iint_A \left(\rho(a,t)-\rho_g\right) V(a,t)\, da\, dt \qquad (2\text{-}3)$$

$$\varsigma_1 = \frac{\rho_f}{\rho_f - \rho_g} \qquad (2\text{-}3a)$$

$$\frac{\dot{m}_g}{\varsigma_2} = \lim_{T\to\infty} \frac{1}{T}\int_0^T \iint_A \left(\rho_f-\rho(a,t)\right) V(a,t)\, da\, dt \qquad (2\text{-}4)$$

$$\varsigma_2 = \frac{\rho_g}{\rho_f - \rho_g} \qquad (2\text{-}4a)$$

Following the method of calculus of variations

$$H_1 = \lim_{T\to\infty} \frac{1}{T}\int_0^T \iint_A \Big[\rho(a,t)V^2(a,t) + \lambda_1(\rho(a,t)-\rho_g) + \lambda_2(\rho_f-\rho(a,t))V(a,t)\Big]\, da\, dt \qquad (2\text{-}5)$$

where λ_1 and λ_2 are constants.

$$\delta H_1 = \lim_{T\to\infty} \frac{1}{T}\int_0^T \iint_A \{[2\rho(a,t)\,V(a,t) + \lambda_1(\rho(a,t)-\rho_g) + \lambda_2(\rho_f-\rho(a,t))]\delta V + [V^2(a,t) + \lambda_1 V(a,t) - \lambda_2 V(a,t)]\delta\rho\}\, da\, dt \tag{2-6}$$

In order that $\delta H = 0$

$$2\rho(a,t)\,V(a,t) + \lambda_1(\rho(a,t)-\rho_g) + \lambda_2(\rho_f-\rho(a,t)) = 0 \tag{2-7}$$

and

$$V^2(a,t) + \lambda_1 V(a,t) - \lambda_2 V(a,t) = 0 \tag{2-8}$$

Equations (2-7) and (2-8) along with the two continuity equations, (2-3) and (2-4), specify the conditions on $\rho(a,t)$, $V(a,t)$, λ_1, and λ_2 for the minimum possible momentum flux.

2.2.3 Minimum Momentum Flux at Specified Void Fraction In addition to the continuity constraints of equations (2-3) and (2-4), an average void fraction constraint may be added.

$$\frac{\alpha}{\varepsilon_3} = \lim_{T\to\infty} \frac{1}{T}\int_0^T \iint_A \rho_f - \rho(a,t)\; da\, dt \tag{2-9}$$

$$\varepsilon_3 = \frac{1}{A(\rho_f-\rho_g)} \tag{2-9a}$$

Equation (2-5) is modified by the additional constraint

$$H_2 = \lim_{T\to\infty} \frac{1}{T}\int_0^T \iint_A [\rho(a,t)\,V^2(a,t) + \lambda_1(\rho(a,t)-\rho_g) + \lambda_2(\rho_f-\rho(a,t))V(a,t) + \lambda_3(\rho_f-\rho(a,t))]\, da\, dt \tag{2-10}$$

where λ_3 is an additional constant.

$$\delta H_2 = \lim_{T\to\infty} \frac{1}{T} \int_0^T \iint_A \Big\{ \Big[2\rho(a,t)V(a,t) + \lambda_1(\rho(a,t)-\rho_g) + \lambda_2(\rho_f-\rho(a,t)) \Big] \delta V + \Big[V^2(a,t) + \lambda_1 V(a,t) - \lambda_2 V(a,t) - \lambda_3 \Big] \delta\rho \Big\} da\, dt \tag{2-11}$$

Again setting $\delta H = 0$ gives

$$V^2(a,t) + \lambda_1 V(a,t) - \lambda_2 V(a,t) - \lambda_3 = 0 \tag{2-12}$$

and equation (2-7) as before. Thus equations (2-7) and (2-12) along with the constraints, equations (2-3), (2-4), and (2-9) specify the conditions for the minimum momentum at a given void fraction.

Although it is difficult to find the solutions to the equations by direct means, it is quite simple to test a suspected solution. Because of its flat velocity profiles, we suspect that the two-velocity model may be a solution for the minimum momentum flux at a given void fraction. That this is true is easily verified. Thus Martinelli's minimum bound is shown to be valid by continuity considerations alone.

2.2.4 Minimum Momentum Flux Model It is suspected that the void fraction in the two-velocity model might be adjusted to give the minimum momentum flux and that the result might satisfy the minimum possible momentum flux requirements. It is noted that as the void

fraction approaches zero or one, the momentum flux value of this model approaches infinity (Figures 18 and 19). Also of note is the fact that void fraction values are not singular, that another void fraction in addition to the homogeneous void fraction gives the homogeneous momentum flux value.

$$M = \left[\frac{\dot{m}_f^2}{(1-\alpha)\rho_f} + \frac{\dot{m}_g^2}{\alpha \rho_g} \right] \frac{1}{A g_c} \tag{2-13}$$

In order that $\frac{dM}{d\alpha} = 0$

$$\alpha = \frac{\left(v_g/v_f\right)^{\frac{1}{2}} X}{1 + \left[\left(v_g/v_f\right)^{\frac{1}{2}} - 1\right] X} \tag{2-14}$$

$$= \frac{1}{1 + \left(\frac{1-X}{X}\right)\left(v_g/v_f\right)^{\frac{1}{2}}} \tag{2-14b}$$

A substitution shows that the two-velocity model at the void fraction given in equation (2-14) satisfies the requirements for the minimum possible momentum.

At the value of void fraction giving the minimum possible momentum flux, the slip ratio is found to be

$$\frac{V_g}{V_f} = \left(v_g/v_f\right)^{\frac{1}{2}} \tag{2-15}$$

a result common in two-phase flow. It can be found by considering the kinetic energy per unit cross sectional area to be the same in each phase. It was also derived by Fauske (11) by a more tortuous route. Fauske's critical flow model is thus the flow with minimum momentum flux.

2.2.5 Unsteady Minimum Momentum Flux It should be recognized that the two-velocity model at the specified void fraction represents only one of many solutions to the minimum momentum flux requirements. The other solutions are all of a time varying nature, however, leaving the two-velocity model as the only steady-state solution.

That time varying solutions exist can be demonstrated by physical reasoning. Consider a liquid jet leaving a nozzle in a steady flow at some angle upward, against gravity. Surface tension acts to break up the stream into droplets which, when they pass through the same elevation as the nozzle, have the same average momentum as at the nozzle. If the stream is enclosed in a frictionless wall duct including a gas phase introduced to give the minimum possible two-phase momentum flux at the jet, the flow will have an unsteady, minimum average momentum flux as it passes the nozzle elevation. Many of the unsteady solutions can be visualized by changing the angle of the jet giving more or less time for the fluid to form droplets.

2.3 Deviations from Minimum Possible Value

Generally speaking, deviation from the minimum possible momentum flux value is caused by deviation of the density and velocity profiles from their minimum functions. These deviations may be classified in one or more of four categories: void fraction phase distribution changes, velocity profile alterations, entrainment phase distribution changes, or time variations. An attempt will be made to investigate the influence of each of the types of deviation.

2.3.1 Void Fraction The large deviation between the homogeneous and two-velocity model momentum fluxes is due entirely to difference in void fraction assumption. The homogeneous void fraction

$$\alpha = \frac{X \, \bar{v}_g/\bar{v}_f}{1+\left(\bar{v}_g/\bar{v}_f - 1\right)X} = \frac{1}{1+\left(\frac{1-X}{X}\right)\bar{v}_f/\bar{v}_g} \qquad (2\text{-}16)$$

$$\frac{V_g}{V_f} = 1 \qquad (2\text{-}17)$$

is considerably greater than minimum momentum flux void fraction. A graphical comparison is provided in Figure 16 at atmospheric pressure.

Several other values of void fraction versus quality have been suggested and are shown on the same figure. Martinelli's curve was reduced from actual data and has been given without mathematical correlation.

Zivi (12) developed the relation

$$\alpha = \frac{\left(v_g/v_f\right)^{\frac{2}{3}} X}{1+\left[\left(\frac{v_g}{v_f}\right)^{2/3}-1\right]X} = \frac{1}{1+\left(\frac{1-X}{X}\right)\left(v_f/v_g\right)^{\frac{2}{3}}} \tag{2-18}$$

$$\frac{V_g}{V_f} = \left(v_g/v_f\right)^{\frac{1}{3}} \tag{2-19}$$

on the basis of a minimum kinetic energy flux.

Bankoff (4) gave the relation

$$\alpha = \frac{\phi\left(v_g/v_f\right) X}{1 + X\left(v_g/v_f - 1\right)} \tag{2-20}$$

$$\phi = 0.71 + .0001\,P \tag{2-20a}$$

on the basis of his assumed density and velocity profiles in bubbly flow. One notes that Bankoff's model certainly fails outside of the low quality region and does not satisfy the known point that the void fraction is unity at single-phase gas flow.

Thom (2) proposes that the general form,

$$\alpha = \frac{\Theta X}{1 + X(\Theta - 1)} \tag{2-21}$$

where Θ should be determined by experimental evidence, best fits all the known data.

The relations of the form

$$\alpha = \frac{C_1 X}{1 + C_2 X} \tag{2-22}$$

are symmetric about the $X = (1-\alpha)$ axis (the expressions are identical when X is replaced by $(1-\alpha)$ and α by $(1-X)$). This is at variance to the Martinelli result which is clearly skewed. The Bankoff model, although intended for low quality is also pleasingly skewed, a shape which seems necessary to best fit the data.

The void fractions reviewed are between the homogeneous and the minimum momentum flux void fractions. They are, excluding the Bankoff model, sufficiently close to the minimum momentum value that they all give nearly the same momentum flux. This is to be expected since they are in the region where $dM/d\alpha$ is small. At lower qualities ($X < .05$) the Martinelli curve does depart by a sufficient difference to make a noticeable difference in the momentum flux. It can be said, with the exception of the Bankoff model and the Martinelli curve at low quality, that the selection of void fraction correlation makes no difference in the momentum flux value. They are all sufficiently close to the minimum momentum flux value (see Figures 18 and 19).

2.3.2 Velocity Distribution In a single-phase flow the minimum momentum velocity profile is the uniform profile where

$$V = \frac{G}{\rho} \qquad (2\text{-}23)$$

The corresponding momentum flux is

$$M = \frac{AG^2}{\rho} \tag{2-24}$$

Integration of universal velocity profiles indicates that the fully developed turbulent flow is 1%-10% greater than the flat profile value (13)(5). Further, the integration is of an averaged curve and, depending upon the fluctuations present, the actual value should be higher still. The laminar velocity profile is

$$V = \frac{2G}{\rho}\left(1 - \left(\frac{r}{r_o}\right)^2\right) \tag{2-25}$$

and results in a momentum flux of

$$M = \frac{4AG^2}{3\rho} \tag{2-26}$$

or 33% greater than the minimum possible. The laminar value is the maximum considering steady flow where viscosity is the only physical force producing factor present.

A laminar model has been investigated. The assumptions made were the following: 1) the phases flow in annular layers with a smooth interface between them (this minimizes the surface energies), 2) pressure is constant across a cross section, 3) no slip boundary conditions, and 4) shear stress matching between the phases. The

Navier-Stokes equation reduces to

$$\frac{dP}{dz} + \rho g = \frac{\mu}{r} \frac{d}{dr}\left(r \frac{dV}{dr}\right) \tag{2-27}$$

whose solution is

$$V = \frac{\frac{dP}{dz} + \rho g}{4\mu} + C_3 r + C_4 \tag{2-28}$$

in each phase.

The void fraction is a function of the flow as well as of the quality and the void fraction is on the opposite side of the minimum momentum flux void fraction from the homogeneous. This is indicative of very high slip ratios. The momentum flux value exceeds the homogeneous value except below 8% quality. At higher qualities, the values are prohibitively high. One can safely conclude that the laminar model bears such small relation to reality as to be useless; the results are not presented graphically.

Anderson and Mantzoranis (5) made the same assumptions as were made for the laminar model. They did not, however, satisfy the laminar flow equations in each phase but used Van Karman's (14) "universal velocity profile." They determined a factor giving the ratio of the actual momentum to the two-velocity momentum. Essentially, they predicted a 1% to 10% increase in the flux.

The work of Anderson and Mantzoranis presents a few conceptual difficulties. For example, they draw the velocity and shear stress

profiles as in Figure 21. Within the liquid phase it is impossible to have a positive sloping shear stress and a concave downward velocity profile. They admitted to the difficulty saying that "the assumption must involve some error .... Nevertheless the universal velocity profile is used here as the best approximation to the truth ..." They go even further to define the double velocity profile also shown in the sketch. The double profile amounts to two universal profiles back to back in the liquid region. There is no substantial reason for the assumption other than it might accidentally predict some results.

Note that velocity profile moves the momentum flux value toward the homogeneous model value without altering the measured void fraction. That the momentum flux values are like the homogeneous model does not imply that the flow is homogeneous, but that other factors have made their addition to the flux predicted by the slip model.

2.3.3 Phase Distribution The phenomena of phase distribtuion has no analogy in the single-phase flow. Here it specifically refers to the phenomena of entrainment, a portion of the liquid phase traveling at the gas velocity. The void fraction may still be specified independently. Entrainment is defined as

$$\epsilon = \frac{\text{entrained } \dot{m}_f}{\text{total } \dot{m}_f} \qquad (2\text{-}29)$$

Real entrained flows have been observed (6) (20) to have very laminar-like velocity profiles in the core region. Here, however, the effect of entrainment is being viewed for its mass distribution effect between the two average velocities of the slip model. The steep profiles are not considered.

The two-phase momentum multiplier is

$$MM = \left(\frac{X(X+(1-X)\epsilon)\,\bar{v}_g}{\alpha} + \frac{(1-X)^2(1-\epsilon)^2\,\bar{v}_f}{\left(1-\alpha-\frac{\epsilon\alpha\bar{v}_f(1-X)}{\bar{v}_g X}\right)} \right) \frac{1}{g_c} \qquad (2\text{-}30)$$

One notes that when $\epsilon = 0$, the momentum multiplier reduces to the two-velocity slip model value

$$MM = \left(\frac{X^2 \bar{v}_g}{\alpha} \quad \frac{(1-X)^2 \bar{v}_f}{(1-\alpha)} \right) \frac{1}{g_c} \qquad (2\text{-}31)$$

However, when $\epsilon = 1$, the value is

$$MM = \frac{X\,\bar{v}_g}{\alpha\, g_c} \qquad (2\text{-}32)$$

which is larger than the homogeneous value,

$$MM = \left(X\,\bar{v}_g + (1-X)\,\bar{v}_f \right) \frac{1}{g_c} \qquad (2\text{-}33)$$

This is because to satisfy the void fraction, some liquid must stand on the wall, reducing the effective tube size. Entrainments larger than 1.0 are possible with back flow in the annular water at the wall. Figure 20 shows the results of the entrainment model

with entrainments of 0, 20, 40, 60, 80, and 100 percent along with the homogeneous result.

2.3.4 Time Variation In a single-phase flow, the average momentum flux may be higher than that predicted by an integration using the average velocity profile. This is because the momentum is a function of the square of the velocity. Consider a flow, with a uniform instantaneous velocity profile, varying sinusoidally about a mean value with amplitude b.

$$\dot{m} = \dot{m}_{mean} + b \sin \omega t \tag{2-34}$$

The average momentum flux is proportional to

$$M \approx \dot{m}^2 + \frac{b^2}{2} \tag{2-35}$$

as opposed to the steady value of

$$M \approx \dot{m}^2 \tag{2-36}$$

Schlicting(13) reproduces turbulent flow measurements of Reichardt as in Figure 22. Using a hot-wire anemometer, Reichardt obtained the average velocity profile and a profile of the root mean square of the fluctuating velocities in the axial and the transverse directions. Considering the velocity to be composed of a steady average and a fluctuating velocity, whose average is zero,

$$V = \overline{V} + V' \tag{2-37}$$

and that the momentum flux is proportional to the velocity squared,

$$M \approx \iint_A (\bar{V}^2 + 2\bar{V}V' + V'^2)\, da \qquad (2\text{-}38)$$

the average momentum flux is proportional to two terms

$$\bar{M} \approx \iint_A (\bar{V}^2 + \bar{V}'^2)\, da \qquad (2\text{-}39)$$

An integration of Reichardt's data shows that the fluctuating component amounts to slightly over one percent of the steady velocity profile integration.

In calibrating his apparatus, Rose (10) consistently measured higher momentum fluxes than he was able to support by integration of universal velocity profile. The difference is of the same magnitude as that which is attributed to fluctuation according to Reichardt's data.

The fluctuating velocity is expected to be large at the air-water interface in annular flow. This is visually evident in the fluid to one observing liquid waves propagating up the wall and in the gas from Reichardt's data. This fluctuation may well explain the inability of Silvestri to integrate steady measured profiles to reasonable momentum pressure drop data.

In the two-phase fluctuation generally, some model must be selected to relate parameters before a calculation similar to

equation (2-35) can be made. For example, one may assume the homogeneous model in which the solution is the same as for a single phase. One may assume that the void fraction remains constant and that the flow variations occur in each phase independently, similar to Reichardt's turbulent data. In a slug flow model the void fraction will have some functional relation to the fluctuating flow rates.

The model taken to represent varying void fraction conditions was the two-velocity model with the following assumptions: 1) constant gas velocity

$$\frac{\dot{m}_g \, \bar{v}_g}{\alpha} = \text{constant} \qquad (2\text{-}40)$$

and 2) constant volume flow rate

$$\dot{m}_f \, \bar{v}_f + \dot{m}_g \, \bar{v}_g = \text{constant}. \qquad (2\text{-}41)$$

For computation, step variations in the parameters were used. Any number of steps (i) can be chosen per cycle, but the percentage of time at each step (t_i) must be chosen so as to total unity.

$$\sum_i t_i = 1. \qquad (2\text{-}42)$$

Void fractions selected must be time weighted to give the known overall average value, $\bar{\alpha}$.

$$\sum_i t_i \, \alpha_i = \bar{\alpha} \qquad (2\text{-}43)$$

The continuity relations are written in terms of the local qualities

η_{fi} and η_{gi} where

$$\eta_{fi} = \frac{\dot{m}_{fi}}{\dot{m}_{Total}} \quad , \quad \eta_{gi} = \frac{\dot{m}_{gi}}{\dot{m}_{Total}} \qquad (2\text{-}44a \text{ \& } b)$$

Equations (2-40) and (2-43) are now

$$\frac{\eta_{gi}\ v_g}{\alpha_i} = C_5 \qquad (2\text{-}45)$$

and

$$\eta_{fi}\ v_f + \eta_{gi}\ v_g = C_6 \qquad (2\text{-}46)$$

Of course,

$$\sum_i \eta_{gi}\ t_i = \bar{X} \qquad (2\text{-}47)$$

and

$$\sum_i \eta_{fi}\ t_i = (\overline{1-X}) \qquad (2\text{-}48)$$

which give

$$C_5 = \frac{\bar{X}\ v_g}{\bar{\alpha}} \qquad (2\text{-}49)$$

and

$$C_6 = (\overline{1-X})\ v_f + X\ v_g \qquad (2\text{-}50)$$

so that all η_{gi} and η_{fi} can be evaluated. The resulting momentum multiplier is

$$MM = \frac{1}{g_c} \sum_i t_i \left[\frac{\eta_{fi}^2 v_f}{(1-\alpha_i)} + \frac{\eta_{gi}^2 v_g}{\alpha_i} \right] \qquad (2\text{-}51)$$

Note that η_{fi} and η_{gi} may have been selected in place of α_i along with t_i to determine the value of the other parameters.

Figures 23 through 28 show computed results of the time varying model using two steps (i = 2). The results are given in terms of γ an average deviation from the average liquid fraction $(\overline{1-\alpha})$

$$\gamma = \sum_i \frac{|\bar{\alpha} - \alpha_i| t_i}{1 - \bar{\alpha}} \qquad (2\text{-}52)$$

The time at each step was varied as well as the value of γ. Figure 23 shows the effect of changing the time at each step while holding γ constant. Figures 24 and 25 show the effect of variable γ while the time at each step remains constant. Figure 26 shows the value of the momentum at each step and the resulting average. Figures 27 and 28 show the ratio of the fluctuation in amplitude to the average value as γ varies.

Assuming that the model and the ensuing calculations have some validity, the last curve is particularly significant. By comparing the given figure with actual experimental data, a sample of which is given in Figure 45, one can estimate the correct values of γ.

2.4 Differential Deviation from Single Phase

The single-phase limits are points where the two-phase models can be checked against single-phase theory. This, of course, is well recognized and virtually all the models give the single phase limits in void fraction and momentum flux if they claim to be valid in the region. Bankoff's model, of course, deviates at the high qualities as discussed because it was intended to apply only to the bubbly flow regime.

In addition to the limiting values, the slope of the values with respect to quality can also be estimated with a little additional reasoning. A differentially small addition of a gas to a single-phase liquid can be imagined best as well dispersed throughout the flow (unless artifically made otherwise). Thus at the low quality limit the homogeneous flow is seen to predict the slopes of the void fraction and momentum multiplier. A differential addition of a liquid, not wetting the walls, can be expected to produce the same result. A differential addition of a wetting liquid could eventually be expected to be found at the wall. Thus the two-velocity model would best predict the slope of values for this phenomenon.

CHAPTER III

EXPERIMENTAL PROGRAM

An experimental program was undertaken to obtain direct measurements on the momentum flux in two-phase pipe flow.

3.1 Feasibility

Two methods were initially considered to measure the momentum flux at a section. The first involved condensing the vapor portion of a pipe flow exhausting into a large chamber. The measurement of the pressure difference between the end of the pipe and the exit of the chamber would then relate the negligible chamber exit section momentum flux to the entering flux of interest. The second, the method actually used, involved turning the two-phase fluid as described in Appendix A, in a tee. Calculations indicated that the second method would give more accurate results. It would also be flexibile to measuring two-component as well as two-phase flow where one phase can condense. As a further incentive, turning arrangements had been successful for other investigators.

3.2 Design Requirements

An apparatus to measure the momentum flux by the method considered must accurately measure the force on the turning tee. It must provide facilities for making the force measurement under a

variety of conditions and must monitor those conditions.

It was decided to work principally with steam-water with adaptation to air-water. This decision was based upon the relative ease of availability of the fluids and their significance in regard to two-phase flow application and current studies.

Laboratory steam was available at 200 psia. This pressure and the corresponding saturation temperature set the upper bounds for which the apparatus was to be designed for both operation and safety. Unfortunately, this upper bound is well below values common in industrial practice. Since, however, momentum effects are accentuated at lower pressures, it was felt that the data could be safely extrapolated from the experimental to higher pressures. Atmospheric pressure was the lower bound on the apparatus.

The parameters to be experimentally varied were the flow rate of each of the phases, the pressure, and the inlet pipe diameter.

3.3 Original Design

The final apparatus evolved, through several design changes, from less successful earlier attempts.

3.3.1 Tank and Internals With the turning tee method, it is necessary that the tee be surrounded by an atmosphere at the pressure being tested. Further, the vessel must be large enough so that exit flow from the tee cannot be diverted so as to affect the measurement being made.

A 0.3125-inch wall steel tank having an internal diameter of 16 inches and a length of 36 inches with welded, dome-shaped heads was selected as the pressure containment vessel. The vessel was designed as a refrigerant receiver tank for use at 300 psi. It was hydrostatically tested to 500 psi.

Several fittings already available were used as steam exit, water exit, gage glass mounts, and thermocouple well header. Additional access ports made in the tank include the inlet pipe fitting, an instrumentation fitting and a 10-inch man hole. The man hole provided an entrance through which parts could be inserted and adjustments made. A 9-inch diameter, 1-inch thick tempered glass plate was inserted and sealed by an O-ring in the man hole flange cover. The glass provided a 7-1/2 inch unsupported diameter window for viewing the internal mechanism in actual operation. External mounting fittings were provided with the tank.

Measurement of the forces in the high temperature, pressure, steam-water environment posed a difficult problem. Temperature compensated strain gages presented a possible solution which would have required a great deal of calibration to prove merit on an unsupported measurement. The solution adopted is that of placing a displacement transducer external to the tank where it is not affected by the adverse environment. The transducer would then measure the deflection of a beam, a displacement proportional to the force on the tee. A Linear

Variable Differential Transformer (LVDT) was selected as the transducer so that the transmission of information could be by magnetic means through the wall of the pressure vessel. The primary LVDT coil was fed a 15 KC signal with a peak and peak amplitude of 16 volts.

The pressure vessel wall at the position of the transducer consists of stainless steel, number ten gage tubing (for hypodermic use) with an inside diameter of 0.113 inches and an outside diameter of 0.133 inches. The LVDT used is a Sanborn Linearsyn Differential Transformer Model 590T-025. As shown in Figure 4, the coil assembly has an inside diameter of 0.136 inches while the core has an outside diameter of 0.100 inches. The core was silversoldered to another stainless steel tube serving as the displacement pushrod.

The electrical output of the coil assembly as a function of the core traverse position is shown in Figure 8. The voltage output is considerably smaller than that which would be achieved in the absence of the stainless steel pressure vessel wall. The end effect of the pushrod is sufficiently far from the core effect and excellent linearity occurs in the test distance.

Fittings to clamp the deflecting beam were welded into the tank. Two beams were initially tried, one a brass beam of 1/8 x 1/2 inch squared section and the other a steel beam of 3/16 x 1/2 inch squared section. The two beams were tried for their different spring rates,

from the point of view of frequency response and sensitivity. The steel beam was selected for its higher natural frequency and sufficient sensitivity. The tee was attached to the beam by a threaded stainless steel 10-30 rod. Both the beam and the tee connections are threaded and locked by nuts.

3.3.2 Turning Tee The function of the turning tee, as can be seen from the momentum equation analysis in Appendix A, is simply to turn the flow through a right angle. As long as this is accomplished, the tee internals are of little importance. In exploratory experiments, the tee used by Rose (10) in bubbly air-water flow, was tested in the present apparatus. Rose's tee, being soft soldered, did not stand the temperatures involved. Further, it was found that Rose's tee, being a double pipe elbow, was suitable only for flows approximating a single phase becuase of the extreme secondary flow patterns encountered in other regimes. Thus it was decided to use a tee of radially symmetric design with flow exiting from between parallel plates to insure perpendicularity to the inlet direction.

It was decided to design the tee as a flat plate deflector with guide walls to prevent splash back not normal to the inlet direction. As might be expected, the solution for a two-phase jet striking an overhead plate has not been attempted for two-phase flow. Thus it was decided to design on the basis of a single phase and modify as was deemed necessary by performance. Note that by designing on the

basis of a deflecting plate rather than in a more gradual turning nozzle, it was hoped to increase the time response of the tee.

The problem of a radially symmetric jet striking a surface has not been solved. Two approaches are taken here which bound the solution. First, a continuity approach, where the depth of the tee aperture at each radius is determined by the criteria that it pass the same flow in a radial direction as entered the tee, provides the minimum guide wall dimension. The two-dimensional jet solution (15)

$$y = \frac{h}{2} + \frac{h}{\pi} \log \coth \frac{\pi}{4}\left(\frac{2z}{h} - 1\right) \qquad (3\text{-}1)$$

h = thickness of arriving flow

provides the other limit. The actual solution must approach the continuity solution at the exit of the tee, and the two-dimensional solution at the inlet. As an approximation to the actual solution, the two-dimensional solution was modified to a radially symmetric solution by the criteria that flow area normal to the inlet be the same. This solution is asymptotic to the two-dimensional solution at the inlet and the continuity solution at the exit as shown in Figure 6. The resulting tee design is that of Figure 7a and b. The material was aluminum.

3.3.3 Feed System City water is supplied at the system pressure by an Aurora Model E5T two-stage, vane pump designed to deliver 5 gpm

at 200 psi. The pump is bypassed so that any intermediate pressure and flow may be achieved without overloading the pump.

The liquid flow is measured by a Fischer & Porter 3000 Series Flowrator Meter measuring 5.70 gpm at full scale. The flowmeter was calibrated by weigh tank measurement presented in Figure 11.

The water was preheated in an Economy Steam and Water Mixer rated at 500 gallons per hour. The steam for the contact mixer was supplied at 200 psia from the laboratory supply through a 1/2-inch pipe. Pressure at the point of temperature measurement was read on a 1% accuracy, 200 psi max. pressure gage (#410R-TD Helicoid Test Gage 8-1/2"). The flow rate of the steam was obtained from a heat balance on the mixer. Copper Constantan thermocouples were provided to establish the temperatures necessary for this balance.

The main steam is supplied from the laboratory steam supply through a two-inch line. The flow rate of the steam is determined by flange tap orificing according to the ASME Power Test Code (16). Two sharp-edged orifices were used of 0.4-inch and of 1.0-inch diameter. Pressure readings are provided by the same Helicoid gage used to measure the heater steam pressure and the temperature by another thermocouple. The differential pressure across the orifice was measured by high pressure manometers filled with mercury or with Meriam #3 Manometer Fluid having a specific gravity of 2.95.

Air is supplied from the laboratory supply at 125 psi. It is measured by a laboratory setup equipped with mercury and oil manometers, a .3102-inch diameter orifice in a 2.067-inch diameter pipe, a thermometer, and a pressure gage. A shop air supply at 300 psi could also be used.

The steam and water are mixed in a jet pump mixing fixture, the inner chamber supplying the steam and the outer the water. The fixture, a McDaniels Suction tee, is fitted with one-inch female pipe connections. A valve is provided in both the steam and water lines immediately proceeding the mixing chamber for control and to introduce a large impedance just before mixing. The impedance is intended to minimize feedback into the feed systems. The exit of the mixing fixture feeds a length of insulated pipe leading to the pressure vessel and tee.

The pressure in the tank is monitored by a #410R 4-1/2" Helicoid gage reading to 200 psi. The pressure is determined for calculational purposes by measuring the saturation temperature in the vessel by a Copper-Constantan thermocouple set in an eight-inch well near the beam. The exhaust steam, after passing through a control valve, is condensed in a two-inch line by contact mixing with tap water and dumped. Water level is determined by a sight glass and valve controlled in a half-inch dump line.

3.4 Modified Design

3.4.1 Tank and Internals The initial assembly proved to have two difficulties: considerable frctional hysteresis and an annoying zero shift during operation. Figure 15a and b shows the decay of the beam vibration following the release of an initial deflection, a pluck. Figure 10 shows a static test in which the hysteresis is of disturbing proportions. Friction between the LVDT core and the stainless steel tube vessel wall was blamed for the hysteresis when it was estimated that a quarter of a pound of normal force there could cause the effect. Also suspect was the clamping arrangement for the beam connection to the pressure vessel. The clamping was further suspect of being somewhat responsible for the zero shift at operating temperatures.

Two modifications were made. One end of the beam was bent into a dogleg and welded to the pressure vessel wall. This was to eliminate any buckling problems and to render the attachment more immobile, absorbing deflections in the elastic beam material. The second change involved an alignment mechanism so that the pushrod could always be aligned with the stainless steel tube within the LVDT coil. A flexible wire, too short to buckle, was built into the alignment mechanism so that no torque could be transmitted to the pushrod providing a normal force at the LVDT core. Figure 2 shows a diagram of the final apparatus.

Figures 10 and 15c show that the modification eliminated the column damping and the hysteresis. An operational zero shift persisted, however. Differential thermal expansions, and differential strains from pressure and water level change were investigated (Appendix B). Thermal expansion differences were shown to be of primary effect with a possible assistance from pressure changes.

The elimination of the zero shift lay either in a complete redesign of the apparatus, reducing the lengths subject to the differential strains and compensating somehow for differential expansion, or in the definition of an operational procedure to account for the change. Of course, the operational solution was chosen. Thermocouples were placed in the wall of the pressure vessel so that equilibrium could be detected through time spaced measurements. At the operating equilibrium, a zero point would be measured and the run would commence. The procedure has worked well and the zero value can be checked many times during a run.

3.4.2 Tee The original tee gave an estimated 5% runback (liquid leaving through the entrance). A new tee was designed, the change being a larger aperture, a larger overall radius, and a larger flat distance on the radius. The redesigned tee is given in Figure 7c and d. Further opening between the deflection plate and the guide walls was provided by the insertion of washers to open the slot from 0.10 inches to 0.35 inches. The tee, also constructed

from aluminum, weighs 0.84 pounds. It has performed to satisfaction at all operating conditions.

3.4.3 Feed System At flow rates only one-third of its specified value, the contact heater become noisy in operation. The noise was detectible in a flowmeter oscillation, an oscillation of the feed system that was considered undesirable. One positive effect was that it led to a consideration of the effect of oscillations on the average momentum flux.

A recirculating line, returning water from the pressure vessel to the feed system, replaced the contact heater. A centrifugal pump made up the small pressure difference in the circuit. The recirculated water, mixed with any makeup water needed is returned to the system preceeding the flowmeter. The final arrangement is shown in Figure 3. The recirculation loop successfully eliminated the undesirable noise and was further beneficial in reducing the number of measurements to be made, and in reducing the difficulty of holding specified conditions.

3.5 Void Fraction Data

A direct measurement of the void fraction for air-water was made by isolating a section of the inlet pipe with quick closing valves. The isolated section was plexiglass pipe of 0.75-inch diameter and 75 cm. length. The ratio of liquid volume to total volume was taken to be the liquid fraction.

3.6 Testing

Several tests to verify the performance of the apparatus have already been mentioned. They will merely be listed here.

Test	Purpose
Core Traverse, Fig. 5	Test operation, determine operating range
Pluck Tests, Fig. 15	Determine damping nature and factors
Static Calibrations, Fig. 10	Calibrate flowmeter

The spring constant of the beam was determined by direct measurement of the deflection under a steady load (Figure 9).

The most significant test is the single-phase steam test for it evaluates the principle and the function of the apparatus against known results. Steam flow was measured by the orifice and the momentum flux was measured by the tee. The single-phase momentum flux as calculated from the measured flow is compared with the measured result in Figure 12. The results are excellent.

3.7 Data System

The data consists of all the pressure, temperature, and flow readings necessary to establish the thermodynamic state of the two-phase flow and the temperature equilibrium state of the pressure vessel, and the LVDT output voltage measuring the deflection of the

beam. The pressure, temperature, and flow conditions are steady state and are not monitored continuously. The LVDT output is monitored in several ways as indicated in Figure 5 as its fluctuating nature as well as the average value is of interest.

3.7.1 Observation All of the pressure, temperature, manometer, and flow readings were recorded for each run. The LVDT signal was read from a vacuum tube volt meter after being averaged by a resistor capacitor circuit with a 15 second time constant. In addition, the flow was visually observed and the LVDT output was viewed on an oscilloscope to detect any irregularities. This data is sufficient to determine the average momentum multiplier values.

3.7.2 Tape Recorder For many runs the LVDT output was recorded by a frequency modulated tape deck. As shown in Figure 5, the LVDT signal was first biased and amplified before recording. The purpose of recording the data was for automatic spectral density later.

3.7.3 Brush Recorder The signal was often recorded directly by a Brush recorder. The same signal was also passed through a standard tee filter (17) (18) designed to zero out the natural beam frequency (43.8 cps) and recorded on the second band of the recorder. A diagram of the filter and its experimental frequency response are shown in Figure 14. Also shown is the combined response of the beam and the filter. Samples of the Brush recordings are shown in Figure 44.

3.8 Data Reduction

3.8.1 Average Force Data The recorded data was reduced on the computer to the parameters presented in Chapter IV. Appendix C gives the equations and approximations used in the computer program.

3.8.2 Fluctuating Data Appendix D gives the equation of motion for the beam, the frequency response of which is plotted in Figure J. This is to be compared with the analog computer spectral analysis, samples of which are shown in Figure 46. A Philbrick Researchers SK Analog computer was used for the analysis with a filter, Dynamic Analizer Model 5D101A, made by Spectral Dynamics Corporation of San Diego. Unfortunately, the extremely long averaging times and narrow, sharp bandwidths required for accuracy at low frequencies limit the accuracy of the actual analog analysis.

CHAPTER IV

RESULTS

4.1 Average Moemntum Flux Data

The average momentum flux data, both raw and reduced, are presented in chart form in Appendix E. Figures 31 through 42 give a graphical presentation of the data. The figures locate the data on a mass velocity versus quality map, scribed with lines of constant homogeneous velocity; and present the momentum flux information as a momentum multiplier versus quality. The lines of homogeneous and minimum possible momentum multiplier values are given for reference. An individual figure is presented for each pressure and pipe size tested; atmospheric pressure, 30 psia, 60 psia, 90 psia, and 120 psia in nominal one-half and one-inch pipes for steam-water, and atmospheric pressure in a one-half inch pipe for air-water.

The temperature of the mixing water at the tee did not have any observable effect on the data. It was concluded that the entrance pipe was of sufficient length to diameter ratio to assure the thermal equilibrium and steady flow development conditions standard for adiabatic two-phase flow.

The two pipe sizes tested had no noticeable effect upon the momentum multiplier values.

Flow rate at a particular quality has a noticeable influence on the momentum multiplier values. In an attempt to correlate this effect, the data was coded according to the homogeneous velocity. It is not meant to suggest that the flow is actually homogeneous; the parameter was selected for calculational purposes as a quantity which varies at each quality in the same way as the mass flow rate. Some lines of constant homogeneous velocity have been drawn through the data on the figures of momentum multiplier versus quality. Further mention will be made later concerning the velocity effect for purposes of extrapolation and interpolation.

A few of the data points fall below the minimum possible momentum multiplier line. They are clearly in error. The principle cause of error is the difficulty of measuring the low forces involved. All of the points in error are characterized by low momentum flux and subsequent difficulty of measurement. Points with a small force measurement, generally less than one-half pound, are plotted with bounds of one-tenth of a pound error in each direction. One-tenth of a pound measurement error is sufficient to explain most of the points which fall into the region of impossibility.

4.2 Rose's Results

The bubbly flow regime momentum flux measurements of Rose (10) are presented in Figure 30. The homogeneous and absolute minimum momentum multipliers are also shown on the figure along with other

predicted values. Rose experimentally determined the void fraction, the results being presented here in Figure 29. The void fraction data was approximated by

$$\alpha = 21.59 \; X^{0.574} \qquad X < 0.001 \tag{4-1}$$

and by

$$\alpha = 4.07 \; X^{0.333} \qquad 0.001 < X < 0.004 \tag{4-2}$$

for calculational purposes. The momentum multiplier calculated from these void values according to the two-velocity model is also presented on Figure 30.

Rose's data did not show a systematic variation with the mass velocities he tested, and thus no velocity correlation has been made.

4.3 Vance's Results

Vance (9) made some careful measurements of the momentum flux in horizontal flow with an apparatus very similar to that proposed by Griffin (19). His results, due to the apparatus, are steady rather than average results. Along with the appropriate reduction, the data is shown in Appendix F. The data is taken at widely varying pressures and it is difficult to present the data on a graph. Figure 43 makes an attempt by plotting momentum multiplier versus quality and showing the range of the homogeneous and minimum

possible value for the same pressure and quality.

The question of the relationship between horizontal and vertical flow can be answered by comparison of Vance's results to the results of this investigation. At the flows tested, it is not expected that the difference due to inclination would be detected since the frictional forces are considerably greater than the body forces throughout the flow. One cannot, however, form a definite conclusion on this basis since some lever mechanism may be involved whereby a small body force would dominate much larger forces in influencing flow formation. The similarity of this investigation's data with that of Vance affirms the predominance of the friction forces in determining the flow.

Vance measured the momentum flux for the purpose of determining the slip ratio (or the void fraction) and this is how he presents his data. This is not a valid method of determining the void fraction, however, as the many additional factors mentioned in Chapter II affect the momentum flux. This is the same error as made by Semenov and discussed in Chapter I.

4.4 Void Fraction Measurements

The void fraction measurements are presented in Appendix E and graphically in Figure 17. Two values are given in the appendix estimating the bounds of the range of reliability. The limiting values are connected by a line on Figure 17.

As can be seen from Figure 29 of Rose's data, the void fraction is essentially that of the homogeneous model at qualities approaching zero. As the quality increases the void fraction deviates toward the minimum momentum void value. By 30% quality the void is substantially the minimum momentum void value.

The momentum multiplier calculated by the two-velocity model from the measured void fraction data is shown on Figure 42. This line is substantially below the data, demonstrating, as did Rose's data, that factors in addition to the void fraction are important in determining the momentum flux. Attention is again called to Figures 18 and 19 which shown that large differences in the void fraction near the minimum possible momentum void fraction result in small changes in the momentum multiplier. Above 15% quality, the minimum possible momentum is essentially the same, with respect to the data, as that predicted by measured voids with the slip model. The void fraction deviation from the minimum momentum void plays only a small role in the deviation of the momentum multiplier from its minimum value at higher qualities.

The voids measured here essentially verify Martinelli's results.

4.5 Fluctuations

Two types of data on the fluctuations were reduced, data maximum fluctuation amplitudes as reduced from Brush recorder

traces and spectral density analysis performed on an analog computer from a taped signal.

4.5.1 Brush Recorder Samples of the Brush records are reproduced in Figure 44. Both the unfiltered and filtered signals were recorded (filter response shown in Figure 14). Figure 45 shows data on the maximum filtered amplitude as a percentage of the average force. The data on this figure represents all pressures and mixtures tested and thus is not intended to be an accurate plot. It is intended to indicate the region in which fluctuations play a major role.

The parameter of fluctuating amplitude divided by average amplitude is used in plotting the results of the fluctuating model. By comparing Figures 27 and 28 and 45, one can estimate values of γ in the fluctuation model.

4.5.2 Spectral Analysis Samples of spectral analysis made on an analog computer from a recorded signal can be seen in Figure 46. Also shown in the figure is an oscilloscope photograph of the raw signal during the analysis. The effect of the beam natural frequency is, of course, predominant. By comparison with the expected beam response with a white noise input, Figure 13, one can determine that the fluctuations are of interest in the lower frequency portion of the spectrum (0 - 10cps).

Very small amplitude fluctuations exist at frequencies higher than the beam natural frequencies due to droplet entrainment. This

can be tested empirically by holding one's hand in front of an expelling two-phase flow. These are difficult to detect with the beam arrangement and may well be impossible with a tee since the period of the fluctuations approaches the transit time in the tee. The fluctuations are still very small and they do not affect the validity of the large amplitude measurements at lower frequencies.

It is difficult to explain the fluctuating period of two seconds in a ten-foot long tube where the homogeneous velocity is perhaps 200 ft/sec. Yet Schlicting (13) reports the same sort of data in the velocity fluctuations in turbulent flow. In the two-phase flow it is suspected that the low frequencies are due to continuity type waves easily visible to investigators standing at a distance from a two-phase flow. Reasonable precautions have been taken to isolate the feed systems and the data is presently understood to be valid.

4.6 Choke Flow

A few of the data points taken approach the choke flow (choke flow predictions shown on the flow map of Figure 47 and on Figures 31, 32, 33, and 34). The momentum flux values are not the minimum possible momentum flux as is the assumption in the Fauske model. The Fauske model may predict the critical flow quite accurately, but it is clear from this investigation that the physical reasoning is incorrect.

Although it is inconceivable that the momentum flux would naturally arrive at its minimum possible value, some of the data in the 20-50% quality range indicates that the momentum multiplier drops as the critical flow is approached.

One may think of two-phase critical flow in the following way: as the pressure drops in a tube, the adiabatic momentum multiplier rises. However, if the pressure drops rapidly enough, the flow may not be able to redistribute itself rapidly enough, and the real momentum multiplier will lag behind the adiabatic value. Of course, it cannot lag too far behind because it runs into the continuity minimum -- but before that, some sort of realisitic minimum momentum multiplier. When the flow reaches this condition it is unable to adjust more rapidly -- the critical flow model must incorporate the situation of maximum adjustment rate before continuing.

The factors influencing the maximum rate of adjustment are 1) thermodynamic metastability, 2) flow adjustment, and as a subtitle under adjustment, 3) fluctuations. The Fauske model assumes that the minimum possible momentum represents the maximum adjustment.

4.7 Non-Adiabatic Flow

In a heated tube, bubbles can be observed to occupy a large fraction of the flow channel although the average quality is known to be subcooled. This metastable effect obviously has an effect on

the momentum flux which is difficult to predict. Clearly in the case described, the momentum flux will be higher than that predicted on an average quality basis. Yet in a mist flow, the cool droplets might lag behind in the accelerating fluid stream and result in a lower momentum flux than predicted on an adiabatic basis. The answer to the question seems to be dependent upon the flow regime and the heating rate.

A condensing tube can be considered more generally. The metastable vapor can have no other effect than to make the momentum flux greater than that predicted on an adiabatic basis.

4.8 Discussion of Effects

The momentum multiplier deviates from the minimum possible for the reasons discussed in Chapter II. At this point it will be attempted to note where the various reasons predominate.

4.8.1 Void Fraction Deviation In the bubbly flow regime, the flow is almost homogeneous. The void fractions and momentum fluxes measured by Rose verify the homogeneous model as the single phase liquid is approached. The deviation of the void fraction from the minimum momentum flux value still plays a small role up to 10% quality, but is insignificant when the quality reaches 20%.

4.8.2 Velocity Distribution Velocity and density distribution are almost always important. This is the lion's share of the reason

that momentum multiplier is greater than the homogeneous model as single-phase liquid is approached. Investigators (6) (20) using velocity traverse probes have noted a significant, laminar like, velocity profile in the entrained annular flow region. As the single-phase gas is approached, the velocity profile approaches the same importance as in turbulent flow. The regime where the velocity profile plays the least role is in the annular flow without entrainment.

4.8.3 Entrainment Entrainment is important where there is droplet entrainment since the gas velocities are higher.

4.8.4 Fluctuations Slug flow momentum flux is predominantly fluctuation. As the void fraction influence tapers off, the fluctuation influence increases (the macroscopic void fraction fluctuation). Well into the slug-annular transition, the fluctuation plays a predominant role.

The continuity waves in the annular layer may be considered to be the same sort of fluctuation, but may also be considered to be axial velocity fluctuation similar to the turbulent flow fluctuation. This type of fluctuation is important even in the limiting single-phases if turbulence is present. This is experimentally demonstrated in the inability to calibrate totally on the basis of the universal velocity profiles.

4.9 Interpolation and Extrapolation

Much of the data is in regions where entrainment is expected. Furthermore, the forces causing entrainment are the same as those causing wavy films and some of the fluctuations. Thus it seemed reasonable to attempt to correlate on the basis of the entrainment.

Steen and Wallis (21) report that

$$\epsilon = f\left(V \rho_g^{(1-n)}\right) \tag{4-3}$$

where n is a constant between .52 and .85, the higher values at higher entrainments. They report that the entrainment is directly proportional to the velocity at lower entrainments and proportional to the square root of the density.

A more recent publication of Minh and Huyghe (22) reports that entrainment may be correlated on the basis of a homogeneous $V^2\rho$ defined as

$$(V^2\rho)_{Homogeneous} = \frac{\dot{m}_g^2}{\rho_g \alpha^2 A^4}\left(1 + \epsilon \frac{\dot{m}_f}{\dot{m}_g}\right) \tag{4-4}$$

This is very similar to that reported by Steen and Wallis, more concise but inconvenient as the entrainment correlation parameter itself includes entrainment.

The data reported in Appendices E and F give the homogeneous

velocity and an entrainment correlation parameter.

$$V_{Homogeneous}\sqrt{\frac{\rho_g}{\rho_{atm}}} \tag{4-5}$$

It is recommended that the data be interpolated to intermediate pressure by means of this correlation parameter.

Appendices E and F give two factors

$$YK = \frac{\text{homogeneous MM - actual MM}}{\text{homogeneous MM - minimum MM}} \tag{4-6}$$

and

$$ZK = \frac{\text{actual MM}}{\text{minimum MM}} \tag{4-7}$$

The factor YK represents the location of the momentum multiplier with respect to the homogeneous and minimum values. It is suggested that this parameter remains relatively constant through pressure changes as the entrainment parameter remains constant. ZK is the ratio of the actual to the minimum momentum multiplier. As with the ratio of the homogeneous to the minimum, the values are expected to diverge with pressure change at lower qualities (see Figure 1). ZK serves as a convenient term when working with higher quality momentum fluxes where the difference between the homogeneous and minimum fluxes is only a small portion of the total value.

The difference between the homogeneous and minimum momentum

flux models is often proportionately a small part of the total flux. Thus the YK given in the appendices is in large error due to a small measuring error. It is recommended to make interpolation and extrapolations by the lines of constant velocity drawn on the data in Figures 31, 33, 35, 37 and 39.

The difference between the homogeneous and minimum fluxes becomes proportionately smaller as the pressure rises. It is considered safe then to extrapolate in that direction. Note that as the critical pressure is approached, the turbulent velocity fluctuation and velocity distribution become increasingly important.

CHAPTER V

SUMMARY

5.1 The Two-Velocity Slip Model

The two-velocity slip model results in the minimum possible momentum flux value for given flow rates of liquid and gas if the slip ratio is taken to be

$$\frac{V_g}{V_f} = \sqrt{\frac{v_g}{v_f}} \qquad (5\text{-}1)$$

No rearrangement of the flow from that assumed in the model can result in a lower average momentum flux.

The two-velocity model results in a minimum momentum flux when a specific void fraction (or slip ratio) is established for that void fraction. No deviations from the steady, flat profile assumed in the model can further decrease the average momentum flux at that void fraction.

No criteria for an upper bound was found.

5.2 The Homogeneous Model

The homogeneous model correlates the experimental momentum flux data more closely than does the slip model. This does not mean that the flow is more homogeneous than like the two-velocity model, but merely that the disturbances from the minimum momentum flux slip

model drive the momentum flux toward a value corresponding to the homogeneous model. The flow cannot possibly achieve an absolute minimum momentum flux configuration nor a local minimum at a given void fraction.

5.3 Deviations from Minimum Momentum Flux

The momentum flux deviates from the minimum possible momentum flux for the following reasons:

a) The void fraction deviates from the void fraction for a minimum momentum flux. At extremely low qualities ($x < .003$), the flow is essentially homogeneous. The void fraction deviates considerably from the minimum momentum void fraction and the contribution to the real momentum is significant. However, by 15% quality the contribution of a non-minimum void fraction is small but detectible. Greater than 30% quality, the contribution is negligible.

b) The velocity profiles are not flat. Velocity profiles always play a significant role. They are especially important at high entrainments and least important when the flow is most nearly annular. The velocity profile effect remains of importance in determining the momentum flux even as the flow approaches single phase limits, either at the quality extremes or at the critical pressure.

c) phase distribution (entrainment).

and d) fluctuation. Two types of fluctuation are distinguished, both of which contribute to the momentum flux, turbulent fluctuation, and void fraction fluctuation. Turbulent like velocity variations are especially important in annular flow with waves. The turbulent fluctuation, like the velocity profile effect, is important even in the single-phase limits. Void fraction fluctuation is of great importance in slug and degenerating slug flows.

5.4 Implications

The implications of the investigation are threefold.

a) to replace the use of the slip model by the homogeneous model in predicting momentum flux values. More exact estimation of the fluxes can be made through direct reference to the data.

b) to reconsider critical flow and other momentum associated phenomena in the light of the data.

and c) to carefully investigate fluctuations. Two-phase flow has been considered for its average steady-state properties when it is basically an unsteady phenomenon where the unsteadinesses play a fundamental role.

APPENDIX A

MOMENTUM EQUATION DERIVATIONS

Pressure Drop in a Pipe

The general momentum equation for a control volume can be written as (23)

$$\vec{F}_s + \iiint_{c.v.} \vec{B}\,\rho\, d\forall = \oiint_{c.s.} \vec{V}(\rho \vec{V}\cdot d\vec{A}) + \frac{\partial}{\partial t}\iiint_{c.v.} \vec{V}(\rho\, d\forall) \qquad \text{(A-1)}$$

In the case of upflow in a tube, the surface force is composed of pressure and shear forces while the body force is gravity.

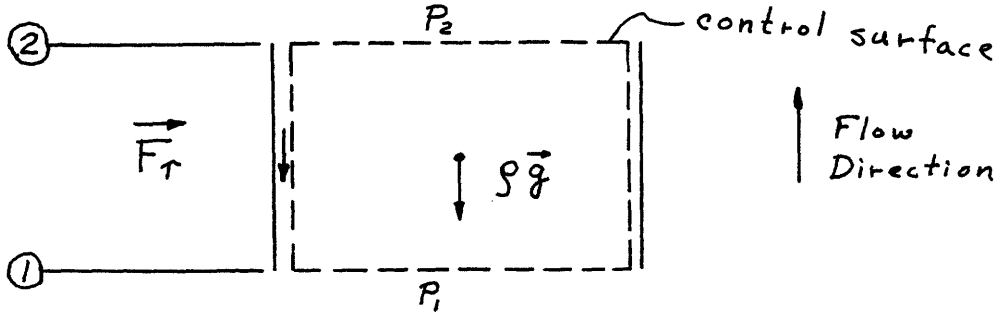

Lumping the shear forces at the control surface into a single fractional term and writing the general momentum equation in the direction of flow, the only non-trivial principal direction, one arrives at an equation for pressure drop in a pipe.

$$F_f + \left[\iint_A P\,dA\right]_{①}^{②} + \iiint_{C.V.} \rho g\,dv = \left[\iint_A \rho V^2\,dA\right]_{②}^{①} + \frac{\partial}{\partial t}\iiint_{C.V.} \rho V\,dv \qquad \text{(A-2)}$$

Considering the pressure to be constant throughout a cross section perpendicular to the flow gives the more simplified relation

$$(P_1 - P_2)A = F_f + \iiint_{C.V.} \rho g\,dv + \left[\iint_A \rho V^2\,dA\right]_{①}^{②} - \frac{\partial}{\partial t}\iiint_{C.V.} \rho V\,dv \qquad \text{(A-3)}$$

(Note: The assumption of constant pressure throughout a cross section is excellent in vertical flow. It is also excellent at the homogeneous velocities tested for flow in any direction, losing validity as the flow begins to stratify due to large relative body forces.)

The pressure change is seen to be composed respectively of a frictional term, an hydrostatic consideration, momentum flux changes, and a transient effect.

Momentum Flux Measurement in a Tee

Writing the general momentum equation for the control volume in a tee which turns the flow through a right-angle bend, one arrives at

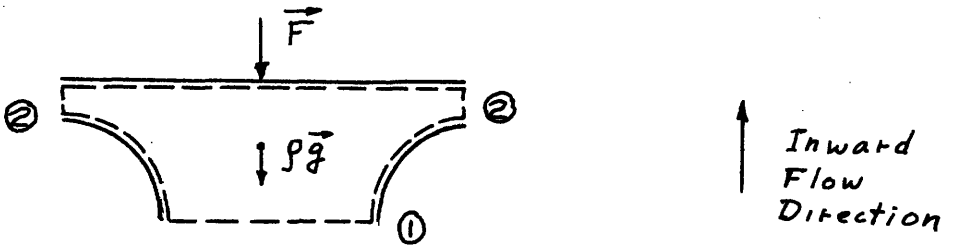

$$F + \iiint_{C.V.} \rho g \, d\mathcal{V} = \iint_{①} \rho V^2 \, dA + \frac{d}{dt} \iiint_{C.V.} \rho V \, d\mathcal{V} \qquad \text{(A-4)}$$

in the direction of the inward flow, again the only non-trivial principal direction. In non-transient flow, the final term vanishes. The other control volume term can be made negligibly small as the size of the control volume is made small. In the case that the term cannot be made negligibly small, it can be estimated with sufficient accuracy to make the maximum possible error negligible. For experimental purposes the equation can be viewed as

$$F = \iint \rho V^2 \, dA \qquad \text{(A-4)}$$

The force on the tee is a direct measurement of the momentum flux entering the turning tee.

Since the measurements of momentum flux made with the tee are to be applied to sections other than exit sections, it is of importance to note a significant difference between exit and other sections. When the flow is reversing, the same fluid passing forward through

a section will return when the flow is reversed as it has been constrained in the pipe forward of the section. If, however, the section is at or near an exit, the forward flowing fluid may be dumped and replaced by the exit atmosphere fluid. The exit condition will persistas far into the tube as the exit fluid replaces the flowing fluid. The tee measurement therefore is inapplicable to measuring in-tube momentum fluxes with flow reversals. This region was avoided in experimentation.

APPENDIX B

CAUSES OF ZERO SHIFT

Thermal Expansion

Coefficients of thermal expansion are given (24) as

	$\frac{\Delta \ell}{\ell\, ^\circ C}$
Stainless steel	17.3×10^{-6}
Steel	10.5×10^{-6}

The differential coefficient is thus

$$6.8 \times 10^{-6} \ \Delta\ell/\ell\, ^\circ C \qquad \text{(B-1)}$$

Over fifteen inches, a 100°C temperature change gives a 0.01 inch which corresponds to a zero shift of 0.0714 volts. This is close to the observed zero shift of 0.077 volts.

Weight of Water

The strain area in the wall of the pressure vessel is

$$\pi\,(16\ in.)(0.3125\ in.) = 15.7\ in.^2 \qquad \text{(B-2)}$$

The cross-sectional area of the tank is

$$\pi\,(8\ in.)^2 \approx 200\ in^2 \approx 1.4\ ft^2 \qquad \text{(B-3)}$$

A one-inch change in the water level adds .12 ft^3 of water on 7.5 lbm of water.

$$\frac{7.5\ lbm}{15.7\ in.^2} = 30 \times 10^6\ psi \cdot \frac{\Delta \ell}{15\ in.} \qquad \text{(B-4)}$$

Therefore, using E = 30 x 10^6 psi, the $\Delta \ell$ over 15 inches is .239 x 10^{-6} inches. This is four orders of magnitude less than that observed in the thermal strains. It can be safely concluded that this effect cannot be detected since the maximum water level change is four inches.

Pressure Change

A 10 psi pressure change would cause a $\Delta \ell$ change of .637 x 10^{-4} inches.

$$\frac{10\ psi\ 200\ in.^2}{15.7\ in.^2} = 30 \times 10^6\ psi\ \frac{\Delta \ell}{15\ in.} \qquad \text{(B-5)}$$

This is small, but detectible, $\sim$ .005 volts for 100 psi pressure change.

APPENDIX C

FUNCTIONS TO FIT CURVES FOR DATA REDUCTION PROGRAM

To obtain water flow rate from the rotometer scale reading, the following equation is used:

$$\text{water flow rate (lbm/hr)} = 27.6 \times \text{scale reading} \qquad \text{(C-1)}$$

Temperature is obtained from Cu-Const. thermocouple millivolt reading by

$$\text{Temp } (^{\circ}\text{F}) = 32.0 + 46.2036R - 0.96412R^2 \qquad \text{(C-2)}$$

R = potentiometer reading in millivolts

when R 4.5, and

$$\text{Temp } (^{\circ}\text{F}) = 40.655 + 41.9795R - 0.44641R^2 \ . \qquad \text{(C-3)}$$

The orifice flow coefficients (16) are functions of Reynolds Number.

$$K = .5974 + \frac{26}{Re + 33.333} \qquad \text{(C-4)}$$

for the 0.4-inch orifice with a diameter ratio of .200, and

$$K = .6250 + \frac{126.884}{Re - 492.063} \qquad \text{(C-5)}$$

for the 1.0-inch orifice with a diameter ratio of .500.

Martinelli's void fraction versus quality curves were found to fit the form

$$X^{c_1} + (1-\alpha)^{c_2} = 1 \qquad \text{(C-6)}$$

quite well. Values of the coefficients for atmospheric and 60 psia steam-water data are

	c_1	c_2
atmospheric pressure	0.116	0.669
60 psia	0.153	0.660

For computational purposes, Rose's void fraction data was fit by

$$\alpha = 21.59 \quad X^{0.574} \qquad \text{for } x < .001$$

and by

$$\alpha = 4.07 \quad X^{0.333} \qquad \text{for } .001 < x < .004$$

APPENDIX D

EQUATION OF MOTION OF THE TEE

$$F = k x + c \frac{dx}{dt} + m \frac{d^2x}{dt^2} \qquad \text{(D-1)}$$

$$F = k' e + c' \frac{de}{dt} + m \frac{d^2e}{dt^2} \qquad \text{(D-2)}$$

where equation (D-2) is written in terms of the LVDT voltage output, e. The relation between e and x is simply

$$x = 7.14 \left(\frac{volts}{in.}\right) e \qquad \text{(D-3)}$$

Values of k and k' have been experimentally determined in static tests.

$$k = 208 \frac{lbf}{in.} \qquad k' = 29.18 \frac{lbf}{volt} \qquad \text{(D-4, a\&b)}$$

The natural frequency is 43.8 $\frac{\text{cycles}}{\text{sec}}$ or 275 $\frac{\text{radians}}{\text{sec}}$

$$\sqrt{\frac{k}{m}} = \sqrt{\frac{k'}{m'}} = 275/sec \qquad \text{(D-5)}$$

$$m = \frac{208 \frac{lbf}{in.}}{75625/sec^2} \qquad m' = \frac{29.18 \frac{lbf}{volt}}{75625/sec^2}$$

$$= .275 \times 10^{-2} \frac{lbf\,sec^2}{in.} = .3855 \times 10^{-3} \frac{lbf\,sec^2}{volt} \qquad \text{(D-6, a\&b)}$$

$$= 1.028\ lbm.$$

The measured mass of the tee was .84 lbm. The effective mass computed includes the pushrod mass and a contribution from the beam itself.

The decay constant β of the envelope was measured to be 0.4/sec.

$$\frac{c}{2m} = \frac{c'}{2m'} = 0.4/\text{sec}. \qquad \text{(D-7)}$$

$$c = 0.22 \times 10^{-2} \frac{\text{lbf sec}}{\text{in.}} \qquad c' = 0.308 \times 10^{-3} \frac{\text{lbf sec}}{\text{volt}} \qquad \text{(D-8, a\&b)}$$

APPENDIX E

DATA

STEAM - WATER DATA

D= 1.0640 1198.000000 2.280000
TEMP= 212.00 PRESS= 14.70

TEST NUMBER	MIXING WATER THERMOCOUPLE READING (millivolts)	ORIFICE MANOMETER READING (in.Hg.)	ROTOMETER READING (% SCALE)	LVDT VOLTAGE (volts)	ZERO VOLTAGE (volts)	MIXING WATER TEMPERATURE (°F)	MIXING WATER FLOW RATE (lbm/hr)	MIXING STEAM FLOW RATE (lbm/hr)	QUALITY	MASS VELOCITY ($lbm/hr\,in^2$)	FORCE ON TEE (lbf)	MOMENTUM MULTIPLIER ($lbf\,hr^2 in^2/lbm^2$)	YK	ZK	ENTRAINMENT CORRELATION FACTOR (ft/sec)	HOMOGENEOUS VELOCITY (ft/sec)
88	3.270	20.60	66.50	.2780	.0659	172.8	.1835E 04	.3664E 03	.1409	2476	6.178	.1133E-05	.1653	4.603	375	375
89	3.160	29.40	56.00	.3200	.0659	168.4	.1546E 04	.4348E 03	.1952	2227	7.402	.1678E-05	.0970	3.859	467	467
90	3.390	16.10	75.50	.2420	.0659	177.6	.2084E 04	.3251E 03	.1108	2709	5.130	.7860E-06	.2829	4.765	324	324
91	3.490	5.00	91.00	.1200	.0659	181.5	.2512E 04	.1827E 03	.0418	3030	1.576	.1930E-06	.5665	4.812	138	138
92	3.120	8.70	76.00	.1460	.0659	166.8	.2098E 04	.2403E 03	.0660	2629	2.333	.3795E-06	.4366	5.122	188	188
93	3.050	15.50	77.00	.2020	.0660	164.0	.2125E 04	.3191E 03	.0939	2749	3.962	.5896E-06	.3805	4.666	278	278
94	3.020	21.40	69.00	.2670	.0662	162.7	.1904E 04	.3732E 03	.1294	2562	5.849	.1003E-05	.2027	4.699	357	357
95	3.620	6.80	49.80	.1470	.0662	186.6	.1374E 04	.2128E 03	.1180	1785	2.354	.8306E-06	.2915	4.544	227	227
96	3.550	10.50	50.00	.1790	.0662	183.9	.1380E 04	.2637E 03	.1439	1849	3.286	.1081E-05	.2363	4.235	286	286
97	3.500	16.40	50.00	.2220	.0662	181.9	.1380E 04	.3280E 03	.1764	1921	4.538	.1383E-05	.1994	3.807	364	364
98	3.510	23.30	48.70	.2675	.0655	182.3	.1344E 04	.3889E 03	.2117	1949	5.884	.1742E-05	.1516	3.466	443	443
99	3.550	32.70	49.50	.3210	.0655	183.9	.1366E 04	.4574E 03	.2414	2051	7.442	.1990E-05	.1554	3.120	532	532
100	3.600	3.60	39.80	.1130	.0655	185.8	.1098E 04	.1553E 03	.1063	1410	1.384	.7827E-06	.2470	5.080	161	161
101	3.530	8.50	39.60	.1420	.0655	183.1	.1093E 04	.2376E 03	.1628	1496	2.228	.1119E-05	.3284	3.543	262	262
102	3.510	14.90	40.00	.1890	.0658	182.3	.1104E 04	.3130E 03	.2079	1594	3.589	.1589E-05	.2353	3.266	356	356
103	3.540	21.70	39.70	.2310	.0662	183.5	.1096E 04	.3758E 03	.2460	1655	4.800	.1971E-05	.1911	2.986	437	437
104	3.500	30.10	39.90	.2770	.0662	181.9	.1101E 04	.4397E 03	.2772	1733	6.140	.2299E-05	.1547	2.797	516	516
105	3.470	3.56	30.00	.0937	.0662	180.7	.8280E 03	.1544E 03	.1377	1105	.801	.7380E-06	.5193	3.117	164	164
106	3.420	9.10	30.00	.1310	.0662	178.7	.8280E 03	.2457E 03	.2136	1208	1.888	.1456E-05	.3576	2.849	277	277
107	3.450	17.10	30.00	.1750	.0662	179.9	.8280E 03	.3347E 03	.2785	1308	3.169	.2084E-05	.2837	2.514	391	391
108	3.490	22.10	29.90	.2030	.0662	181.5	.8252E 03	.3791E 03	.3087	1354	3.985	.2443E-05	.2251	2.433	449	449
109	3.590	28.70	29.50	.2310	.0662	185.4	.8142E 03	.4298E 03	.3445	1399	4.800	.2758E-05	.2219	2.235	517	517
110	3.380	6.30	20.00	.0980	.0662	177.2	.5520E 03	.2049E 03	.2578	851	.926	.1438E-05	.5702	1.998	236	236
111	3.460	10.70	19.90	.1260	.0662	180.3	.5492E 03	.2661E 03	.3204	917	1.742	.2330E-05	.3378	2.164	315	315
112	3.490	17.20	20.00	.1550	.0663	181.5	.5520E 03	.3357E 03	.3772	998	2.584	.2915E-05	.2851	1.992	404	404
113	3.510	23.10	19.80	.1825	.0664	182.3	.5465E 03	.3873E 03	.4172	1050	3.382	.3449E-05	.1987	1.946	470	470
114	3.500	32.00	20.00	.2170	.0665	181.9	.5520E 03	.4527E 03	.4557	1130	4.384	.3861E-05	.1692	1.840	552	552
115	3.550	32.00	30.00	.2550	.0666	183.9	.8280E 03	.4527E 03	.3521	1440	5.488	.2975E-05	.1454	2.315	544	544
116	3.580	32.00	40.00	.2910	.0668	185.1	.1104E 04	.4527E 03	.2854	1751	6.531	.2396E-05	.1402	2.761	536	536
117	3.350	32.00	50.00	.3190	.0700	176.0	.1380E 04	.4527E 03	.2312	2061	7.253	.1920E-05	.1441	3.257	512	512

Mixing
Steam
Enthalpy = 1198 BTU/lbm

Specific
Volume = 2.28 ft^3/lbm

Pipe Diameter = 1.064 in.
Pressure = 14.7 psia

STEAM-WATER DATA

TEST NUMBER	MIXING WATER THERMOCOUPLE READING (millivolts)	ORIFICE MANOMETER READING (in. Hg.)	ROTOMETER READING (% SCALE)	LVDT VOLTAGE (volts)	ZERO VOLTAGE (volts)	MIXING WATER TEMPERATURE (°F)	MIXING WATER FLOW RATE (lbm/hr)	MIXING STEAM FLOW RATE (lbm/hr)	QUALITY	MASS VELOCITY (lbm/hr in^2)	FORCE ON TEE (lbf)	MOMENTUM MULTIPLIER (lbf hr^2 in^2/lbm^2)	YK	ZK	ENTRAINMENT CORRELATION FACTOR (ft/sec)	HOMOGENEOUS VELOCITY (ft/sec)
TEMP= 291.61 PRESS= 59.00																
118	3.770	13.30	30.00	.0999	.0820	192.5	.8280E 03	.2961E 03	.1893	1264	.521	.3669E-06	.3299	2.726	135	70
119	4.140	13.50	38.00	.1040	.0820	206.8	.1049E 04	.2983E 03	.1539	1515	.641	.3140E-06	.2663	3.220	132	69
120	4.410	13.30	48.00	.1060	.0802	217.0	.1325E 04	.2961E 03	.1199	1823	.752	.2543E-06	.2203	3.766	124	65
121	4.440	23.80	47.10	.1260	.0820	218.1	.1300E 04	.3929E 03	.1754	1904	1.282	.3977E-06	.1495	3.331	189	98
122	4.620	24.00	58.00	.1300	.0825	225.1	.1601E 04	.3945E 03	.1436	2244	1.384	.3090E-06	.2067	3.519	183	95
123	4.660	24.10	81.00	.1300	.0825	226.6	.2236E 04	.3953E 03	.0930	2959	1.384	.1777E-06	.3225	3.717	157	82
124	4.230	24.10	17.50	.1100	.0825	210.2	.4830E 03	.3953E 03	.4111	988	.801	.9234E-06	.2182	1.806	228	119
125	4.480	31.50	21.10	.1210	.0830	219.6	.5824E 03	.4494E 03	.4008	1160	1.107	.9246E-06	.1676	1.894	261	136
126	4.990	31.60	50.00	.1435	.0830	239.0	.1380E 04	.4500E 03	.2080	2058	1.762	.4679E-06	.1625	2.985	241	126
127	5.000	31.80	76.00	.1565	.0835	239.4	.2098E 04	.4514E 03	.1339	2867	2.126	.2910E-06	.1952	3.674	218	114
128	4.890	31.70	98.50	.1535	.0842	235.3	.2719E 04	.4507E 03	.0924	3564	2.019	.1787E-06	.3113	3.770	188	98
129	4.850	12.90	27.80	.1010	.0842	233.8	.7673E 03	.2917E 03	.2357	1191	.489	.3880E-06	.5181	2.012	158	82
130	4.900	12.90	70.50	.1080	.0842	235.6	.1946E 04	.2917E 03	.0799	2516	.693	.1231E-06	.4996	3.121	116	60
131	4.980	12.80	100.00	.1083	.0842	238.6	.2760E 04	.2906E 03	.0448	3431	.702	.6707E-07	.5284	3.179	90	47
132	4.900	25.60	94.90	.1390	.0842	235.6	.2619E 04	.4069E 03	.0844	3403	1.596	.1550E-06	.3579	3.673	165	86
133	3.900	31.10	53.50	.1320	.0842	197.5	.1477E 04	.4466E 03	.1582	2163	1.392	.3347E-06	.2276	3.291	194	101
134	5.100	31.30	99.00	.1610	.0842	243.1	.2732E 04	.4480E 03	.0984	3577	2.237	.1967E-06	.2796	3.822	201	105
135	5.630	31.20	49.80	.1505	.0842	262.8	.1374E 04	.4473E 03	.2273	2049	1.931	.5174E-06	.1501	2.851	262	137
136	4.960	31.20	50.00	.1435	.0842	237.9	.1380E 04	.4473E 03	.2058	2055	1.727	.4600E-06	.1705	2.984	239	124
137	2.850	31.20	51.20	.1200	.0842	155.8	.1413E 04	.4473E 03	.1327	2092	1.043	.2679E-06	.2736	3.427	158	82
138	4.930	18.40	48.60	.1185	.0842	236.8	.1341E 04	.3469E 03	.1623	1899	.999	.3117E-06	.3311	2.947	174	91
TEMP= 212.00 PRESS= 14.70																
139	4.210	3.10	52.80	.1135	.0665	209.4	.1457E 04	.1441E 03	.0920	1801	1.369	.4747E-06	.5204	3.878	179	179
140	4.230	3.64	51.80	.1200	.0665	210.2	.1430E 04	.1561E 03	.1016	1784	1.558	.5510E-06	.4917	3.846	195	195
141	4.210	3.66	59.70	.1270	.0665	209.4	.1648E 04	.1565E 03	.0886	2029	1.762	.4813E-06	.4845	4.172	194	194
142	4.210	3.70	70.00	.1350	.0665	209.4	.1932E 04	.1574E 03	.0766	2350	1.995	.4064E-06	.4948	4.405	194	194
143	4.250	3.70	80.10	.1410	.0665	211.0	.2211E 04	.1574E 03	.0687	2663	2.170	.3441E-06	.5282	4.379	198	198
144	4.250	3.74	95.60	.1500	.0665	211.0	.2639E 04	.1582E 03	.0583	3145	2.432	.2765E-06	.5564	4.446	199	199
145	4.250	3.72	39.80	.1105	.0665	211.0	.1098E 04	.1578E 03	.1308	1413	1.282	.7221E-06	.4945	3.325	199	199
146	4.210	3.67	30.00	.1010	.0665	209.4	.8280E 03	.1568E 03	.1648	1108	1.005	.9214E-06	.5038	2.858	196	196
147	4.210	3.67	19.80	.0902	.0665	209.4	.5465E 03	.1568E 03	.2318	791	.690	.1241E-05	.5833	2.096	197	197
148	4.210	8.90	49.70	.1720	.0665	209.4	.1372E 04	.2430E 03	.1556	1816	3.073	.1048E-05	.3446	3.588	304	304
149	4.250	8.90	60.00	.1880	.0665	211.0	.1656E 04	.2430E 03	.1333	2136	3.539	.8726E-06	.3610	3.892	306	306
150	4.250	9.00	70.00	.2010	.0665	211.0	.1932E 04	.2444E 03	.1168	2448	3.918	.7354E-06	.3872	4.089	308	308
151	4.260	9.20	80.00	.2125	.0665	211.3	.2208E 04	.2470E 03	.1049	2761	4.253	.6274E-06	.4229	4.156	312	312
152	4.260	9.20	90.70	.2230	.0665	211.3	.2503E 04	.2470E 03	.0936	3093	4.559	.5358E-06	.4501	4.261	312	312
153	4.260	9.20	40.20	.1600	.0665	211.3	.1110E 04	.2470E 03	.1905	1526	2.724	.1316E-05	.3342	3.161	312	312
154	4.260	9.20	30.00	.1425	.0665	211.3	.8280E 03	.2470E 03	.2405	1209	2.214	.1703E-05	.3303	2.688	312	312
155	4.230	9.20	20.00	.1230	.0665	210.2	.5520E 03	.2470E 03	.3231	899	1.646	.2292E-05	.3693	2.096	312	312
156	4.140	9.20	9.80	.1030	.0682	206.8	.2705E 03	.2470E 03	.4980	582	1.014	.3365E-05	.5869	1.353	311	311
157	4.250	14.90	40.20	.2023	.0682	211.0	.1110E 04	.3130E 03	.2300	1600	3.906	.1716E-05	.2690	2.939	395	395
158	4.250	15.30	50.00	.2275	.0682	211.0	.1380E 04	.3171E 03	.1951	1909	4.640	.1433E-05	.2747	3.297	400	400
159	4.260	15.30	60.10	.2470	.0682	211.3	.1659E 04	.3171E 03	.1678	2222	5.208	.1186E-05	.3032	3.564	401	401
160	4.260	15.30	69.50	.2660	.0682	211.3	.1918E 04	.3171E 03	.1482	2514	5.762	.1025E-05	.3171	3.819	401	401
161	4.260	15.50	80.00	.2815	.0682	211.3	.2208E 04	.3191E 03	.1319	2842	6.213	.8651E-06	.3584	3.931	403	403
162	4.260	15.50	87.20	.2903	.0682	211.3	.2407E 04	.3191E 03	.1222	3066	6.470	.7742E-06	.3840	3.996	403	403
163	4.220	15.50	29.70	.1810	.0682	209.8	.8197E 03	.3191E 03	.2923	1281	3.286	.2253E-05	.2535	2.483	402	402
164	4.200	15.30	20.00	.1550	.0682	209.0	.5520E 03	.3171E 03	.3808	977	2.528	.2976E-05	.2707	1.997	399	399
165	4.140	15.20	10.00	.1260	.0682	206.8	.2760E 03	.3161E 03	.5575	666	1.684	.4271E-05	.4313	1.380	398	398
166	4.140	23.90	35.00	.2430	.0682	206.8	.9660E 03	.3937E 03	.2999	1529	5.092	.2449E-05	.1810	2.574	492	492
167	4.230	24.00	44.30	.2730	.0682	210.2	.1223E 04	.3945E 03	.2545	1819	5.966	.2028E-05	.2000	2.887	497	497
168	4.230	24.20	54.60	.3010	.0685	210.2	.1507E 04	.3961E 03	.2169	2140	6.773	.1663E-05	.2346	3.167	499	499
169	4.270	24.30	69.60	.3390	.0690	211.7	.1921E 04	.3968E 03	.1794	2607	7.865	.1302E-05	.2814	3.478	503	503
170	4.220	24.40	23.40	.2070	.0695	209.8	.6458E 03	.3976E 03	.3984	1174	4.005	.3271E-05	.2031	2.015	502	502
171	4.220	24.40	14.00	.1720	.0705	209.8	.3864E 03	.3976E 03	.5309	882	2.957	.4277E-05	.3047	1.519	502	502
D= 1.0640 1198.000000 2.280000																
TEMP= 291.61 PRESS= 59.00																
172	6.250	.80	58.50	.1650	.0930	285.6	.1615E 04	.4787E 03	.2288	2354	2.097	.4256E-06	.3901	2.320	304	158
173	6.290	.80	71.00	.1770	.0930	287.0	.1960E 04	.4787E 03	.1967	2742	2.447	.3659E-06	.3759	2.554	305	159
174	6.300	.80	84.00	.1880	.0930	287.4	.2318E 04	.4787E 03	.1712	3146	2.767	.3145E-06	.3782	2.738	305	159
175	6.260	.80	94.00	.1950	.0930	286.0	.2594E 04	.4787E 03	.1541	3456	2.971	.2797E-06	.3832	2.866	302	157

P = 14.7

Pressure=14.7 psia

Pressure = 59.0 psia

Pipe Diameter = 1.064 in.

STEAM - WATER DATA

TEST NUMBER	MIXING WATER THERMOCOUPLE READING (millivolts)	ORIFICE MANOMETER READING (in. Hg.)	ROTOMETER READING (% scale)	LVDT VOLTAGE (volts)	ZERO VOLTAGE (volts)	MIXING WATER TEMPERATURE (°F)	MIXING WATER FLOW RATE (lbm/hr)	MIXING STEAM FLOW RATE (lbm/hr)	QUALITY	MASS VELOCITY (lbm/hr in^2)	FORCE ON TEE (lbf)	MOMENTUM MULTIPLIER (lbf hr^{2}in^2/lbm^2)	YK	ZK	ENTRAINMENT CORRELATION FACTOR (ft/sec)	HOMOGENOUS VELOCITY (ft/sec)	
176	6.220	.80	50.20	.1580	.0930	284.5	.1386E 04	.4787E 03	.2568	2097	1.893	.4844E-06	.3889	2.174	303	158	
177	6.190	.80	39.60	.1470	.0930	283.4	.1093E 04	.4787E 03	.3052	1768	1.573	.5662E-06	.4367	1.886	303	158	
178	6.140	.80	29.90	.1360	.0930	281.6	.8252E 03	.4787E 03	.3685	1467	1.253	.6550E-06	.5396	1.562	303	158	
179	6.140	.80	20.00	.1230	.0930	281.6	.5520E 03	.4787E 03	.4690	1159	.874	.7314E-06	.8495	1.123	305	159	
180	5.950	.80	9.50	.1115	.0930	274.6	.2622E 03	.4787E 03	.6541	833	.539	.8729E-06	1.7953	.718	305	159	
181	6.250	2.89	37.00	.2510	.0930	285.6	.1021E 04	.9098E 03	.4783	2172	4.602	.1097E-05	.2063	1.625	582	304	
182	6.290	3.02	50.00	.2740	.0930	287.0	.1380E 04	.9300E 03	.4087	2598	5.272	.8785E-06	.2920	1.737	596	311	
183	6.250	2.92	60.00	.3080	.0930	285.6	.1656E 04	.9145E 03	.3596	2891	6.263	.8427E-06	.1304	2.100	584	304	
184	6.320	2.76	69.50	.3160	.0930	288.1	.1918E 04	.8893E 03	.3213	3157	6.496	.7328E-06	.1653	2.230	570	297	
185	5.090	2.68	80.00	.3020	.0930	242.8	.2208E 04	.8763E 03	.2522	3469	6.088	.5690E-06	.1661	2.633	493	257	
186	4.930	2.73	58.00	.2670	.0940	236.8	.1601E 04	.8844E 03	.3252	2795	5.039	.7255E-06	.1994	2.162	511	266	
187	4.820	2.78	35.00	.2280	.0950	232.6	.9660E 03	.8924E 03	.4574	2090	3.874	.9974E-06	.2952	1.604	536	280	
188	5.040	2.75	11.90	.1700	.0965	240.9	.3284E 03	.8876E 03	.7314	1368	2.141	.1287E-05	1.6513	.855	560	292	
189	5.760	5.30	29.00	.3110	.0965	267.6	.8C04E 03	.1230E 04	.6090	2283	6.248	.1348E-05	.3956	1.269	779	406	
190	5.560	5.90	50.30	.3940	.0965	260.3	.1388E 04	.1297E 04	.4761	3020	8.666	.1069E-05	.2493	1.597	806	420	
191	5.500	4.70	64.00	.4400	.0965	258.0	.1766E 04	.1158E 04	.3828	3290	10.006	.1040E-05	-.1403	2.316	707	369	
192	5.490	7.50	62.00	.5100	.0965	257.7	.1711E 04	.146CE 04	.4507	3567	12.045	.1065E-05	.1370	1.760	901	470	
193	5.500	9.50	60.20	.5900	.0965	258.C	.1662E 04	.1641E 04	.4895	3714	14.375	.1172E-05	.1192	1.663	1019	531	
194	5.500	11.00	60.00	.6350	.0965	258.0	.1656E 04	.1763E 04	.5C95	3846	15.686	.1193E-05	.1762	1.571	1098	573	Pressure = 14.7 psia
D= 1.0640 1198.CCCCCC 2.280CCCC																	
TEMP= 320.27 PRESS= 90.00																	
195	6.970	2.36	39.80	.1980	.1100	311.6	.1098E 04	.8226E 03	.4287	2161	2.563	.6176E-06	.3223	1.605	426	182	
196	7.000	2.36	50.00	.2090	.1100	312.6	.1380E 04	.8226E 03	.3734	2477	2.884	.5285E-06	.3191	1.756	426	182	
197	7.050	2.39	60.50	.2260	.1100	314.4	.1670E 04	.8278E 03	.3317	2809	3.379	.4816E-06	.2605	1.966	430	184	
198	7.070	2.42	70.40	.2385	.1100	315.1	.1943E 04	.833CE 03	.3003	3122	3.743	.4319E-06	.2622	2.091	433	185	
199	7.060	2.47	81.00	.2525	.1100	314.8	.2236E 04	.8415E 03	.2729	3461	4.151	.3898E-06	.2621	2.216	437	187	
200	7.110	2.44	89.80	.2680	.1100	316.6	.2478E 04	.8364E 03	.2528	3728	4.602	.3724E-06	.2150	2.402	436	187	
201	7.110	2.45	100.00	.2790	.1100	316.6	.2760E 04	.8381E 03	.2330	4047	4.923	.3381E-06	.2305	2.488	437	187	
202	6.970	2.45	29.10	.1820	.1100	311.6	.8032E 03	.8381E 03	.5131	1846	2.097	.6923E-06	.5289	1.297	435	186	
203	6.900	2.45	20.00	.1680	.1100	309.1	.5520E 03	.8381E 03	.6064	1563	1.689	.7774E-06	.8342	1.068	435	186	
204	6.700	2.45	9.00	.1610	.1100	301.9	.2484E 03	.8381E 03	.7776	1222	1.486	.1119E-05	1.3060	.960	436	186	
205	6.950	7.00	35.00	.3360	.1100	310.8	.9660E 03	.1411E 04	.5977	2674	6.583	.1036E-05	-.0745	1.463	734	314	
206	7.000	6.50	49.70	.3365	.1100	312.6	.1372E 04	.1360E 04	.5007	3073	6.598	.7859E-06	.1875	1.541	707	302	
207	6.250	6.60	72.00	.4220	.1100	285.6	.1987E 04	.1371E 04	.3909	3777	9.088	.7167E-06	-.1540	2.196	680	291	
208	6.950	6.50	84.60	.4550	.1100	310.8	.2335E 04	.1360E 04	.3666	4156	10.050	.6544E-06	-.0920	2.244	703	300	
209	6.110	6.20	16.00	.2660	.1100	280.5	.4416E 03	.1329E 04	.7501	1991	4.544	.1289E-05	-.1054	1.185	685	293	
210	6.870	10.50	35.10	.4190	.1100	308.0	.9688E 03	.1724E 04	.6443	3028	9.001	.1104E-05	-.0454	1.354	896	383	
211	6.470	10.50	51.10	.4670	.1100	293.6	.1410E 04	.1724E 04	.5442	3525	10.399	.9414E-06	-.0562	1.583	882	377	
212	6.310	10.20	71.30	.5220	.1100	287.8	.1968E 04	.1699E 04	.4503	4124	12.001	.7935E-06	-.0837	1.887	855	365	
213	6.500	10.00	83.60	.5600	.1100	294.7	.2307E 04	.1683E 04	.4110	4488	13.108	.7321E-06	-.0981	2.051	849	363	
214	6.110	10.10	21.40	.3620	.1100	280.5	.5906E 03	.1691E 04	.7400	2566	7.341	.1254E-05	-.0049	1.183	871	372	
215	6.550	10.20	10.10	.3230	.1100	296.5	.2788E 03	.1699E 04	.8675	2225	6.204	.1410E-05	1.9305	.981	885	378	
216	6.550	18.00	30.20	.5080	.1100	296.5	.8335E 03	.2244E 04	.7322	3461	11.593	.1089E-05	.7524	1.048	1163	497	
217	5.140	13.80	49.00	.5300	.1100	244.6	.1352E 04	.1971E 04	.5668	3738	12.234	.9849E-06	-.0749	1.536	973	416	
218	5.850	13.80	63.00	.6880	.1100	271.C	.1739E 04	.1971E 04	.5128	4172	16.837	.1088E-05	-.6462	2.041	984	420	
219	6.330	13.70	82.80	.6570	.1100	288.5	.2285E 04	.1964E 04	.4495	4779	15.934	.7846E-06	-.0618	1.872	989	423	
220	5.760	14.10	13.80	.4130	.1100	267.6	.3809E 03	.1992E 04	.8419	2668	8.826	.1394E-05	.4515	1.027	1030	440	
221	5.510	16.60	33.00	.5380	.1100	258.4	.9108E 03	.2157E 04	.6924	3450	12.467	.1178E-05	-.0219	1.261	1096	469	
222	6.290	16.50	48.00	.5900	.1100	287.0	.1325E 04	.2151E 04	.6133	3909	13.982	.1029E-05	.0343	1.385	1101	471	
TEMP= 250.33 PRESS= 30.00																	
223	5.150	2.79	30.00	.3930	.1200	245.0	.8280E 03	.8940E 03	.5351	1937	7.952	.2384E-05	.1535	1.579	796	570	
224	4.560	2.76	41.50	.4370	.1200	222.8	.1145E 04	.8893E 03	.4363	2288	9.234	.1983E-05	.0870	1.933	768	550	
225	4.840	2.76	58.50	.5100	.1200	233.4	.1615E 04	.8893E 03	.3563	2816	11.360	.1611E-05	.0847	2.289	772	553	
226	4.400	2.76	19.80	.3330	.1200	216.6	.5465E 03	.8893E 03	.6280	1615	6.204	.2676E-05	.3298	1.304	779	558	
227	4.400	2.73	8.80	.2730	.1200	216.6	.2429E 03	.8844E 03	.8030	1268	4.457	.3118E-05	1.4067	.939	784	561	
228	4.620	5.50	30.60	.6110	.1200	225.1	.8446E 03	.1252E 04	.6079	2358	14.302	.2892E-05	-.0044	1.500	1101	789	
229	4.460	5.50	40.80	.6730	.1200	218.9	.1126E 04	.1252E 04	.5296	2675	16.108	.2532E-05	-.0143	1.709	1089	780	
230	4.640	5.50	47.00	.7070	.1200	225.8	.1297E 04	.1252E 04	.4956	2867	17.099	.2339E-05	.0160	1.792	1092	782	
231	3.300	5.50	16.80	.5190	.1200	174.0	.4637E 03	.1252E 04	.7341	1930	11.622	.3509E-05	-.0323	1.264	1088	779	
232	1.300	5.60	8.50	.4720	.1200	90.4	.2346E 03	.1264E 04	.8471	1685	10.253	.4062E-05	-.1121	1.107	1096	785	
233	3.270	7.80	33.00	.5730	.1200	172.8	.9108E 03	.1489E 04	.6115	2699	13.195	.2038E-05	.9078	1.045	1268	908	

P=30 psia Pressure = 90 psia

STEAM-WATER DATA

TEST NUMBER	MIXING WATER THERMOCOUPLE READING (millivolts)	ORIFICE MANOMETER READING (in.Hg.)	ROTOMETER READING (% SCALE)	LVDT VOLTAGE (volts)	ZERO VOLTAGE (volts)	MIXING WATER TEMPERATURE (°F)	MIXING WATER FLOW RATE (lbm/hr)	MIXING STEAM FLOW RATE (lbm/hr)	QUALITY	MASS VELOCITY (lbm/hr in^2)	FORCE ON TEE (lbf)	MOMENTUM MULTIPLIER (lbf hr^2 in^2/lbm^2)	YK	ZK	ENTRAINMENT CORRELATION FACTOR (ft/sec)	HOMOGENEOUS VELOCITY (ft-sec)
234	3.740	7.90	39.00	.8000	.1200	191.3	.1076E 04	.1498E 04	.5766	2895	19.808	.2657E-05	.0826	1.525	1283	919
235	3.950	7.70	44.00	.8230	.1200	199.5	.1214E 04	.1479E 04	.5445	3029	20.478	.2510E-05	.0761	1.607	1268	908
236	2.760	7.70	26.40	.7240	.1200	152.2	.7286E 03	.1479E 04	.6597	2483	17.594	.3209E-05	-.0864	1.422	1258	901
237	1.930	7.70	20.00	.6860	.1200	117.6	.5520E 03	.1479E 04	.7161	2284	16.487	.3553E-05	-.2012	1.343	1257	900
238	.800	7.60	14.00	.6480	.1200	68.3	.3864E 03	.1470E 04	.7800	2087	15.380	.3970E-05	-.4573	1.271	1251	896
239	.440	11.95	13.20	.8520	.1200	52.1	.3643E 03	.1837E 04	.8296	2475	21.322	.3914E-05	.0618	1.111	1577	1129
240	1.340	11.80	17.50	.8790	.1200	92.2	.4830E 03	.1825E 04	.7840	2596	22.109	.3689E-05	.0595	1.169	1563	1120
241	3.240	11.90	30.30	.9280	.1200	171.6	.8363E 03	.1833E 04	.6852	3002	23.536	.2937E-05	.3839	1.209	1580	1132
TEMP= 320.27 PRESS= 90.00																
242	7.070	3.04	68.60	.2900	.1270	315.1	.1893E 04	.9330E 03	.3309	3179	4.748	.5285E-06	.1099	2.167	486	208
243	7.090	2.81	80.80	.3100	.1270	315.8	.2230E 04	.8972E 03	.2874	3517	5.331	.4846E-06	.0191	2.526	467	200
244	7.090	2.78	90.00	.3220	.1270	315.8	.2484E 04	.8924E 03	.2644	3797	5.680	.4430E-06	.0300	2.654	465	199
245	7.090	2.73	98.50	.3100	.1270	315.8	.2719E 04	.8844E 03	.2452	4052	5.331	.3651E-06	.1991	2.475	460	197
246	7.070	2.76	55.00	.2680	.1270	315.1	.1518E 04	.8893E 03	.3710	2707	4.107	.6302E-06	.0028	2.117	463	198
247	7.040	2.78	39.80	.2390	.1270	314.1	.1098E 04	.8924E 03	.4508	2239	3.262	.7318E-06	.0979	1.737	464	199
248	6.950	2.79	25.00	.2120	.1270	310.8	.6900E 03	.8940E 03	.5678	1782	2.476	.8774E-06	.2673	1.363	465	199
249	6.700	2.79	9.00	.1830	.1270	301.9	.2484E 03	.8940E 03	.7892	1285	1.631	.1111E-05	1.6382	.927	465	199
250	7.010	7.40	38.00	.3760	.1270	313.0	.1049E 04	.1450E 04	.5852	2811	7.253	.1032E-05	-.1303	1.517	756	323
251	7.080	7.40	53.00	.4200	.1280	315.5	.1463E 04	.1450E 04	.5022	3276	8.506	.8911E-06	-.1146	1.737	757	323
252	7.100	7.40	70.00	.4720	.1290	316.2	.1932E 04	.1450E 04	.4323	3804	9.991	.7765E-06	-.1225	1.988	757	324
253	7.150	7.40	82.00	.5080	.1290	318.0	.2263E 04	.1450E 04	.3945	4177	11.040	.7118E-06	-.1209	2.145	759	325
254	6.190	7.20	87.00	.5050	.1300	283.4	.2401E 04	.1431E 04	.3527	4310	10.923	.6614E-06	-.1864	2.428	701	300
255	6.120	7.20	21.80	.3210	.1300	280.8	.6017E 03	.1431E 04	.7008	2286	5.564	.1197E-05	-.0457	1.253	735	314
256	5.710	7.20	8.90	.2830	.1300	265.8	.2456E 03	.1431E 04	.8566	1886	4.457	.1410E-05	.8589	1.005	741	317
257	6.340	12.00	38.00	.4870	.1310	288.9	.1049E 04	.1840E 04	.6332	3249	10.370	.1105E-05	-.1117	1.400	945	404
258	6.190	12.10	54.90	.5420	.1320	283.4	.1515E 04	.1848E 04	.5386	3782	11.943	.9388E-06	-.0770	1.609	936	400
259	6.150	11.90	70.00	.5960	.1330	281.9	.1932E 04	.1833E 04	.4716	4234	13.487	.8460E-06	-.1323	1.850	919	393
260	6.510	11.90	83.00	.6420	.1340	295.0	.2291E 04	.1833E 04	.4350	4638	14.798	.7737E-06	-.1012	1.958	929	397
261	6.180	12.00	23.90	.4380	.1350	283.0	.6596E 03	.1840E 04	.7355	2812	8.826	.1256E-05	-.0521	1.198	949	406
262	5.720	12.10	11.20	.3880	.1360	266.2	.3091E 03	.1848E 04	.8601	2426	7.341	.1403E-05	1.2860	.992	957	409
263	6.340	15.80	43.00	.5950	.1370	288.9	.1187E 04	.2106E 04	.6359	3703	13.341	.1094E-05	-.0599	1.376	1081	462
264	5.670	15.60	61.00	.6450	.1380	264.3	.1684E 04	.2093E 04	.5339	4247	14.768	.9208E-06	-.0460	1.604	1042	445
265	6.370	15.40	83.00	.7300	.1390	290.0	.2291E 04	.2080E 04	.4647	4915	17.215	.8014E-06	-.0363	1.800	1051	449
266	5.820	15.90	26.00	.5300	.1400	269.9	.7176E 03	.2112E 04	.7426	3183	11.360	.1261E-05	-.0223	1.182	1084	463
267	4.670	15.90	13.00	.4700	.1400	227.0	.3588E 03	.2112E 04	.8517	2779	9.613	.1400E-05	.7722	1.009	1085	464
TEMP= 341.25 PRESS= 120.00																
268	7.660	2.20	79.90	.2315	.1220	336.0	.2205E 04	.7944E 03	.2627	3374	3.190	.3152E-06	.1307	2.390	359	134
269	7.700	2.37	99.10	.2510	.1220	337.4	.2735E 04	.8243E 03	.2302	4003	3.758	.2637E-06	.1929	2.463	374	140
270	7.650	2.36	60.00	.2160	.1220	335.7	.1656E 04	.8226E 03	.3305	2788	2.738	.3963E-06	.1405	2.058	372	139
271	7.600	2.36	39.10	.1930	.1220	333.9	.1079E 04	.8226E 03	.4315	2139	2.068	.5084E-06	.1996	1.664	371	138
272	7.490	2.36	23.40	.1760	.1220	330.0	.6458E 03	.8226E 03	.5594	1652	1.573	.6486E-06	.3163	1.329	371	138
273	7.180	2.36	9.10	.1590	.1220	319.1	.2512E 03	.8226E 03	.7668	1208	1.078	.8311E-06	1.4520	.944	371	138
274	7.450	5.95	29.00	.2590	.1220	328.6	.8004E 03	.1302E 04	.6191	2365	3.991	.8027E-06	-.0153	1.363	587	219
275	7.570	5.90	43.50	.2920	.1220	332.9	.1201E 04	.1297E 04	.5191	2809	4.952	.7060E-06	-.1415	1.658	585	218
276	7.660	5.95	60.80	.3250	.1230	336.0	.1678E 04	.1302E 04	.4373	3352	5.884	.5891E-06	-.0890	1.883	590	220
277	7.700	5.90	72.00	.3520	.1230	337.4	.1987E 04	.1297E 04	.3956	3693	6.671	.5500E-06	-.1472	2.097	588	219
278	7.700	5.90	93.00	.3930	.1240	337.4	.2567E 04	.1297E 04	.3356	4345	7.836	.4668E-06	-.1282	2.362	589	220
279	7.250	6.00	8.80	.2220	.1240	321.5	.2429E 03	.1308E 04	.8471	1744	2.855	.1056E-05	1.3148	.992	591	220
280	6.790	8.80	29.90	.3140	.1250	305.1	.8252E 03	.1580E 04	.6483	2705	5.505	.8462E-06	-.0477	1.319	703	262
281	7.260	8.20	49.90	.3500	.1250	321.9	.1377E 04	.1526E 04	.5196	3265	6.554	.6914E-06	-.0796	1.621	681	254
282	7.450	8.10	67.30	.3880	.1260	328.6	.1857E 04	.1517E 04	.4454	3795	7.632	.5960E-06	-.0757	1.844	680	254
283	7.650	8.10	90.80	.4450	.1260	335.7	.2506E 04	.1517E 04	.3763	4524	9.292	.5106E-06	-.0898	2.124	686	256
284	5.180	8.40	10.00	.2690	.1270	246.1	.2760E 03	.1544E 04	.8391	2047	4.136	.1110E-05	-.8025	1.062	687	256
285	6.920	13.20	31.20	.3920	.1280	309.8	.8611E 03	.1928E 04	.6861	3137	7.690	.8786E-06	.0386	1.232	863	322
286	7.300	13.00	49.90	.4400	.1280	323.3	.1377E 04	.1914E 04	.5780	3702	9.088	.7459E-06	.0033	1.439	858	320
287	7.500	12.70	67.20	.4910	.1290	330.4	.1855E 04	.1892E 04	.5032	4214	10.545	.6678E-06	-.0678	1.660	852	318
288	7.410	12.60	89.90	.5540	.1300	327.2	.2481E 04	.1885E 04	.4263	4911	12.351	.5760E-06	-.0934	1.927	842	314
289	4.590	13.60	17.70	.3620	.1300	223.9	.4885E 03	.1957E 04	.7802	2750	6.758	.1005E-05	.0104	1.105	859	320
290	6.450	13.90	9.20	.3390	.1310	292.9	.2539E 03	.1978E 04	.8876	2510	6.059	.1082E-05	-2.9663	.929	891	332
291	6.350	18.30	31.30	.4730	.1320	289.2	.8639E 03	.2262E 04	.7133	3515	9.933	.9040E-06	.1062	1.178	1005	375
292	6.980	17.50	48.50	.5220	.1330	311.9	.1339E 04	.2213E 04	.6158	3995	11.331	.7986E-06	-.0163	1.370	986	368

Pressure = 120 psia

Pressure = 90 psia

P = 30 psia

STEAM-WATER DATA

TEST NUMBER	MIXING WATER THERMOCOUPLE READING (millivolts)	ORIFICE MANOMETER READING (in. Hg.)	ROTOMETER READING (% scale)	LVDT VOLTAGE (volts)	ZERO VOLTAGE (volts)	MIXING WATER TEMPERATURE (°F)	MIXING WATER FLOW RATE (lbm/hr)	MIXING STEAM FLOW RATE (lbm/hr)	QUALITY	MASS VELOCITY (lbm/hr in^2)	FORCE ON TEE (lbf)	MOMENTUM MULTIPLIER (lbf hr^2 in^2/lbm^2)	YK	ZK	ENTRAINMENT CORRELATION FACTOR (ft/sec)	HOMOGENOUS VELOCITY (ft/sec)	
293	6.900	17.40	72.00	.5920	.1340	309.1	.1987E 04	.2207E 04	.5132	4717	13.341	.6743E-06	-.0428	1.617	972	363	
294	7.200	16.80	81.00	.6400	.1350	319.8	.2236E 04	.2170E 04	.4842	4954	14.710	.6740E-06	-.1886	1.796	964	360	
295	5.950	18.70	20.00	.4440	.1350	274.6	.5520E 03	.2286E 04	.7975	3192	9.001	.9938E-06	.4308	1.048	1019	380	
D=	1.0640	1198.000000		2.280000													
TEMP=	250.33	PRESS=	30.00														
296	5.220	7.00	80.80	.1640	.1080	247.6	.2230E 04	.2159E 03	.0888	2751	1.631	.2424E-06	.5166	3.475	190	136	
297	5.220	7.00	99.00	.1740	.1080	247.6	.2732E 04	.2159E 03	.0732	3316	1.923	.1967E-06	.5216	3.685	189	136	
298	5.220	7.00	59.90	.1520	.1080	247.6	.1653E 04	.2159E 03	.1171	2102	1.282	.3262E-06	.5152	3.102	191	137	
299	5.180	7.00	40.10	.1390	.1080	246.1	.1107E 04	.2159E 03	.1653	1488	.903	.4590E-06	.5448	2.514	190	136	
300	5.120	7.00	22.00	.1240	.1080	243.9	.6072E 03	.2159E 03	.2666	926	.466	.6117E-06	.7708	1.471	190	136	
301	5.000	7.00	8.20	.1120	.1080	239.4	.2263E 03	.2159E 03	.4998	497	.117	.5298E-06	1.7590	.400	191	137	
302	5.080	14.10	24.90	.1510	.1080	242.4	.6872E 03	.3047E 03	.3123	1116	1.253	.1132E-05	.3800	2.046	268	192	
303	5.140	14.20	39.90	.1700	.1080	244.6	.1101E 04	.3057E 03	.2204	1582	1.806	.8112E-06	.3179	2.728	269	193	
304	5.200	14.30	60.00	.1930	.1080	246.9	.1656E 04	.3068E 03	.1588	2207	2.476	.5714E-06	.3187	3.345	271	194	
305	5.220	14.40	79.80	.2165	.1080	247.6	.2202E 04	.3078E 03	.1245	2823	3.161	.4459E-06	.3126	3.856	272	195	
306	5.240	14.40	99.00	.2320	.1080	248.4	.2732E 04	.3078E 03	.1030	3419	3.612	.3475E-06	.3602	4.011	273	196	
307	5.250	20.30	98.90	.2720	.1080	248.7	.2730E 04	.3638E 03	.1203	3479	4.777	.4439E-06	.2841	4.046	324	232	
308	5.220	20.30	80.90	.1515	.1080	247.6	.2233E 04	.3638E 03	.1427	2920	1.267	.1671E-06	.9562	1.164	322	231	
309	5.220	20.30	61.90	.2260	.1080	247.6	.1708E 04	.3638E 03	.1795	2331	3.437	.7117E-06	.2243	3.399	323	231	
310	5.130	20.50	39.80	.1935	.1080	244.3	.1098E 04	.3656E 03	.2538	1647	2.491	.1033E-05	.2127	2.711	322	231	
311	5.110	20.40	21.70	.1630	.1080	243.5	.5989E 03	.3647E 03	.3875	1084	1.602	.1534E-05	.3029	1.865	323	231	
312	4.980	20.40	9.00	.1400	.1090	238.6	.2484E 03	.3647E 03	.6112	690	.903	.2136E-05	.8033	1.097	324	232	
313	4.870	30.30	13.90	.1710	.1080	234.5	.3836E 03	.4411E 03	.5462	928	1.835	.2399E-05	.1921	1.527	389	279	
314	5.100	30.50	24.40	.1930	.1080	243.1	.6734E 03	.4425E 03	.4061	1255	2.476	.1768E-05	.1583	1.970	392	281	
315	5.190	30.60	39.90	.2270	.1080	246.5	.1101E 04	.4432E 03	.2944	1737	3.466	.1292E-05	.1209	2.601	394	282	
316	5.230	30.70	58.50	.2625	.1080	248.0	.1615E 04	.4439E 03	.2214	2315	4.500	.9444E-06	.1473	3.150	395	283	
317	5.260	30.70	79.90	.3025	.1080	249.1	.2205E 04	.4439E 03	.1725	2979	5.666	.7178E-06	.1687	3.665	397	284	
318	5.280	30.80	91.30	.3200	.1080	249.9	.2520E 04	.4446E 03	.1549	3334	6.175	.6248E-06	.2005	3.810	399	286	
D=	.6250	1198.000000		2.280000													
TEMP=	212.00	PRESS=	14.70														
319	3.480	4.85	9.00	.1680	.1020	181.1	.2484E 03	.1800E 03	.4223	1396	1.923	.3214E-05	.3330	1.771	633	633	
320	.480	8.55	13.20	.2120	.1020	54.0	.3643E 03	.2383E 03	.3163	1964	3.204	.2707E-05	.1193	2.576	667	667	
321	.480	13.85	11.20	.2570	.1020	54.0	.3091E 03	.3020E 03	.4360	1992	4.515	.3709E-05	.1563	1.923	932	932	
322	.470	19.90	10.00	.3000	.1020	53.5	.2760E 03	.3603E 03	.5232	2074	5.768	.4370E-05	.2253	1.597	1164	1164	
323	.470	26.55	8.00	.3330	.1020	53.5	.2208E 03	.4141E 03	.6274	2069	6.729	.5121E-05	.3588	1.316	1392	1392	
324	.470	33.10	8.00	.3760	.1020	53.5	.2208E 03	.4601E 03	.6559	2219	7.981	.5282E-05	.4320	1.245	1561	1561	
325	.450	33.60	21.00	.4270	.1020	52.6	.5796E 03	.4633E 03	.3747	3399	9.467	.2670E-05	.3956	1.847	1367	1367	
326	.450	23.60	20.00	.4240	.1020	52.6	.5520E 03	.3913E 03	.3390	3075	9.380	.3234E-05	-.0476	2.702	1119	1119	
327	.490	21.60	24.90	.3290	.1020	54.4	.6872E 03	.3749E 03	.2652	3462	6.612	.1798E-05	.3883	2.373	986	986	
328	.470	11.50	28.80	.2330	.1020	53.5	.7949E 03	.2757E 03	.1488	3490	3.816	.1021E-05	.3247	3.777	559	559	
329	.450	11.20	33.00	.2080	.1020	52.6	.9108E 03	.2722E 03	.1148	3856	3.088	.6769E-06	.4376	3.873	477	477	
330	.450	12.80	32.00	.2140	.1020	52.6	.8832E 03	.2906E 03	.1360	3826	3.262	.7265E-06	.5209	3.131	560	560	
331	.460	22.80	26.50	.3590	.1020	53.0	.7314E 03	.3848E 03	.2543	3638	7.486	.1843E-05	.3107	2.627	994	994	
332	.470	33.10	22.00	.4290	.1023	53.5	.6072E 03	.4601E 03	.3592	3479	9.516	.2563E-05	.3839	1.920	1341	1341	
333	.480	33.40	31.00	.4360	.1026	54.0	.8556E 03	.4620E 03	.2620	4295	9.712	.1716E-05	.4226	2.315	1209	1209	
334	.480	23.00	40.80	.4280	.1030	54.0	.1126E 04	.3865E 03	.1467	4930	9.467	.1270E-05	.0851	4.810	778	778	
TEMP=	250.33	PRESS=	30.00														
335	.640	23.70	10.30	.2385	.1120	61.2	.2843E 03	.3921E 03	.5162	2205	3.685	.2471E-05	-.0170	1.752	875	626	
336	.640	31.50	9.90	.2705	.1120	61.2	.2732E 03	.4494E 03	.5683	2355	4.617	.2713E-05	-.0123	1.601	1029	737	
337	.640	12.10	11.00	.1800	.1120	61.2	.3036E 03	.2827E 03	.3956	1911	1.981	.1768E-05	.1105	2.069	581	416	
338	.640	8.20	10.00	.1565	.1120	61.2	.2760E 03	.2334E 03	.3660	1660	1.296	.1532E-05	.2083	2.072	468	335	
339	.610	5.45	21.10	.1270	.1118	59.8	.5824E 03	.1907E 03	.1034	2520	.443	.2273E-06	.6573	2.609	202	145	
340	.570	10.60	21.20	.1720	.1116	58.0	.5851E 03	.2649E 03	.1824	2771	1.759	.7471E-06	.1888	3.472	390	279	
341	.550	18.50	20.00	.2270	.1114	57.1	.5520E 03	.3478E 03	.2747	2933	3.367	.1276E-05	.0373	2.908	621	444	
342	.530	24.30	19.70	.2600	.1112	56.2	.5437E 03	.3968E 03	.3181	3066	4.334	.1503E-05	.0115	2.629	751	538	
343	.510	32.90	19.90	.3040	.1110	55.3	.5492E 03	.4587E 03	.3588	3285	5.622	.1698E-05	.0093	2.381	907	650	
344	.490	32.90	29.20	.3105	.1108	54.4	.8059E 03	.4587E 03	.2434	4122	5.817	.1116E-05	.0544	3.154	773	554	
345	.470	25.20	31.80	.2580	.1105	53.5	.8777E 03	.4039E 03	.1835	4177	4.297	.8026E-06	.1113	3.693	592	424	
346	.460	18.30	30.00	.2160	.1102	53.0	.8280E 03	.3460E 03	.1577	3827	3.082	.6860E-06	.1158	4.061	466	334	
347	.450	11.60	32.80	.1480	.1100	52.6	.9053E 03	.2769E 03	.0821	3853	1.107	.2430E-06	.4570	3.893	246	176	
TEMP=	292.71	PRESS=	60.00														

P=120

Pressure=30psia

Pressure=14.7psia

Diameter=0.625in.

Pressure=30psia

STEAM-WATER DATA

TEST NUMBER	MIXING WATER THERMOCOUPLE READING (millivolts)	ORIFICE MANOMETER READING (in. Hg.)	ROTOMETER READING (% scale)	LVDT VOLTAGE (volts)	ZERO VOLTAGE (volts)	MIXING WATER TEMPERATURE (°F)	MIXING WATER FLOW RATE (lbm/hr)	MIXING STEAM FLOW RATE (lbm/hr)	QUALITY	MASS VELOCITY (lbm/hr in.^{2})	FORCE ON TEE (lbf)	MOMENTUM MULTIPLIER (lbf hr^{2}in^2/lbm^2)	YK	ZK	ENTRAINMENT CORRELATION FACTOR (ft/sec)	HOMOGENOUS VELOCITY (ft/sec)	
348	5.350	15.00	10.00	.1690	.1220	252.5	.2760E 03	.3140E 03	.5234	1923	1.369	.1207E-05	.1819	1.533	560	290	
349	5.450	20.50	8.50	.1790	.1220	256.2	.2346E 03	.3656E 03	.6070	1956	1.660	.1414E-05	.1977	1.360	660	341	
350	.830	28.00	9.00	.1910	.1220	69.7	.2484E 03	.4248E 03	.5547	2194	2.010	.1361E-05	.0330	1.551	676	350	
351	.760	32.60	9.00	.2015	.1220	66.6	.2484E 03	.4567E 03	.5747	2298	2.316	.1429E-05	-.0047	1.524	734	380	
352	.670	33.30	19.40	.2130	.1220	62.5	.5354E 03	.4614E 03	.3374	3249	2.651	.8184E-06	.0442	2.317	611	316	
353	.550	20.70	21.80	.1774	.1220	57.1	.6017E 03	.3673E 03	.2269	3158	1.614	.5273E-06	.1016	2.954	401	207	
354	.540	12.70	20.20	.1475	.1220	56.7	.5575E 03	.2895E 03	.1788	2761	.743	.3177E-06	.3989	2.617	277	143	
D=	.6250	1198.000000		2.280000													P = 30 psia
TEMP=	292.71	PRESS=	60.00														
355	6.300	3.70	49.50	.1235	.0723	287.4	.1366E 04	.1574E 03	.1004	4966	1.491	.1971E-06	.2825	3.769	283	146	
356	6.240	3.70	40.00	.1185	.0723	285.2	.1104E 04	.1574E 03	.1204	4111	1.346	.2595E-06	.1862	3.866	279	145	
357	6.190	3.55	30.00	.1105	.0723	283.4	.8280E 03	.1542E 03	.1519	3201	1.113	.3539E-06	.0959	3.750	273	141	
358	6.130	3.55	21.00	.1010	.0723	281.2	.5796E 03	.1542E 03	.2048	2392	.836	.4763E-06	.0996	3.155	274	142	
359	6.000	3.45	16.00	.0960	.0723	276.5	.4416E 03	.1520E 03	.2485	1935	.690	.6011E-06	.0466	2.890	269	139	
360	5.920	3.60	12.00	.0900	.0723	273.5	.3312E 03	.1553E 03	.3119	1586	.516	.6684E-06	.2314	2.173	276	143	
361	5.620	3.55	8.00	.0858	.0723	262.5	.2208E 03	.1542E 03	.4008	1222	.393	.8580E-06	.2691	1.783	273	141	
362	5.980	2.05	23.10	.0900	.0720	275.7	.6376E 03	.1173E 03	.1432	2461	.524	.2823E-06	.2838	3.268	198	103	
362	5.980	2.05	23.10	.0900	.0710	275.7	.6376E 03	.1173E 03	.1432	2461	.553	.2979E-06	.2264	3.450	198	103	
363	6.200	2.05	32.10	.0952	.0720	283.8	.8860E 03	.1173E 03	.1109	3270	.676	.2060E-06	.3367	3.441	205	106	
363	6.200	2.05	32.10	.0952	.0710	283.8	.8860E 03	.1173E 03	.1109	3270	.705	.2148E-06	.2964	3.589	205	106	
364	6.300	2.13	44.00	.1015	.0720	287.4	.1214E 04	.1196E 03	.0864	4348	.859	.1481E-06	.4042	3.443	214	111	
364	6.300	2.13	44.00	.1015	.0710	287.4	.1214E 04	.1196E 03	.0864	4348	.888	.1532E-06	.3757	3.560	214	111	
365	6.320	2.13	60.60	.1090	.0720	288.1	.1673E 04	.1196E 03	.0635	5842	1.078	.1029E-06	.4514	3.444	213	110	
365	6.320	2.13	60.60	.1090	.0710	288.1	.1673E 04	.1196E 03	.0635	5842	1.107	.1057E-06	.4305	3.537	213	110	
366	6.120	2.15	16.10	.0868	.0720	280.8	.4444E 03	.1202E 03	.2073	1840	.431	.4150E-06	.2839	2.695	214	111	
366	6.120	2.15	16.10	.0868	.0710	280.8	.4444E 03	.1202E 03	.2073	1840	.460	.4431E-06	.2070	2.877	214	111	
367	5.920	2.15	11.50	.0821	.0720	273.5	.3174E 03	.1202E 03	.2655	1426	.294	.4714E-06	.4440	2.027	211	109	
367	5.920	2.15	11.50	.0821	.0710	273.5	.3174E 03	.1202E 03	.2655	1426	.323	.5181E-06	.3354	2.227	211	109	
368	5.800	2.15	8.00	.0792	.0720	269.1	.2208E 03	.1202E 03	.3435	1111	.210	.5535E-06	.6150	1.518	213	110	
368	5.800	2.15	8.00	.0792	.0710	269.1	.2208E 03	.1202E 03	.3435	1111	.239	.6303E-06	.4583	1.729	213	110	
369	6.140	7.20	30.00	.1370	.0710	281.6	.8280E 03	.2189E 03	.2041	3412	1.923	.5382E-06	-.0768	3.586	390	202	
370	6.100	7.15	21.10	.1210	.0710	280.1	.5824E 03	.2181E 03	.2685	2609	1.456	.6973E-06	-.0637	2.939	391	202	
371	6.010	7.25	13.50	.1085	.0710	276.8	.3726E 03	.2196E 03	.3682	1930	1.092	.9554E-06	-.0783	2.315	396	205	
372	5.900	7.40	8.70	.0992	.0710	272.8	.2401E 03	.2219E 03	.4796	1506	.821	.1181E-05	.0207	1.765	402	208	
TEMP=	320.27	PRESS=	90.00														
373	6.930	6.75	43.80	.1300	.0795	310.1	.1209E 04	.2120E 03	.1416	4631	1.471	.2235E-06	.1172	3.487	307	131	
374	6.940	6.80	34.50	.1225	.0795	310.5	.9522E 03	.2128E 03	.1763	3797	1.253	.2831E-06	.0925	3.216	312	133	
375	6.840	6.80	24.90	.1140	.0795	306.9	.6872E 03	.2128E 03	.2283	2934	1.005	.3806E-06	.0390	2.895	311	133	
376	6.800	6.75	18.40	.1070	.0795	305.5	.5078E 03	.2120E 03	.2870	2346	.801	.4742E-06	.0513	2.479	311	133	
377	6.630	6.75	11.90	.0990	.0795	299.4	.3284E 03	.2120E 03	.3836	1762	.568	.5966E-06	.1654	1.890	311	133	
378	6.330	6.75	8.10	.0952	.0795	288.5	.2236E 03	.2120E 03	.4753	1420	.457	.7395E-06	.1964	1.594	310	133	
379	6.860	12.50	28.00	.1380	.0790	307.6	.7728E 03	.2872E 03	.2644	3455	1.719	.4692E-06	-.0621	2.811	423	181	
380	6.810	12.60	19.00	.1250	.0790	305.8	.5244E 03	.2883E 03	.3493	2649	1.340	.6223E-06	-.0849	2.323	427	182	
381	6.660	12.67	13.30	.1140	.0790	300.4	.3671E 03	.2891E 03	.4344	2139	1.020	.7264E-06	.0334	1.843	428	183	
382	6.440	12.67	8.00	.1060	.0790	292.5	.2208E 03	.2891E 03	.5615	1662	.786	.9279E-06	.0749	1.472	429	183	
383	6.300	21.30	8.80	.1220	.0790	287.4	.2429E 03	.3724E 03	.5992	2006	1.253	.1015E-05	.0018	1.427	552	236	
384	6.430	21.10	13.00	.1340	.0790	292.1	.3588E 03	.3707E 03	.4998	2378	1.602	.9236E-06	-.2223	1.817	546	234	
385	6.650	21.40	16.70	.1423	.0790	300.1	.4609E 03	.3732E 03	.4412	2719	1.844	.8130E-06	-.1846	2.006	552	236	
386	7.040	2.30	71.80	.1055	.0777	314.1	.1982E 04	.1243E 03	.0533	6864	.810	.5602E-07	.5290	2.724	178	76	
387	7.050	2.25	51.00	.0960	.0777	314.4	.1408E 04	.1229E 03	.0754	4989	.533	.6982E-07	.6088	2.396	180	77	
388	6.940	2.22	30.00	.0887	.0777	310.5	.8280E 03	.1221E 03	.1207	3097	.320	.1089E-06	.6369	2.112	176	75	
389	6.800	2.20	14.30	.0840	.0777	305.5	.3947E 03	.1215E 03	.2260	1683	.184	.2113E-06	.6821	1.633	176	75	
390	6.600	2.14	8.00	.0792	.0777	298.3	.2208E 03	.1199E 03	.3408	1110	.044	.1155E-06	1.4363	.450	175	75	
TEMP=	341.25	PRESS=	120.00														
391	7.350	8.55	37.60	.1210	.0835	325.1	.1038E 04	.2383E 03	.1732	4159	1.092	.2058E-06	.1411	2.941	295	110	
392	7.580	8.60	48.00	.1310	.0835	333.2	.1325E 04	.2390E 03	.1463	5097	1.384	.1736E-06	.1449	3.138	306	114	
393	7.490	8.80	29.50	.1170	.0835	330.0	.8142E 03	.2417E 03	.2209	3442	.976	.2685E-06	.1098	2.673	309	115	
394	7.320	8.55	18.30	.1090	.0835	324.0	.5051E 03	.2383E 03	.3099	2423	.743	.4124E-06	-.0400	2.387	303	113	
395	7.150	8.90	13.00	.1028	.0835	318.0	.3588E 03	.2430E 03	.3914	1962	.562	.4762E-06	.1256	1.850	309	115	
396	6.900	8.90	8.00	.0980	.0835	309.1	.2208E 03	.2430E 03	.5109	1512	.422	.6023E-06	.2365	1.456	310	116	
397	7.340	17.55	31.00	.1415	.0825	324.7	.8556E 03	.3390E 03	.2726	3894	1.719	.3695E-06	-.0649	2.639	430	160	
398	7.290	17.70	19.80	.1265	.0825	323.0	.5465E 03	.3404E 03	.3742	2891	1.282	.4999E-06	-.0578	2.100	436	163	
399	7.170	18.15	12.60	.1160	.0825	318.7	.3478E 03	.3446E 03	.4890	2257	.976	.6245E-06	.0325	1.635	443	165	
400	7.020	18.05	8.30	.1090	.0825	313.4	.2291E 03	.3437E 03	.5924	1867	.772	.7219E-06	.1942	1.331	444	165	
401	7.650	4.00	64.40	.1100	.0800	335.7	.1777E 04	.1636E 03	.0791	6327	.874	.7116E-07	.4490	2.689	211	79	
402	7.620	4.00	46.60	.1025	.0800	334.6	.1286E 04	.1636E 03	.1071	4725	.655	.9567E-07	.4488	2.577	210	78	
403	7.530	3.94	28.00	.0965	.0800	331.4	.7728E 03	.1624E 03	.1658	3048	.481	.1686E-06	.3272	2.564	207	77	
404	7.390	3.95	17.90	.0919	.0800	326.5	.4940E 03	.1626E 03	.2370	2140	.347	.2467E-06	.3192	2.202	206	77	
405	7.240	3.82	12.60	.0887	.0800	321.2	.3478E 03	.1599E 03	.3019	1655	.253	.3017E-06	.4013	1.823	202	75	
406	7.040	3.80	8.50	.0860	.0800	314.1	.2346E 03	.1595E 03	.3896	1285	.175	.3453E-06	.6402	1.352	202	75	
D=	0.	0.		0.													

P = 120 psia P = 90 psia P = 60 psia

AIR - WATER DATA

TEST NUMBER	ORIFICE MANOMETER READING (in. Hg)	ORIFICE AIR DENSITY (lbm/ft^3)	ROTOMETER READING (% scale	LVDT VOLTAGE (volts)	ZERO VOLTAGE (volts)	WATER FLOW RATE (lbm/hr)	AIR FLOW RATE (lbm/hr)	QUALITY	MASS VELOCITY ($lbm/hr\ in^2$)	FORCE ON TEE (lbf)	MOMENTUM MULTIPLIER ($lbf\ hr^2\ in^2/lbm^2$)	YK	ZK	ENTRAINMENT CORRELATING FACTOR (ft/sec)	HOMOGENEOUS VELOCITY (ft/sec)
1	7.20	.2160	63.60	.0825	.0305	-.17554E 04	.92680E 02	.0502	6024	1.515	-.13607E-06	.4810	4.303	232.0	162.5
2	6.30	.2193	79.00	.0915	.0305	.21804E 04	.87426E 02	.0386	7392	1.777	-.10800E-06	.4744	4.477	220.4	154.4
3	8.10	.2102	45.00	.0660	.0305	-.12420E 04	.96897E 02	.0724	4364	1.034	-.17897E-06	.6524	3.534	240.8	168.6
4	9.20	.2098	29.10	.0594	.0305	.80316E 03	.10307E 03	.1137	2954	.842	-.31448E-06	.4859	3.279	254.6	178.3
5	10.00	.2030	15.00	.0485	.0305	-.41400E 03	.10563E 03	.2033	1694	.524	-.59574E-06	.4870	2.413	259.7	181.8
6	11.80	.2295	20.00	.0607	.0295	.55200E 03	.12180B 03	.1808	2196	.909	-.61413E-06	.3385	3.037	299.7	209.8
7	10.30	.2365	40.00	.0720	.0295	-.11040E 04	.11566E 03	.0948	3975	1.238	-.25532E-06	.4970	3.492	286.3	200.5
8	8.90	.2396	61.00	.0880	.0295	.16836E 04	.10835E 03	.0605	5841	1.704	-.16281E-06	.4867	4.105	270.1	189.2
9	10.85	.2327	30.30	.0676	.0295	-.83628E 03	.11770E 03	.1234	3109	1.110	-.37413E-06	.4180	3.440	290.5	203.4
10	12.20	.2290	13.70	.0522	.0295	.37812E 03	.12368E 03	.2465	1636	.661	-.80565E-06	.4079	2.332	303.7	212.7
11	12.65	.2290	8.80	.0442	.0295	-.24288E 03	.12589E 03	.3414	1202	.428	-.96601E-06	.6301	1.554	308.7	216.2
12	15.50	.2677	8.80	.0516	.0292	.24288E 03	.15030E 03	.3823	1282	.652	-.12949E-05	.4559	1.691	368.5	258.0
13	14.20	.2677	22.00	.0735	.0292	-.60720E 03	.14401E 03	.1917	2449	1.290	-.70155E-06	.2655	3.141	354.2	248.0
14	13.20	.2708	39.10	.0896	.0292	.10792E 04	.13976E 03	.1147	3973	1.759	-.36830E-06	.3782	3.742	345.2	241.7
15	11.80	.2770	58.00	.1180	.0292	-.16008E 04	.13379E 03	.0771	5654	2.587	-.26375E-06	.3041	4.031	332.1	232.6
16	11.15	.2870	74.00	.1170	.0292	.20424E 04	.13245E 03	.0609	7089	2.558	-.16589E-06	.4789	4.145	330.2	231.2
17	15.20	.2690	13.00	.0594	.0292	-.35880E 03	.14923E 03	.2937	1656	.880	-.10457E-05	.3370	2.212	366.2	256.4
18	14.60	.2940	39.50	.1000	.0305	.10902E 04	.14934E 03	.0942	5165	2.170	-.26517E-06	.4651	3.660	369.7	258.9
19	13.90	.2940	52.00	.1050	.0305	-.14352E 04	.15297E 03	.1230	4052	2.024	-.40189E-06	.3547	3.711	377.5	264.4
20	14.80	.2880	30.70	.0923	.0305	.84732E 03	.15241E 03	.1524	3259	1.800	-.55259E-06	.2645	3.625	375.4	262.9
21	15.65	.2860	21.70	.0819	.0305	-.59892E 03	.15607E 03	.2067	2461	1.497	-.80586E-06	.1985	3.171	383.7	268.7
22	16.20	.2835	14.60	.0702	.0305	.40296E 03	.15803E 03	.2817	1829	1.156	-.11273E-05	.1836	2.572	387.9	271.6
23	17.20	.2870	8.60	.0570	.0305	-.23736E 03	.16370E 03	.4082	1307	.772	-.14723E-05	.3871	1.701	401.2	281.0
24	16.40	.2910	18.00	.0750	.0305	.49680E 03	.16106E 03	.2448	2144	1.296	-.91890E-06	.2537	2.892	395.6	277.0
25	18.55	.3125	12.00	.0707	.0305	-.33120E 03	.17720E 03	.3485	1657	1.171	-.13899E-05	.2079	2.153	434.5	304.3
26	17.35	.3115	23.00	.0931	.0307	.63480E 03	.17126E 03	.2125	2627	1.818	-.85828E-06	.1571	3.221	420.9	294.7
27	16.80	.3140	30.80	.1040	.0309	.85008E 03	.16927E 03	.1661	3323	2.129	-.62870E-06	.2222	3.583	416.7	291.8
28	16.05	.3230	40.50	.1110	.0311	-.11178E 04	.16790E 03	.1306	4191	2.327	-.43196E-06	.3458	3.634	414.2	290.0
29	16.00	.3560	55.50	.1300	.0313	.15318E 04	.17599E 03	.1031	5567	2.875	-.30243E-06	.4364	3.660	435.2	304.7
30	18.30	.3060	16.00	.0810	.0315	-.44160E 03	.17420E 03	.2829	2007	1.442	-.11666E-05	.1432	2.642	427.5	299.4
31	18.90	.3040	8.00	.0608	.0315	.22080E 03	.17637E 03	.4441	1255	.853	-.18600E-05	.3566	1.638	432.2	302.6

Pipe Diameter = 0.625 in.

ρ_{water} = 62.2 lbm/ft^3

ρ_{air} = 0.076 lbm/ft^3

VOID FRACTION DATA

TEST NUMBER	ORIFICE MANOMETER READING (in.Hg.)	ORIFICE AIR DENSITY (lbm/ft^3)	ROTOMETER READING (% SCALE)	LENGTH FILLED WITH WATER (cm.)	WATER FLOW RATE (lbm/hr)	AIR FLOW RATE (lbm/hr)	MASS VELOCITY (lbm/hr in^2)	QUALITY	α MINIMUM POSSIBLE	α MAXIMUM POSSIBLE
1	5.40	.1620	25.10	6.70	.69277E 03	.69662E 02	1726	.0914	.9107	.9219
2	4.63	.1630	40.00	8.60	.11146E 04	.64757E 02	2646	.0554	.8853	.8959
3	4.30	.1670	50.00	9.90	.13300E 04	.63189E 02	3267	.0438	.8680	.8781
4	3.85	.1685	58.50	9.70	.16146E 04	.60091E 02	3791	.0359	.8707	.8808
5	3.50	.1720	75.00	12.20	.20700E 04	.57910E 02	4817	.0272	.8373	.8466
6	2.90	.1740	91.30	13.70	.25195E 04	.53062E 02	5824	.0206	.8173	.8260
7	2.70	.1750	98.00	15.50	.27148E 04	.51361E 02	6239	.0186	.7933	.8014
8	5.70	.1580	19.90	4.90	.54124E 03	.70663E 02	1403	.1140	.9347	.9466
9	6.10	.1570	10.00	4.40	.27600E 03	.72839E 02	790	.2088	.9413	.9534
10	5.70	.1570	20.00	5.90	.55200E 03	.70439E 02	1409	.1132	.9213	.9329
11	5.25	.1628	30.00	6.70	.82800E 03	.68867E 02	2030	.0768	.9107	.9219
12	8.40	.2080	28.30	4.20	.78108E 03	.98132E 02	1990	.1116	.9440	.9562
13	7.95	.2175	41.20	5.20	.11371E 04	.97657E 02	2795	.0791	.9307	.9425
14	7.10	.2179	50.00	6.70	.13800E 04	.92445E 02	3333	.0628	.9107	.9219
15	6.90	.2225	60.50	7.90	.16698E 04	.92105E 02	3988	.0523	.8947	.9055
16	6.68	.2180	60.70	7.70	.16753E 04	.89725E 02	3995	.0508	.8973	.9082
17	6.60	.2278	70.00	7.50	.19310E 04	.91170E 02	4580	.0451	.9000	.9110
18	6.05	.2255	79.90	8.70	.22012E 04	.86894E 02	5188	.0379	.8840	.8945
19	5.90	.2310	94.00	9.80	.25914E 04	.86860E 02	6069	.0324	.8693	.8795
20	5.70	.2295	94.00	9.60	.25914E 04	.85115E 02	6065	.0318	.8720	.8822
21	8.50	.2065	26.00	3.80	.71710E 03	.98350E 02	1847	.1205	.9493	.9616
22	12.25	.2640	27.50	3.50	.75913E 03	.13304E 03	2019	.1491	.9533	.9658
23	11.80	.2715	40.00	4.40	.11014E 04	.13246E 03	2799	.1071	.9413	.9534
24	10.55	.2690	50.00	5.40	.13810E 04	.12480E 03	3406	.0829	.9280	.9397
25	10.35	.2760	60.80	6.30	.16711E 04	.12523E 03	4082	.0694	.9160	.9274
26	9.43	.2735	71.00	6.90	.19516E 04	.11908E 03	4705	.0573	.9080	.9192
27	9.15	.2810	84.50	8.00	.23312E 04	.11893E 03	5548	.0485	.8933	.9041
28	8.50	.2830	95.50	7.50	.26318E 04	.11509E 03	6227	.0418	.9000	.9110
29	10.70	.3100	88.00	7.00	.24218E 04	.13489E 03	5803	.0526	.9067	.9178
30	11.00	.2970	66.00	5.60	.18216E 04	.13384E 03	4426	.0684	.9253	.9370
31	1.36	.1447	99.90	26.80	.27572E 04	.33260E 02	6316	.0119	.6427	.6466
32	1.74	.1428	80.00	19.50	.22080E 04	.37334E 02	5082	.0166	.7400	.7486
33	2.32	.1398	58.00	14.20	.16008E 04	.42604E 02	3720	.0259	.8107	.8192
34	1.17	.1202	61.00	19.20	.16836E 04	.28154E 02	3875	.0164	.7440	.7507
35	.83	.1212	79.00	22.20	.21804E 04	.23851E 02	4989	.0108	.7040	.7096
36	.55	.1248	97.30	27.00	.26855E 04	.19742E 02	6123	.0073	.6400	.6438

APPENDIX F

DATA OF VANCE

VANCE'S DATA, STEAM-WATER

TEST NUMBER	WATER SPECIFIC VOLUME (ft^3/lbm)	STEAM SPECIFIC VOLUME (ft^3/lbm)	MASS VELOCITY (lbm/hr ft^2)	FORCE (lbf)	QUALITY	MOMENTUM MULTIPLIER (lbf hr^2 in^2/lbm^2)	MINIMUM MOMENTUM MULTIPLIER	HOMOGENEOUS MOMENTUM MULTIPLIER	YK	ZK	HOMOGENEOUS VELOCITY/25 (ft/sec)	ENTRAINMENT CORRELATING FACTOR/25 (ft/sec)
1	.0176	5.4720	293.4100	10.5440	.5246	.9803E-06	.5748E-06	.9942E-06	.3306E-01	.1706E 01	.3379E 02	.7477E 02
2	.0176	5.4720	295.6900	6.8220	.3979	.6245E-06	.3527E-06	.7555E-06	.3252E 00	.1771E 01	.2588E 02	.5726E 02
3	.0176	5.5370	297.3400	7.4810	.4168	.6773E-06	.3866E-06	.8006E-06	.2979E 00	.1752E 01	.2757E 02	.6066E 02
4	.0176	5.4720	290.4400	5.4530	.3244	.5174E-06	.2486E-06	.6172E-06	.2708E 00	.2081E 01	.2076E 02	.4595E 02
5	.0172	9.0250	295.0000	19.4030	.6416	.1785E-05	.1347E-05	.2002E-05	.3317E 00	.1325E 01	.6841E 02	.1179E 03
6	.0173	8.6780	297.3800	15.6000	.5357	.1412E-05	.9277E-06	.1608E-05	.2884E 00	.1522E 01	.5539E 02	.9734E 02
7	.0173	8.5150	196.1200	10.7400	.7431	.2235E-05	.1675E-05	.2187E-05	.9432E-01	.1335E 01	.4967E 02	.8812E 02
8	.0173	8.5150	199.3400	12.2000	.8090	.2457E-05	.1966E-05	.2380E-05	.1868E 00	.1250E 01	.5495E 02	.9749E 02
9	.0173	8.5150	297.3800	12.1300	.4287	.1098E-05	.6073E-06	.1264E-05	.2530E 00	.1808E 01	.4354E 02	.7724E 02
10	.0173	8.5150	294.9900	8.3880	.3311	.7715E-06	.3837E-06	.9776E-06	.3470E 00	.2011E 01	.3340E 02	.5926E 02
11	.0171	10.7500	293.7300	14.6400	.4353	.1358E-05	.7782E-06	.1619E-05	.3105E 00	.1745E 01	.5509E 02	.8699E 02
12	.0173	8.5150	197.3000	5.5360	.4377	.1138E-05	.6306E-06	.1291E-05	.2308E 00	.1805E 01	.2949E 02	.5232E 02
13	.0173	8.3590	398.1800	20.2240	.4248	.1021E-05	.5872E-06	.1230E-05	.3250E 00	.1739E 01	.5672E 02	.1016E 03
14	.0172	8.8480	416.3900	26.7500	.4422	.1235E-05	.6658E-06	.1354E-05	.1735E 00	.1855E 01	.6532E 02	.1137E 03
15	.0174	7.1750	289.7600	10.3970	.4440	.9911E-06	.5506E-06	.1104E-05	.2034E 00	.1800E 01	.3704E 02	.7158E 02
16	.0175	3.8160	295.6100	8.5900	.4209	.7711E-06	.2790E-06	.5582E-06	.7627E 00	.2763E 01	.1931E 02	.5116E 02
17	.0168	23.0000	287.9000	9.3090	.2365	.8989E-06	.5249E-06	.1883E-05	.7245E 00	.1712E 01	.6278E 02	.6777E 02
17	.0169	16.3030	287.9000	7.5460	.2262	.7287E-06	.3550E-06	.1278E-05	.5950E 00	.2053E 01	.4261E 02	.5463E 02
18	.0170	14.6530	423.0800	14.8990	.2273	.6662E-06	.3257E-06	.1156E-05	.5897E 00	.2046E 01	.5663E 02	.7656E 02
19	.0171	11.2940	321.6300	24.4580	.6150	.1892E-05	.1548E-05	.2401E-05	.5961E 00	.1223E 01	.8944E 02	.1378E 03
20	.0169	16.3030	234.1400	23.6840	.8300	.3458E-05	.3930E-05	.4674E-05	.1634E 01	.8799E 00	.1268E 03	.1625E 03
21	.0169	16.5000	243.1400	25.1600	.8100	.3406E-05	.3795E-05	.4617E-05	.1473E 01	.8976E 00	.1300E 03	.1657E 03
22	.0173	8.5150	301.5700	4.9950	.2113	.4396E-06	.1791E-06	.6260E-06	.4171E 00	.2454E 01	.2187E 02	.3879E 02
22	.0173	8.5150	305.5800	4.9520	.2067	.4245E-06	.1728E-06	.6125E-06	.4277E 00	.2456E 01	.2168E 02	.3846E 02
23	.0173	8.5150	297.8900	11.7750	.4229	.1062E-05	.5926E-06	.1247E-05	.2827E 00	.1792E 01	.4303E 02	.7634E 02
24	.0173	8.5150	399.0700	7.2010	.2157	.3619E-06	.1853E-06	.6389E-06	.6106E 00	.1954E 01	.2953E 02	.5239E 02
25	.0173	8.3590	499.8600	11.1370	.2129	.3568E-06	.1785E-06	.6192E-06	.5955E 00	.1979E 01	.3585E 02	.6419E 02
26	.0173	8.5150	400.4900	18.0750	.4209	.9020E-06	.5875E-06	.1241E-05	.5188E 00	.1535E 01	.5757E 02	.1021E 03
27	.0173	8.5150	496.4600	5.0060	.1045	.1626E-06	.6172E-07	.3128E-06	.5983E 00	.2634E 01	.1799E 02	.3191E 02
28	.0170	13.7460	399.0500	4.3890	.1061	.2206E-06	.8983E-07	.5090E-06	.6880E 00	.2456E 01	.2353E 02	.3285E 02
29	.0170	13.7460	598.2300	3.5910	.0496	.8031E-07	.3270E-07	.2408E-06	.7712E 00	.2456E 01	.1669E 02	.2330E 02
30	.0172	10.2580	699.5300	3.7660	.0484	.6160E-07	.2701E-07	.1771E-06	.7695E 00	.2281E 01	.1435E 02	.2319E 02
31	.0173	8.5150	497.6000	2.2800	.0580	.7370E-07	.2967E-07	.1763E-06	.6996E 00	.2484E 01	.1016E 02	.1802E 02
32	.0173	8.5150	396.2700	1.4000	.0611	.7136E-07	.3141E-07	.1852E-06	.7401E 00	.2272E 01	.8498E 01	.1508E 02
33	.0173	8.5150	801.3500	5.1600	.0503	.6432E-07	.2547E-07	.1535E-06	.6967E 00	.2525E 01	.1425E 02	.2528E 02
34	.0173	8.5150	397.2400	3.5900	.1123	.1821E-06	.6817E-07	.3355E-06	.5738E 00	.2671E 01	.1544E 02	.2738E 02
35	.0173	8.3590	797.6600	11.7300	.1061	.1476E-06	.6220E-07	.3118E-06	.6580E 00	.2372E 01	.2880E 02	.5157E 02
36	.0173	8.4000	297.6200	2.0900	.1163	.1889E-06	.7096E-07	.3427E-06	.5662E 00	.2661E 01	.1181E 02	.2110E 02
37	.0170	13.5000	298.8700	7.7500	.2215	.6945E-06	.2894E-06	.1037E-05	.4584E 00	.2400E 01	.3591E 02	.5059E 02
38	.0170	13.3300	402.5900	12.4300	.2188	.6138E-06	.2801E-06	.1012E-05	.5438E 00	.2191E 01	.4717E 02	.6689E 02
39	.0170	13.7000	400.1800	2.1700	.0603	.1085E-06	.4128E-07	.2908E-06	.7308E 00	.2627E 01	.1348E 02	.1885E 02
40	.0176	5.4720	296.6400	3.6100	.2210	.3284E-06	.1329E-06	.4224E-06	.3248E 00	.2471E 01	.1451E 02	.3212E 02
41	.0173	8.5150	398.1300	.7000	.0212	.3535E-07	.1253E-07	.6818E-07	.5900E 00	.2821E 01	.3144E 01	.5578E 01
42	.0173	8.4000	798.8000	1.7300	.0120	.2170E-07	.9360E-08	.4068E-07	.6059E 00	.2319E 01	.3764E 01	.6722E 01

Pipe Diameter = 0.5045 in.

REFERENCES

1) Martinelli, R.C., and D.B. Nelson, "Prediction of Pressure Drop During Forced Circulation Boiling of Water," Trans. Am. Soc. Mech. Engrs., 70, 695, 1948.

1a) Martinelli, R. C., L.M.K. Boelter, T.H.M. Taylor, E.G. Thomson, and E.H. Morrin, "Isothermal Pressure Drop for Two-Phase, Two-Component Flow in a Horizontal Pipe," Trans. Am. Soc. Mech. Engrs., 66, 139, 1944.

1b) Lockhart, R.W., and R. C. Martinelli, "Proposed Correlation of Data for Isothermal, Two-Phase, Two-Component Flow in Pipes," Chem. Eng. Prog., 45, 39, 1949.

2) Thom, J.R.S., "Predicition of Pressure Drop During Forced Circulation of Boiling of Water," International Journal of Heat and Mass Transfer, 7, 709, 1964.

3) Magiros, P.G. and A.E. Dukler, "Entrainment and Pressure Drop in Concurrent Gas-Liquid Flow II. Liquid Property and Momentum Effects," Developments in Mechanics, Vol. I, Plenum Press, New York, 1961.

4) Bankoff, S.G., "A Variable Density Single-Fluid Model for Two-Phase Flow with Particular Reference to Steam-Water Flow," Trans. Am. Soc. Mech. Engrs., Series C, 84, 265, 1960.

5) Anderson, G.H., and B.C. Mantzoranis, "Two-Phase (gas-liquid) Flow Phenomena - Part I," Chem. Eng. Sci., 12, 109, 1960.

6) Silvestri, M., et al., "A Research Program in Two-Phase Flow," Centro Informazioni Studi Esperienze, EURATOM Contract No. 002-59-11, ROI (CAN-1), January, 1963.

7) Linning, D.L., "The Adiabatic Flow of Evaporating Fluids in Pipes of Uniform Bore," Proc. Inst. Mech. Engrs., London, 1B 2, 64, 1952.

8) Semenov, N.I., "Pressure Pulsations During the Flow of Gas-Liquid Mixtures in Pipes," Heat Power Engineering Part I, U.S.A.E.C., Division of Technical Information, AEC-tr-4496, Dec. 1961, translated.

9) Vance, W.H., "A Study of Slip Ratios for the Flow of Steam-Water Mixtures at High Void Fractions," Ph.D. thesis, University of Washington, 1962.

10) Rose, S., "Some Hydrodynamic Characteristics of Bubbly Mixtures Flowing Vertically Upward in Tubes," Sc.D. thesis, Massachusetts Institute of Technology, 1964.

11) Fauske, H.K., "Two-Phase Critical Flow," Two-Phase Gas-Liquid Flow, ed. by P. Griffith and S. W. Gouse, Jr., Special Summer Program, MIT, Cambridge, Mass., 1964.

12) Zivi, S.M., "Estimation of Steady-State Steam Void-Fraction by Means of the Principle of Minimum Entropy Production," Trans. Am. Soc. Mech. Engrs., Series C, 86, 247, 1964.

13) Schlicting, H., Boundary Layer Theory, McGraw-Hill, New York, 1960.

14) Von Karman, T., "Mechanische Ahnlichkeit und Turbalenz," Proc. 3rd Intern. Congress Appl. Mech., Stockholm, 1930.

15) Pai, Fluid Dynamics of Jets, D. Van Nostrand, New York, 1954.

16) ASME Power Test Codes; Chapter 4, Flow Measurement; Part 5, Measurement of Quantity of Materials, PTC 19.5, 4-1959, New York.

17) Radiotron Designers' Handbook, F. Langford-Smith, Amalgomated Wireless Valve Company Ptg, Ltd., Sidney, Australia, 1953.

18) Electronic Designers' Handbook, R. W. Landee, D. C. Davis, and A. P. Alvrecht, McGraw Hill, New York, 1957.

19) Griffin, E. and T. F. Crang, "Steam Flow in Nozzles: Velocity Coefficient at Low Steam Speeds," Proc. of Inst. of Mech. Eng., 155, 83, 1946.

20) Gill, L.E., G.F. Hewitt, and P.M.C. Lacey, "Sampling Probe Studies of the Gas Core in Annular Two-Phase Flow, Part III, Studies of the Effect of Phase Flow Rates on Phase and Velocity Distributions," AERE-R3955, Harwell, England, 1963.

21) Wallis, G.B., D. S. Steen, S.N. Brenner, and J.M. Turner, Thayer School of Engineering, Dartmouth College, Hanover, New Hampshire, Report NYO 10, 489, 1964.

22) Minh, Q.T. and J.D. Huyghe, "Mesure et Correlation de la Fraction D'Entrainment en Ecoulement Diphasé a Deux Composants en Regime Annulaire Dispersé," Centre D'Etudes Nucléaires de Grenoble, Commissariat a l'Energie Atomic, Grenoble, France, Rapport TT No. 52, 1965.

23) Shames, I.H., Mechanics of Fluids, McGraw-Hill, New York, 1962.

24) Handbook of Chemistry and Physics, 35th edition, C. D. Hodgman, Chemical Rubber Publishing Co., Cleveland, 1953.

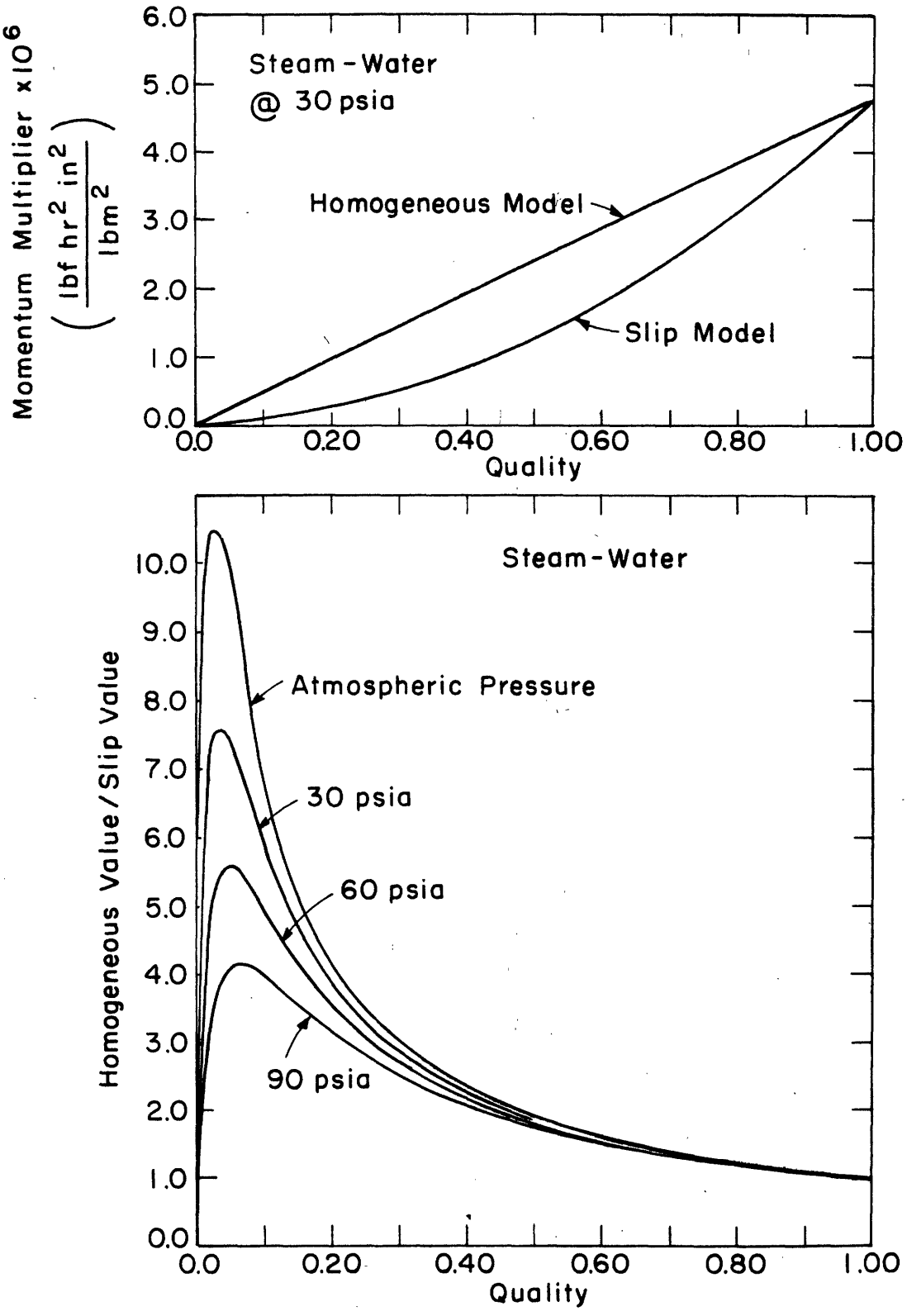

FIGURE 1. COMPARISON BETWEEN HOMOGENEOUS AND SLIP MODELS

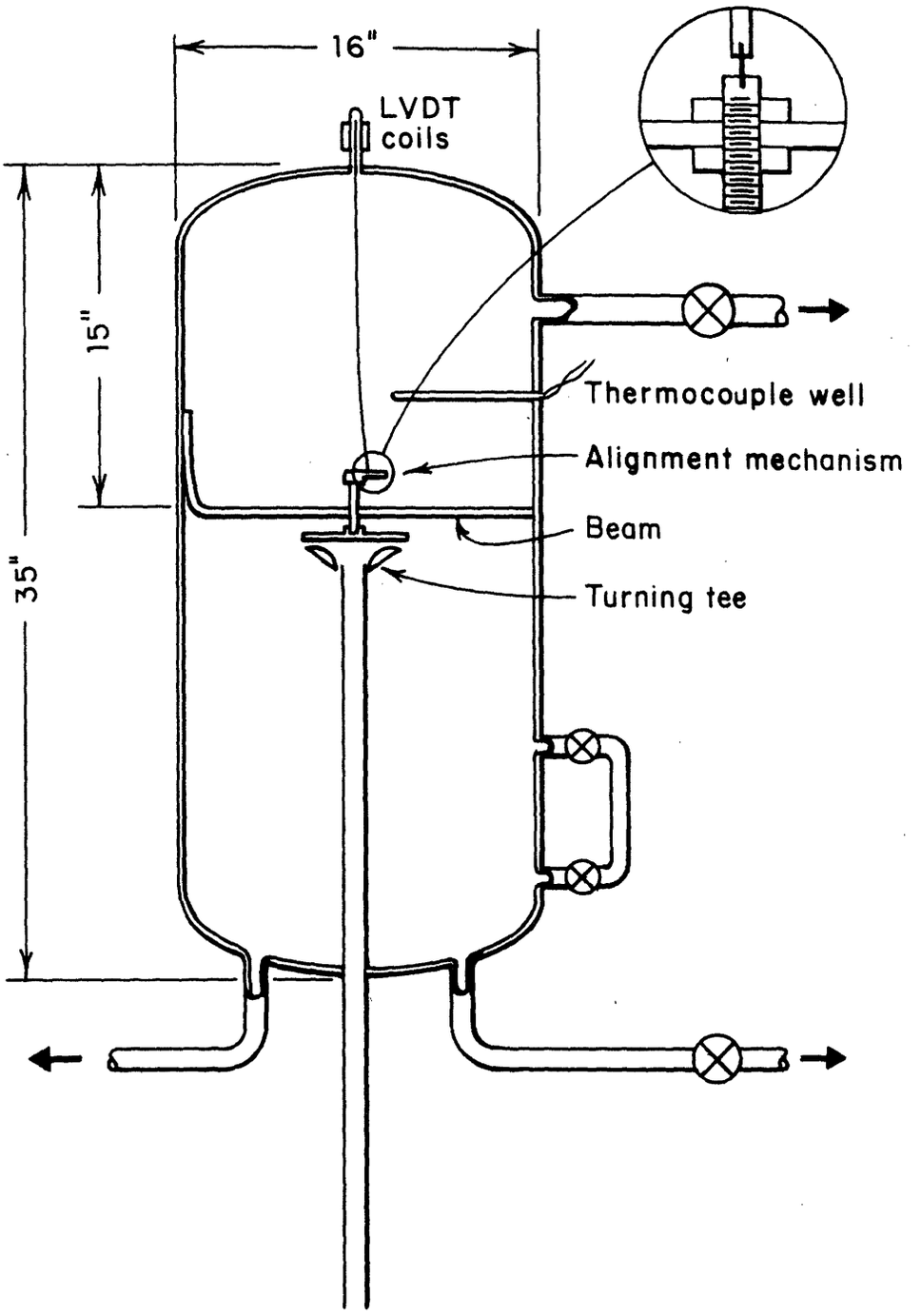

FIGURE 2. CROSS SECTION OF PRESSURE VESSEL SHOWING INTERNALS

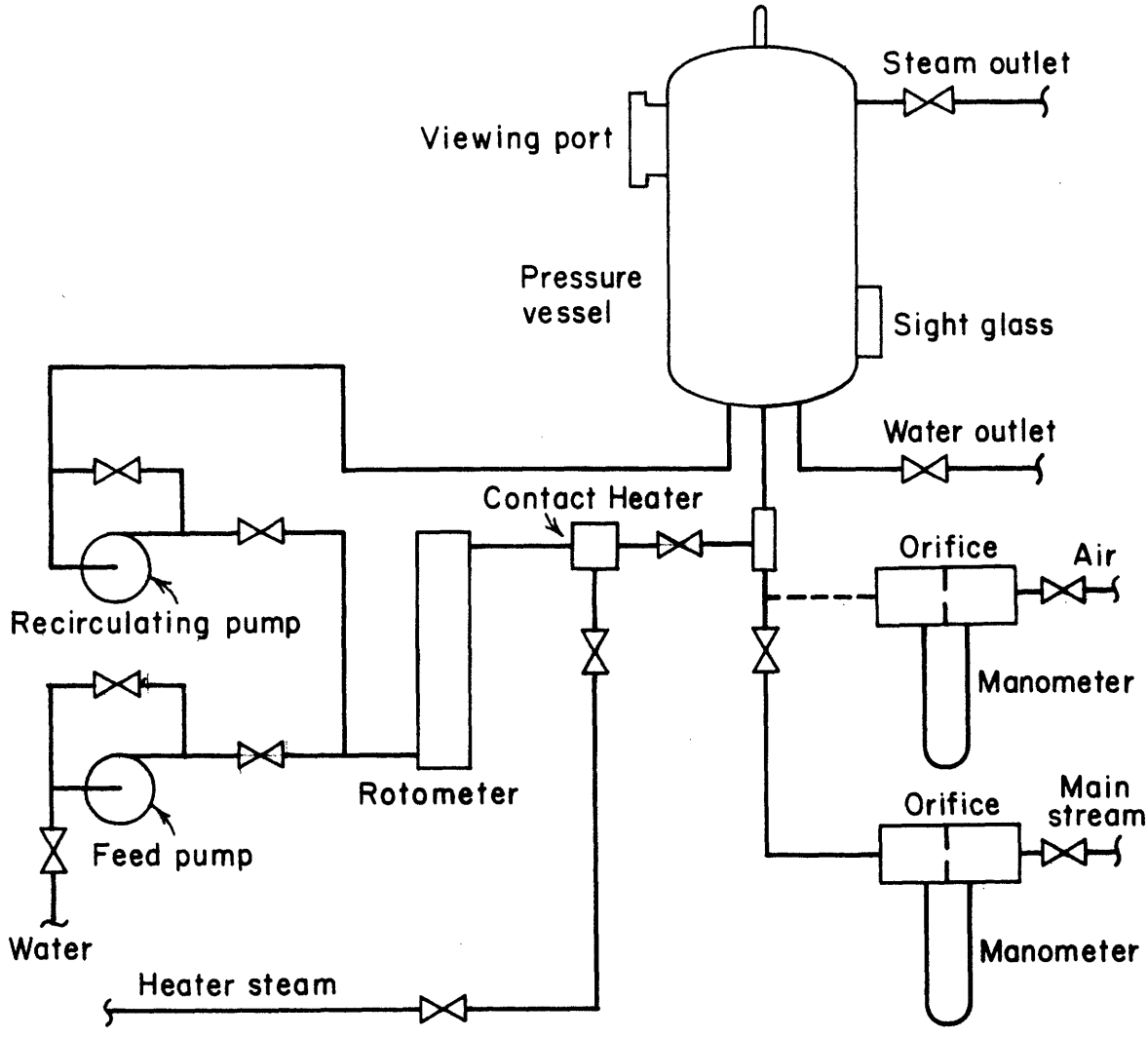

FIGURE 3. SCHEMATIC OF TEST APPARATUS

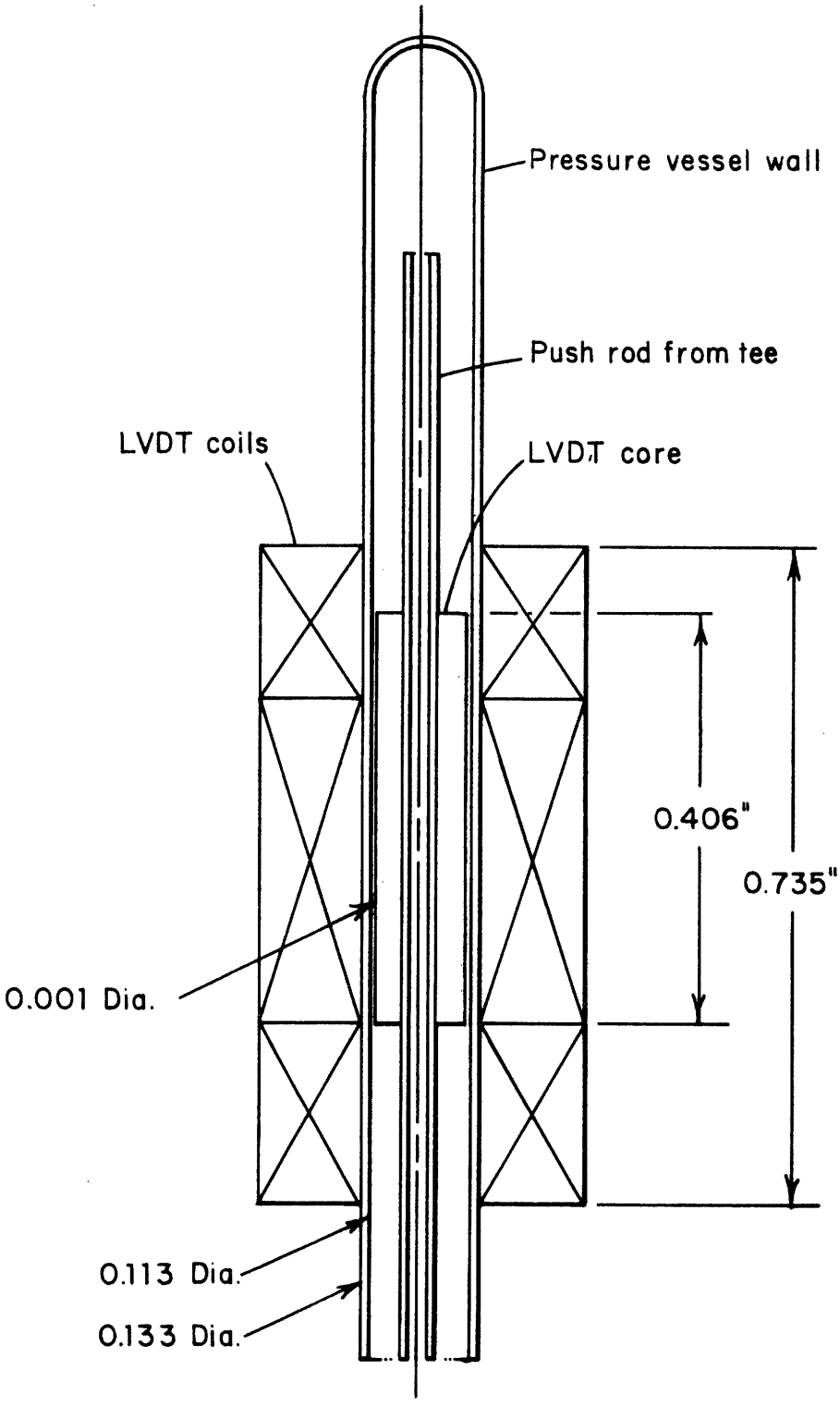

FIGURE 4. LVDT ARRANGEMENT

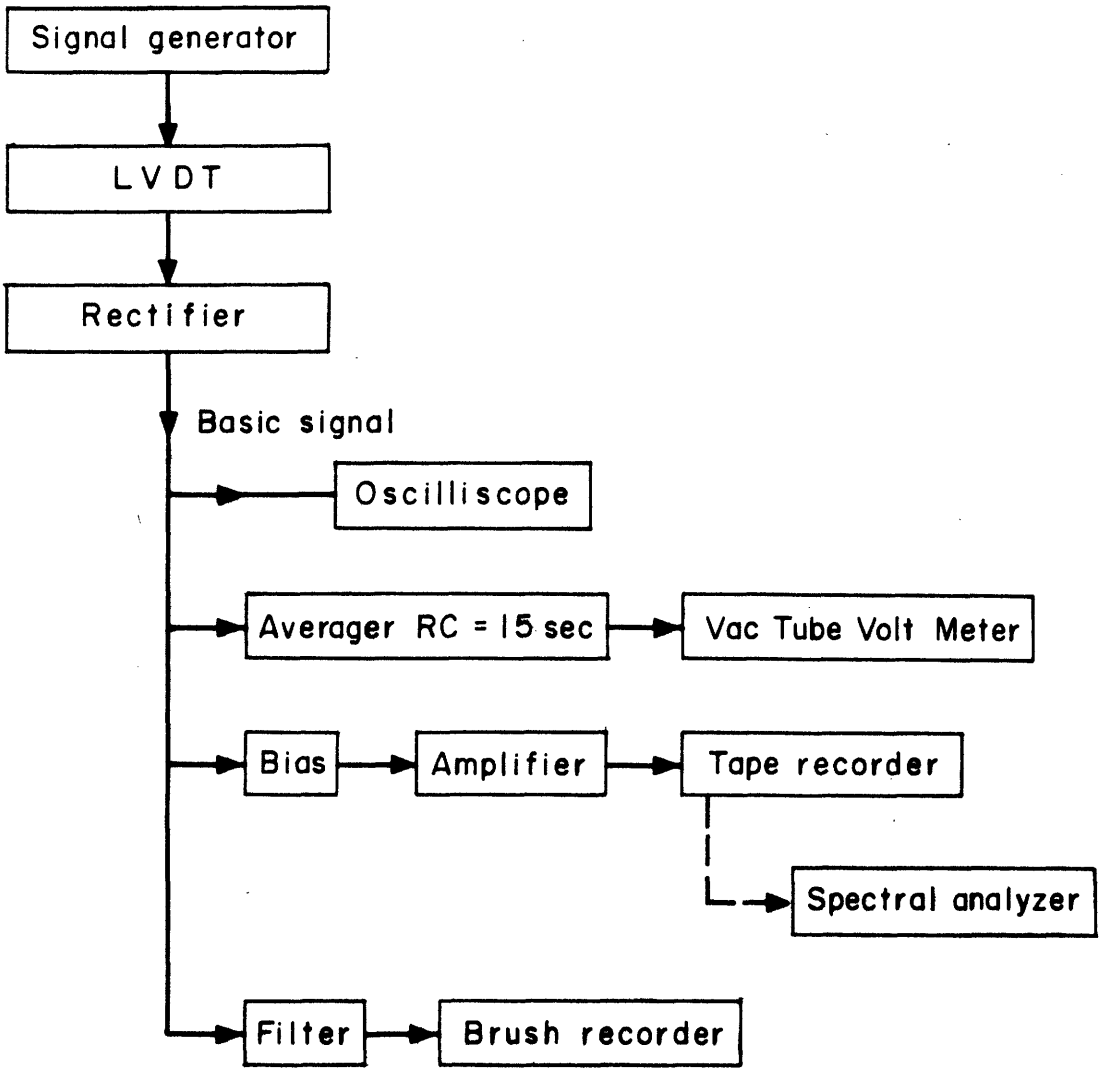

ELECTRICAL APPARATUS

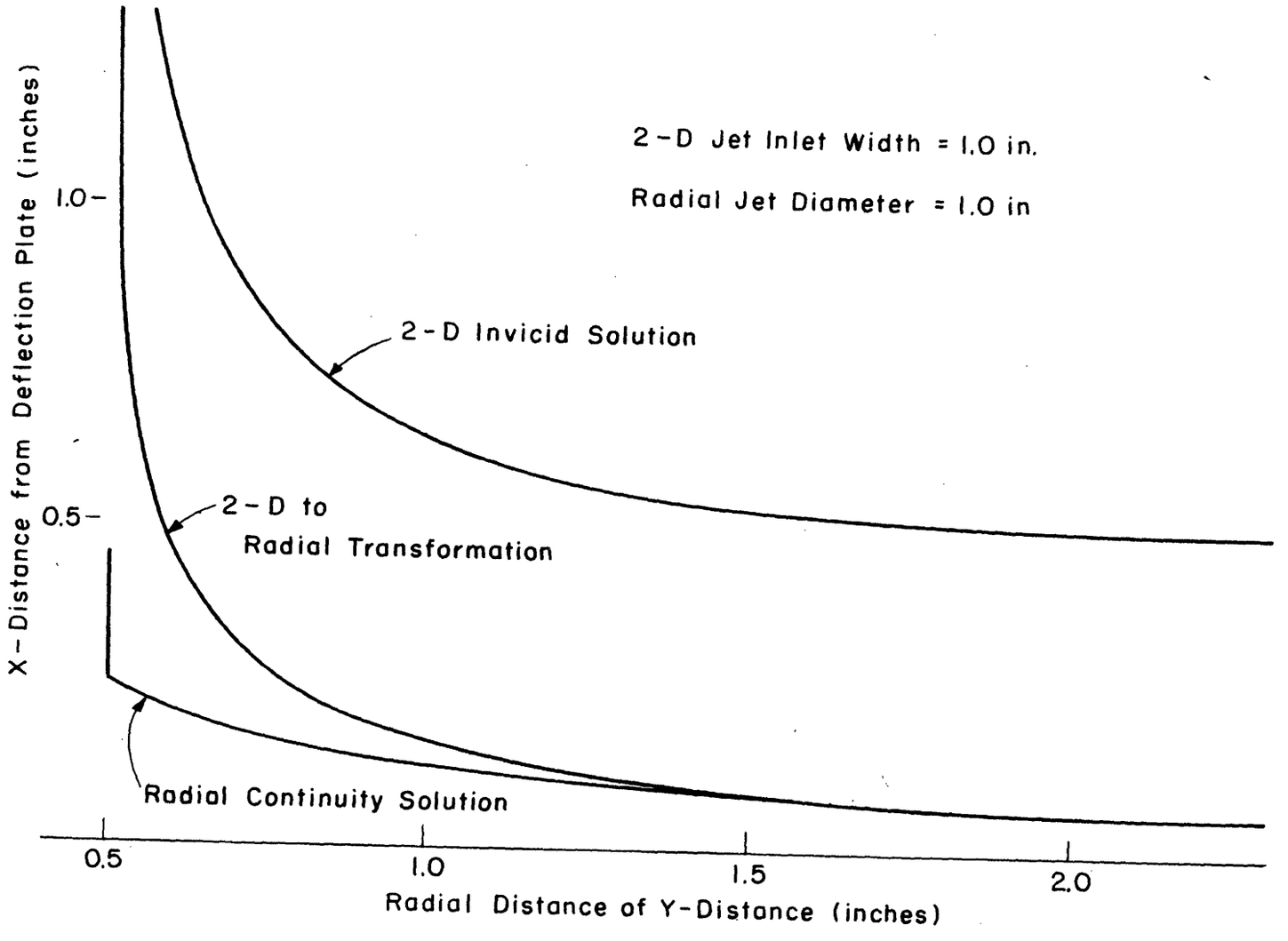

FIGURE 6. JET SURFACE PROFILES

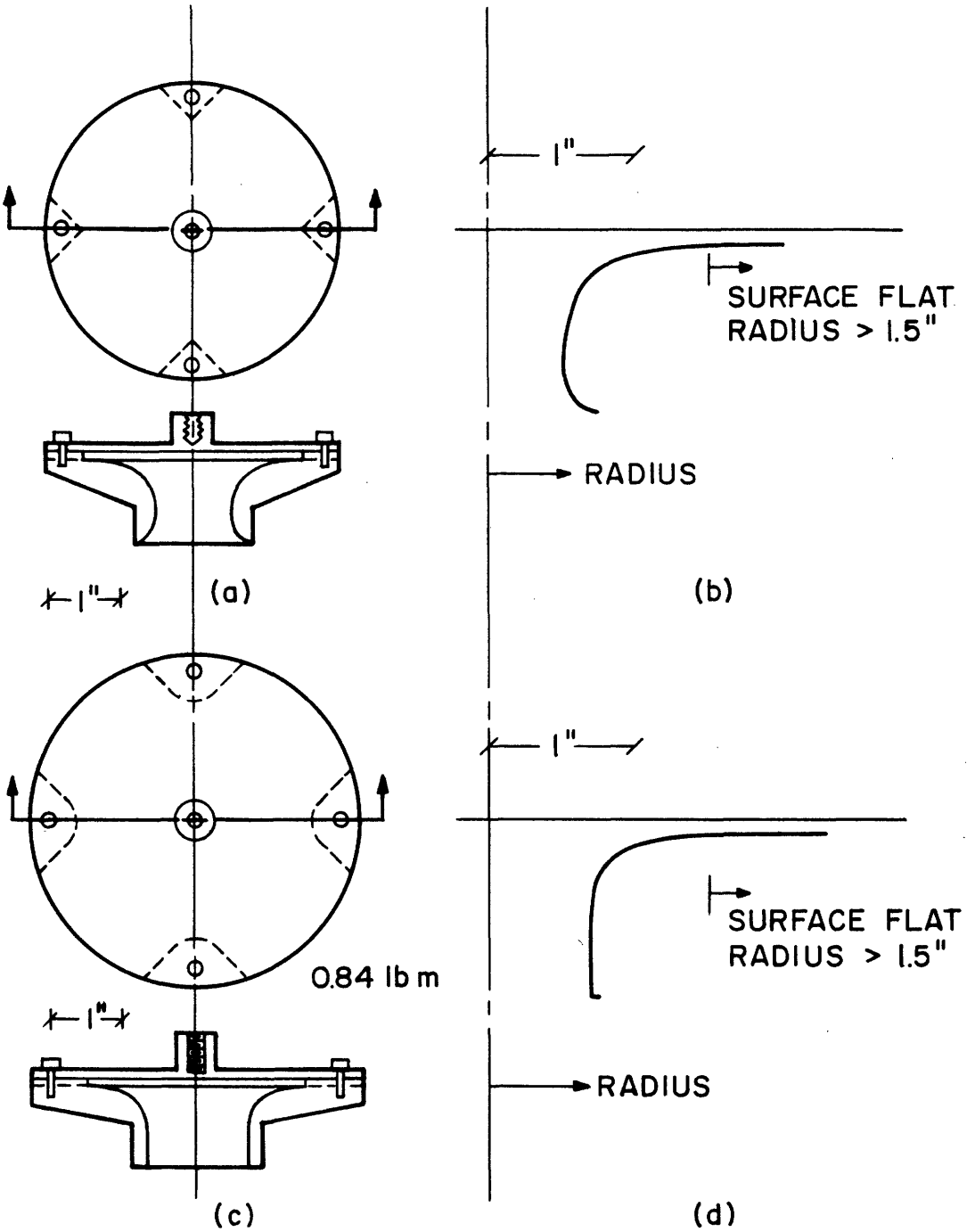

FIGURE 7. TURNING TEE DESIGNS

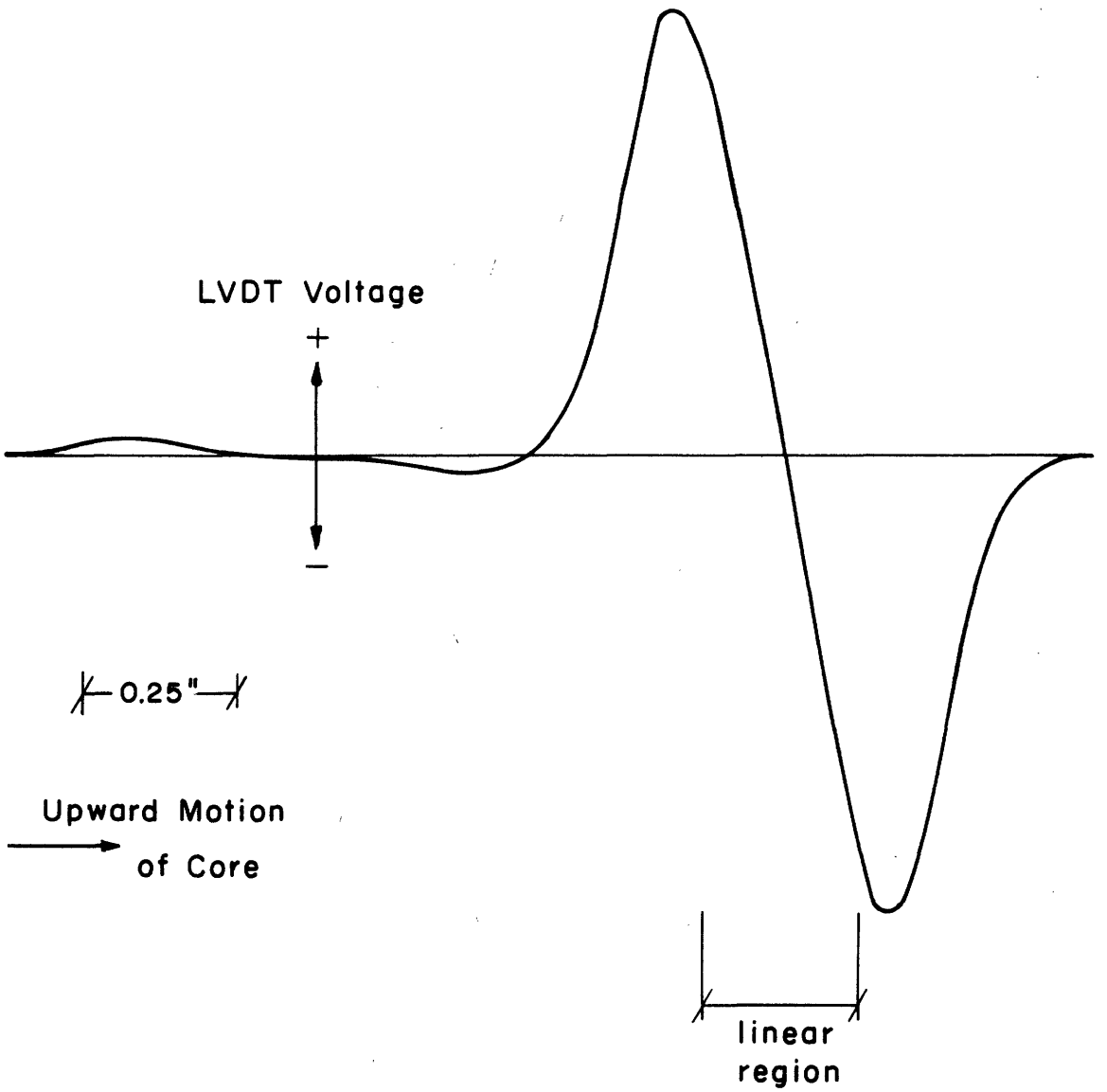

FIGURE 8. CORE TRAVERSE

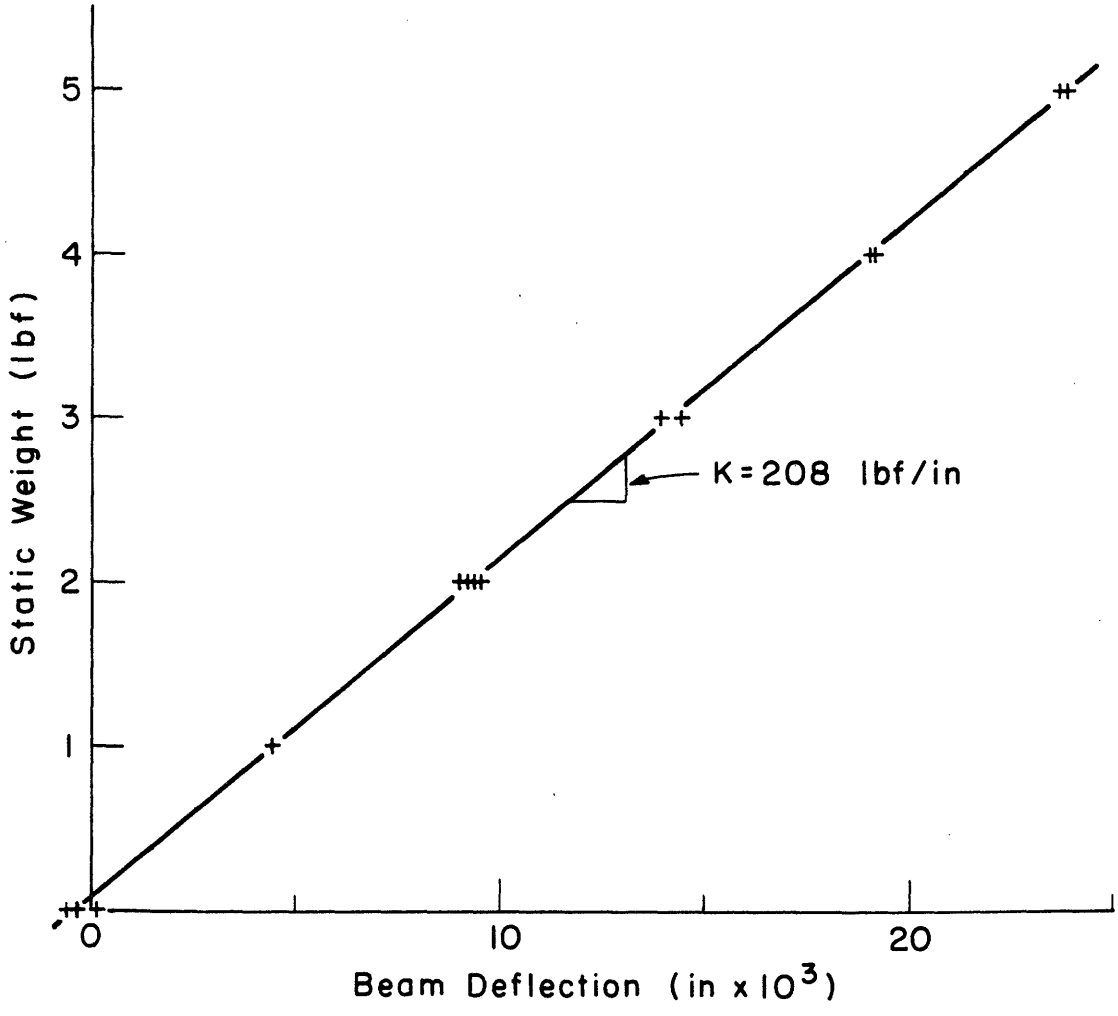

FIGURE 9. BEAM CONSTANT

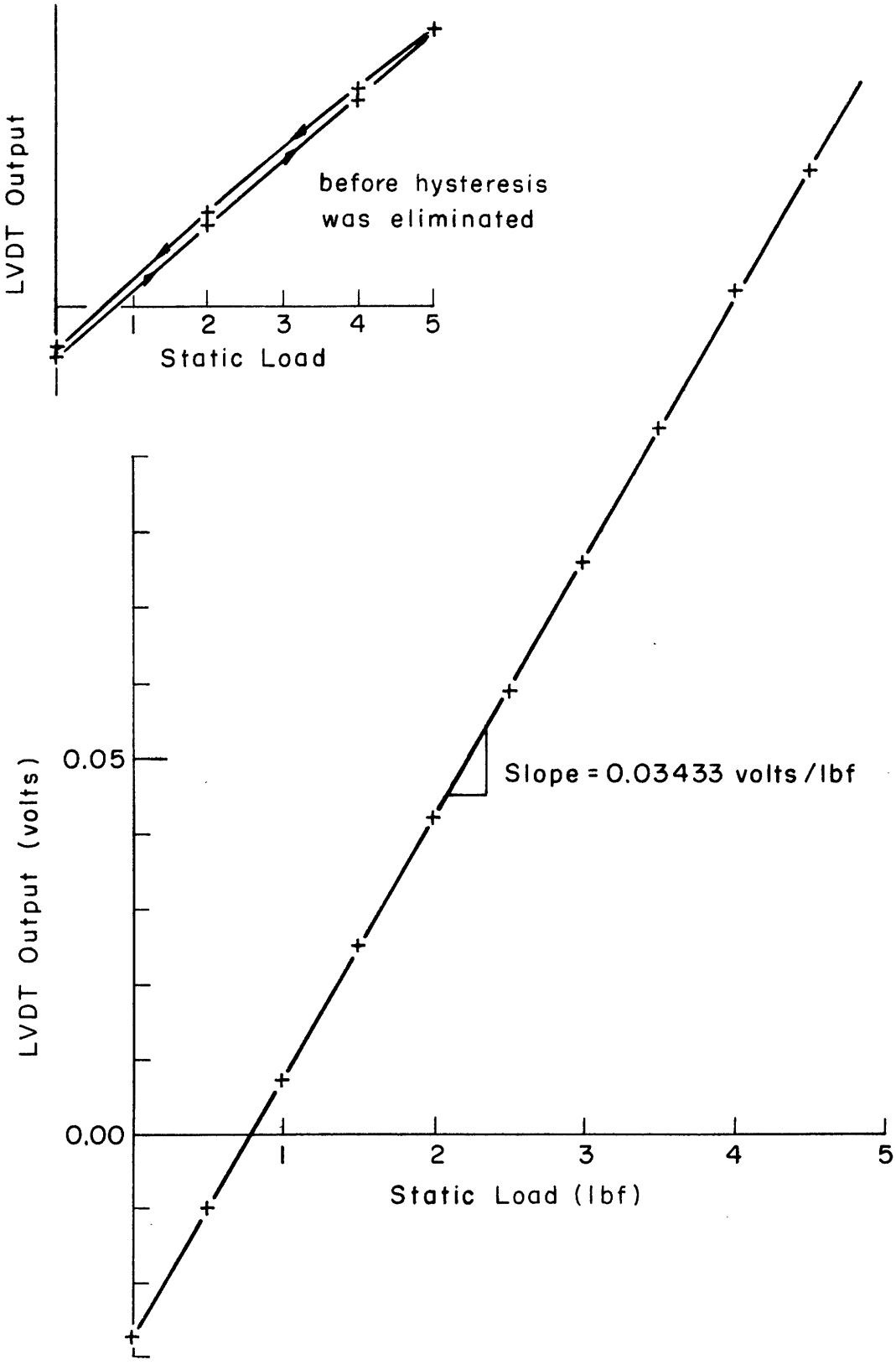

FIGURE 10. STATIC TEST

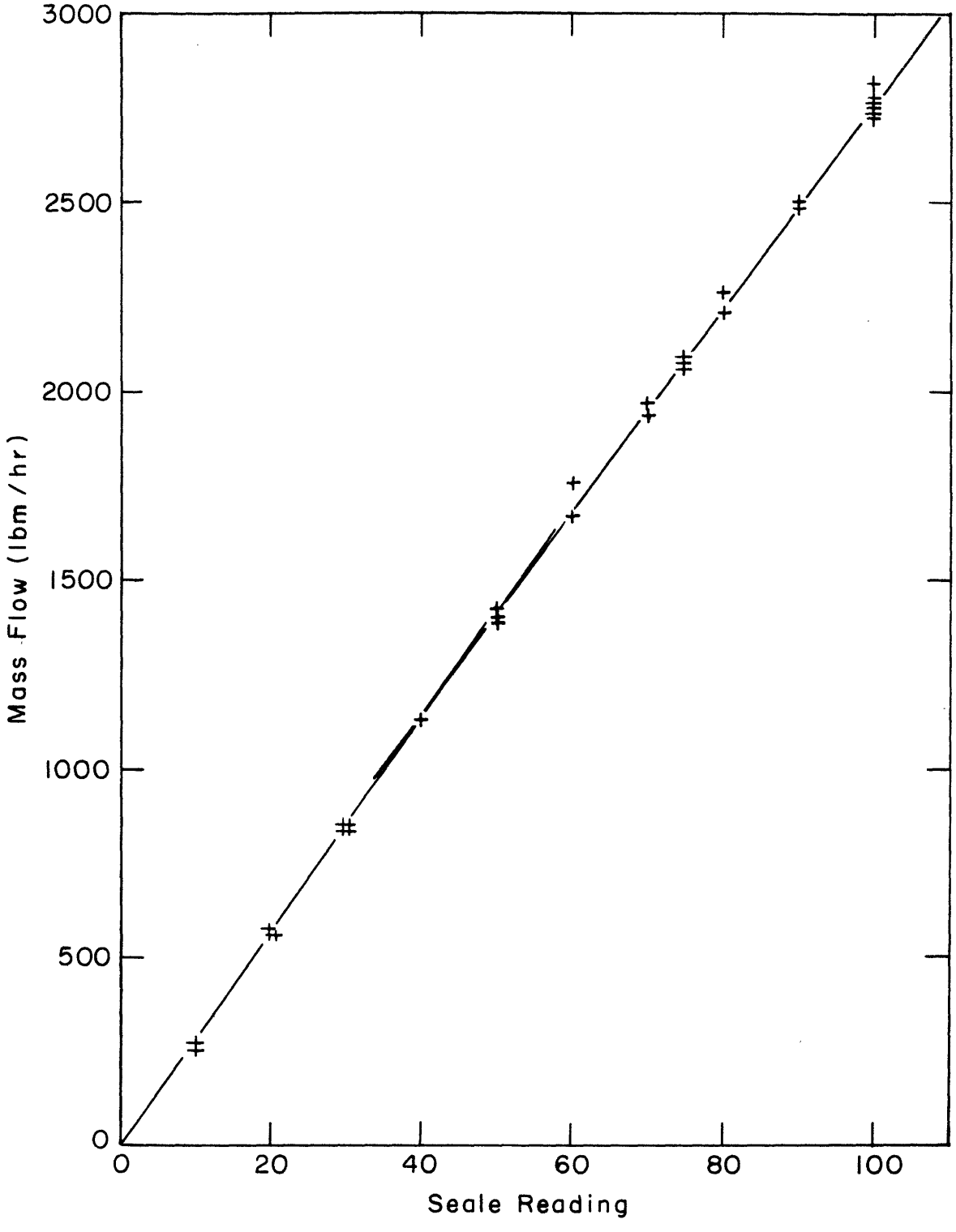

FIGURE II. WEIGH TANK CALIBRATION

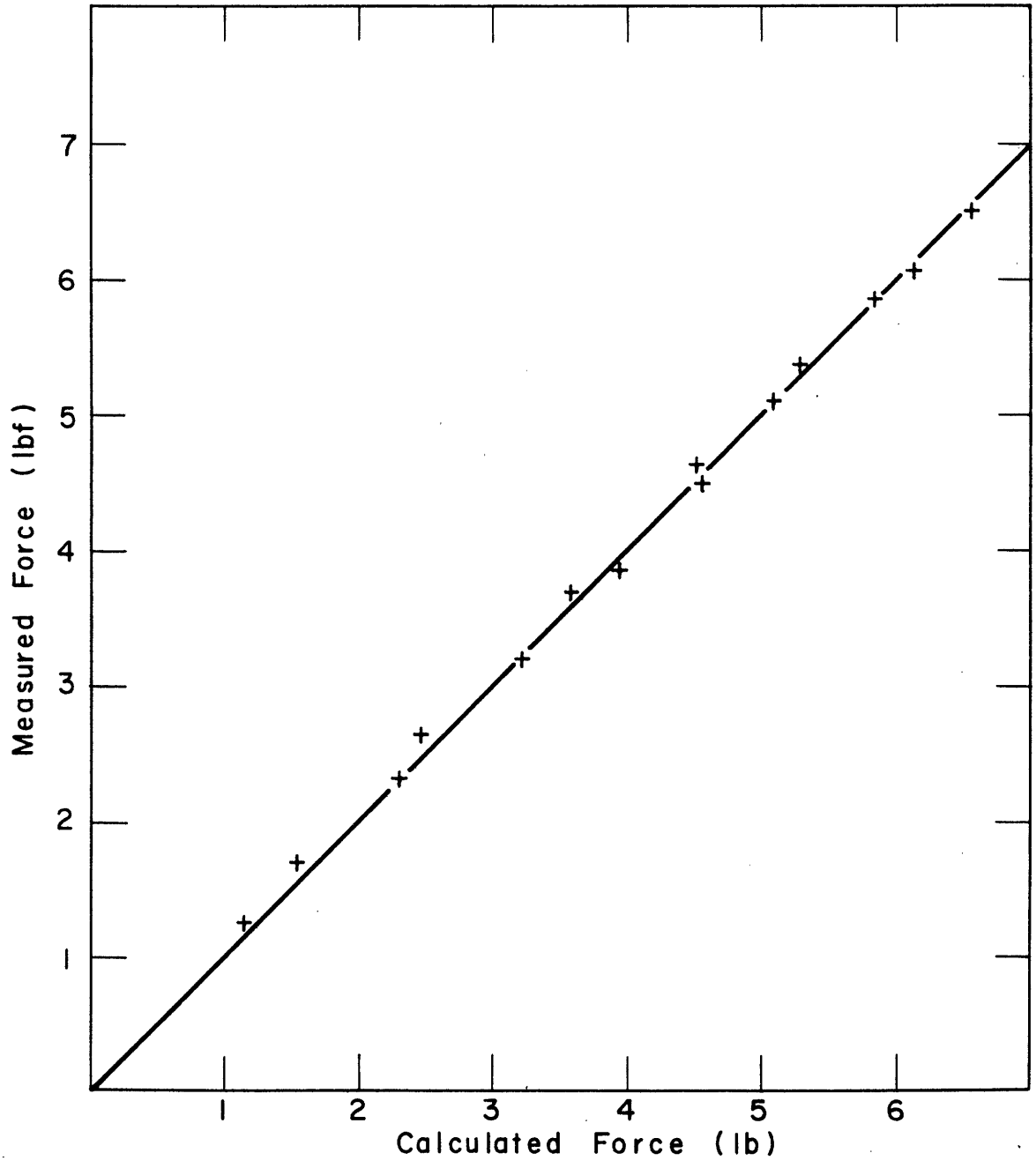

FIGURE 12. STEAM CALIBRATION TEST

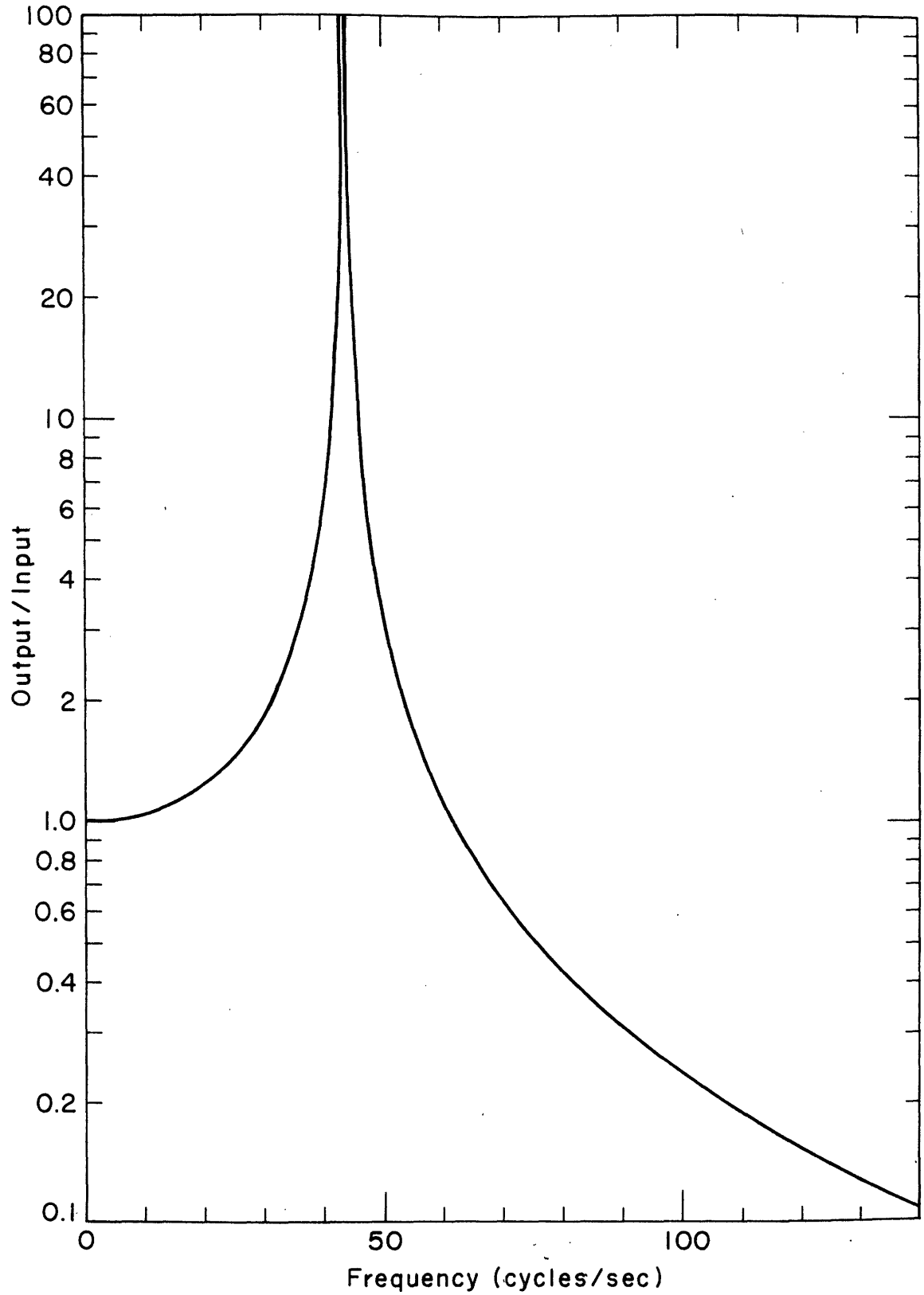

FIGURE 13. BEAM RESPONSE

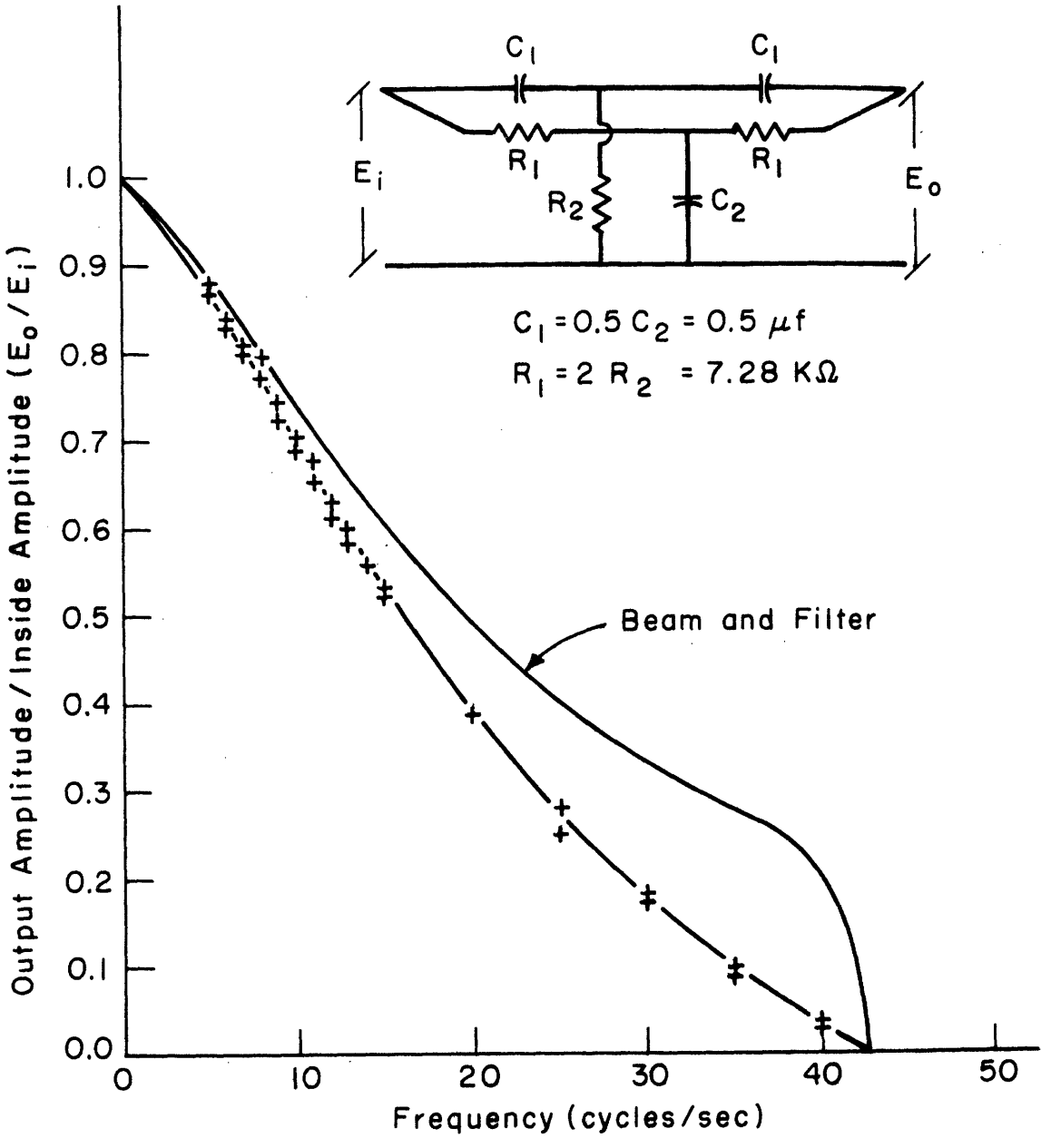

FIGURE 14. FILTER PERFORMANCE

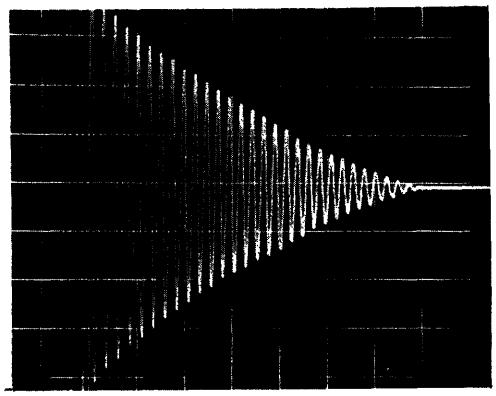

(b) Horiz. Scale 0.1 sec/unit
Vert. Scale 0.05 volts/units

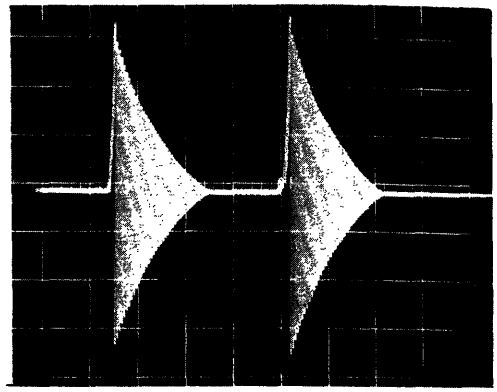

(b) Horiz. Scale 0.5 sec/unit
Vert. Scale 0.1 volts/units

with frictional damping

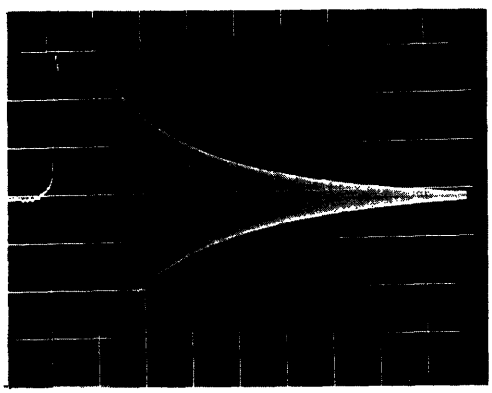

(c) Horiz. Scale 1.0 sec/unit
Vert. Scale 0.02 volts/units

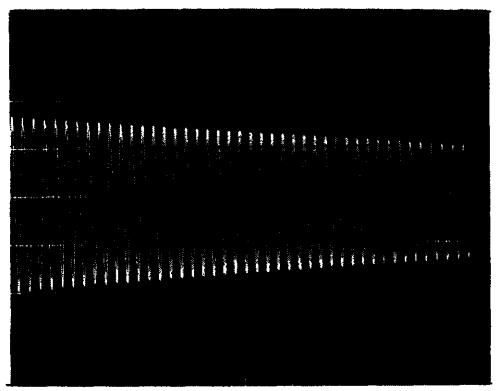

(d) Horiz. Scale 0.1 sec/unit
Vert. Scale 0.02 volt/units

frictional damping eliminated

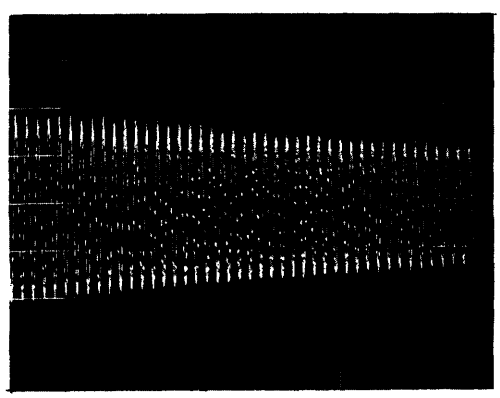

(e) Horiz. Scale 0.1 sec/unit
Vert. Scale 0.5 volts/units

as playback from tape deck

FIGURE 15. PLUCK TESTS

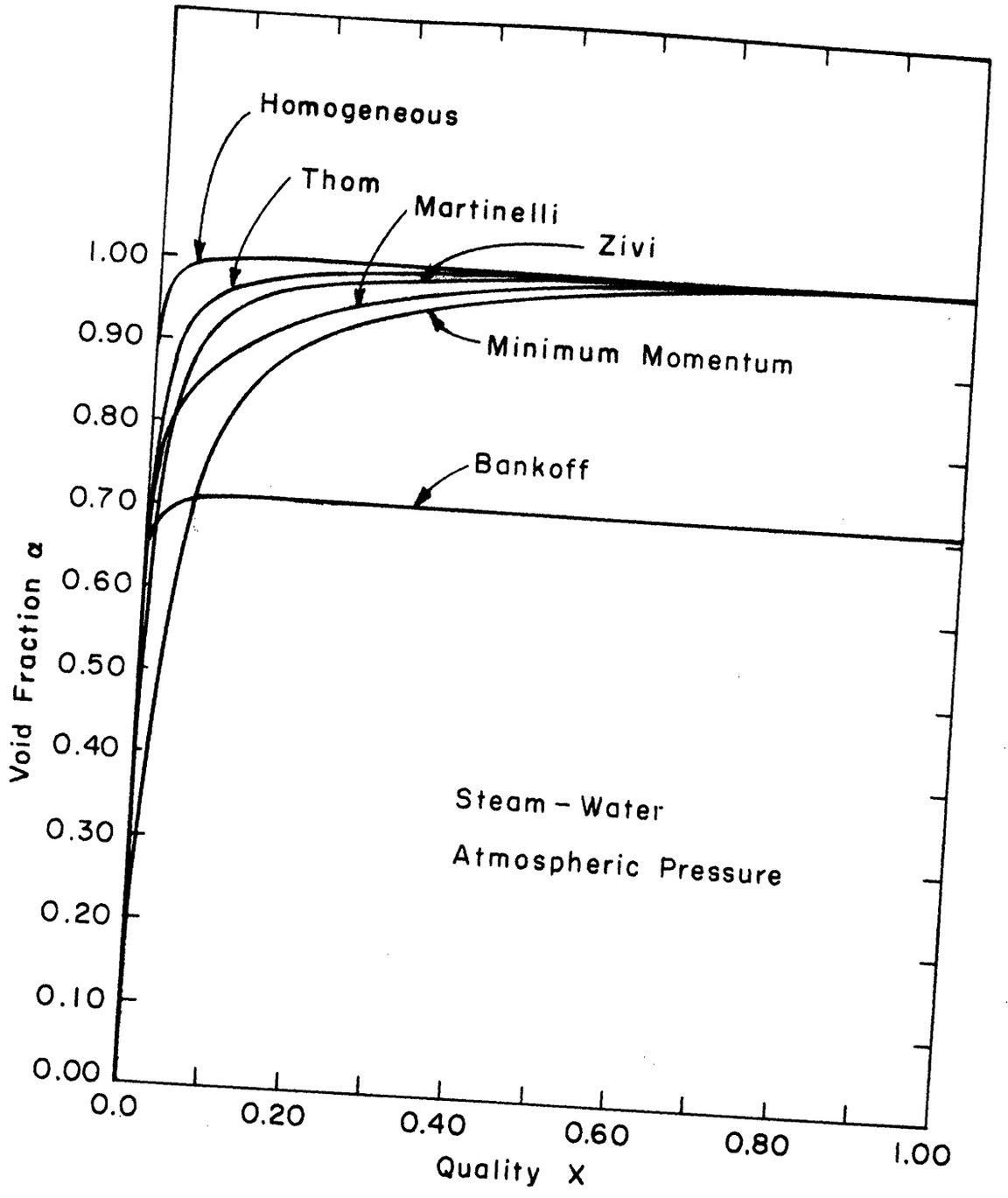

FIGURE 16. QUALITY-VOID FRACTION RELATIONSHIP

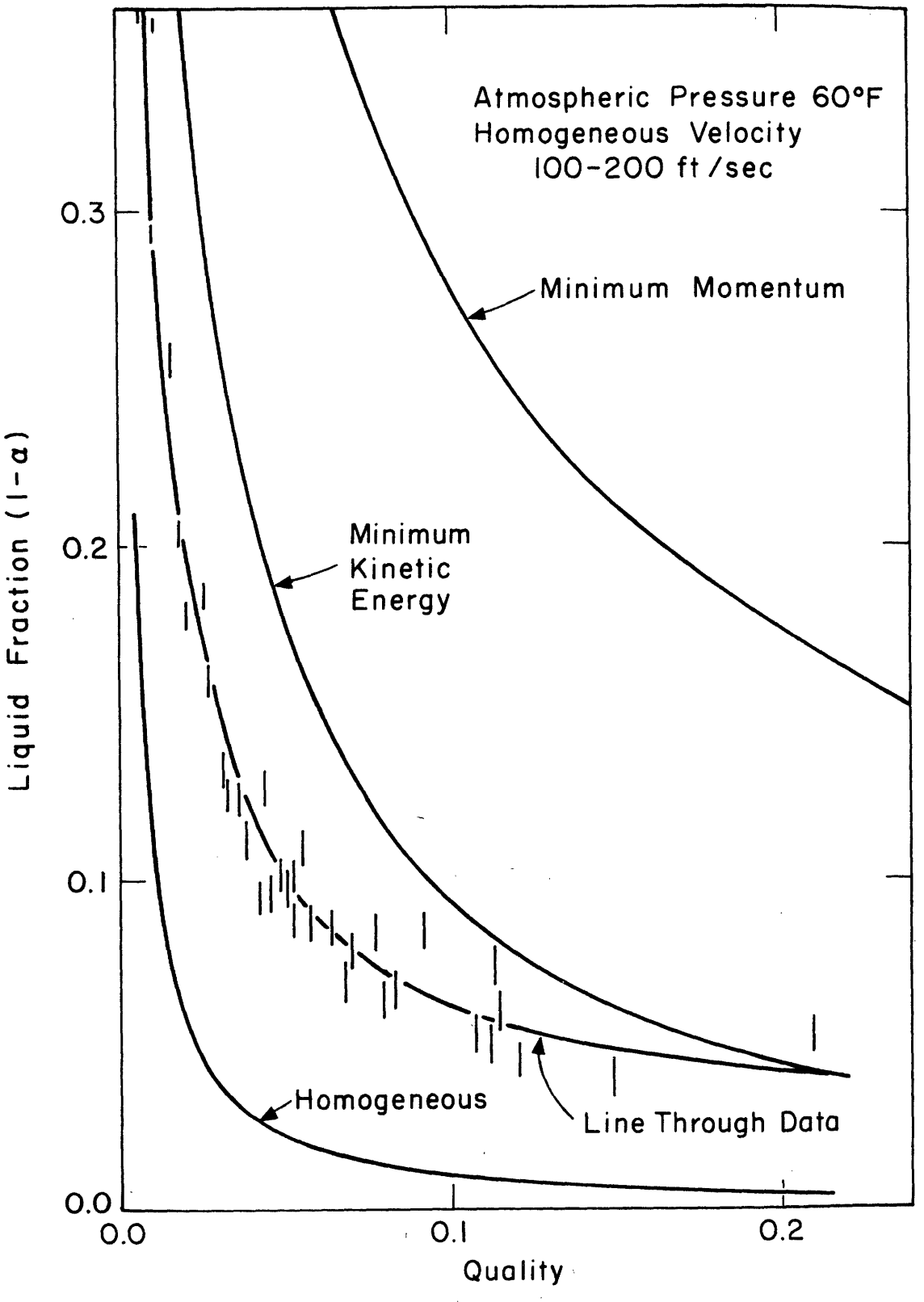

FIGURE 17. AIR-WATER LIQUID FRACTION

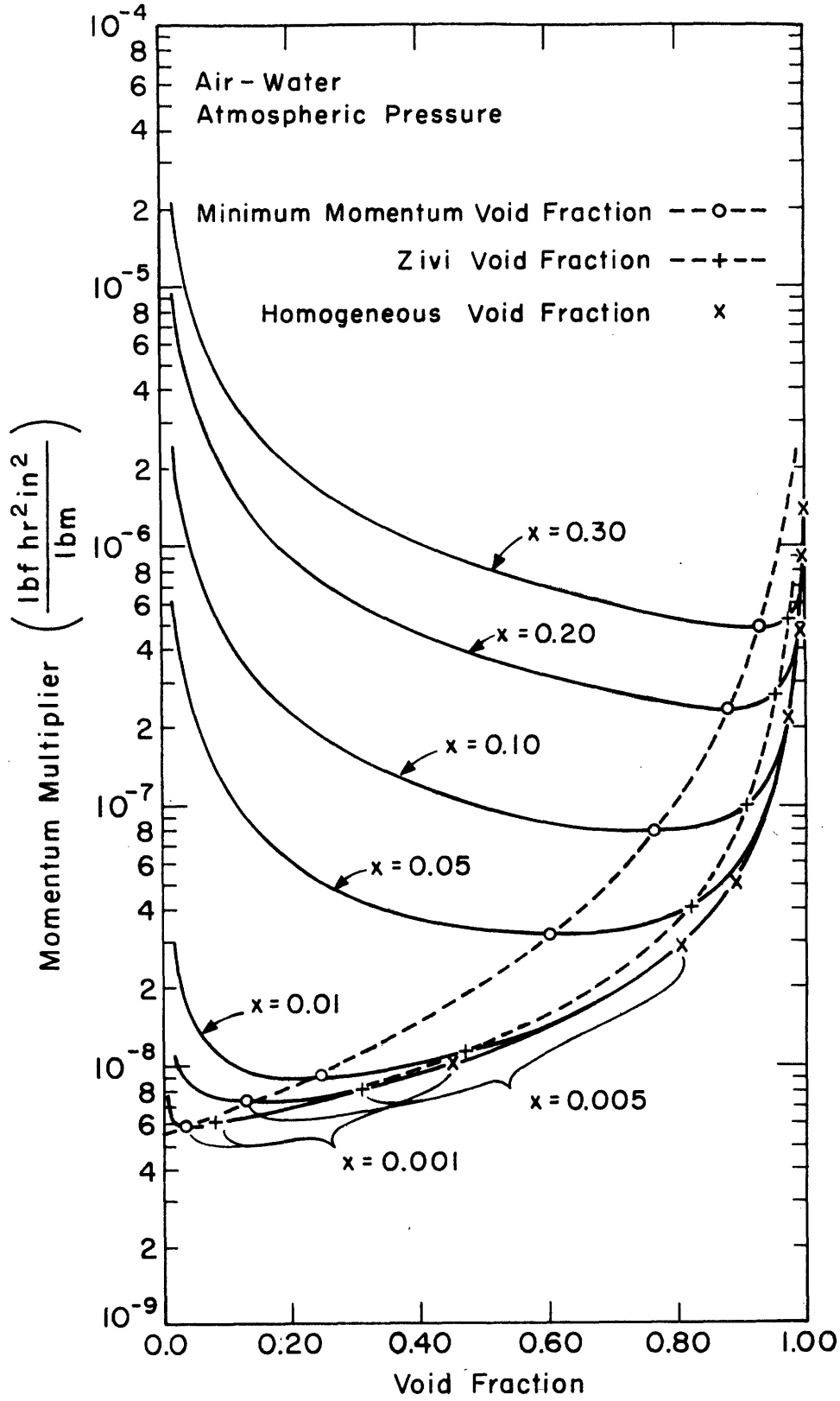

FIGURE 18. EFFECT OF VOID FRACTION ON SLIP MODEL MOMENTUM AMPLIFIER

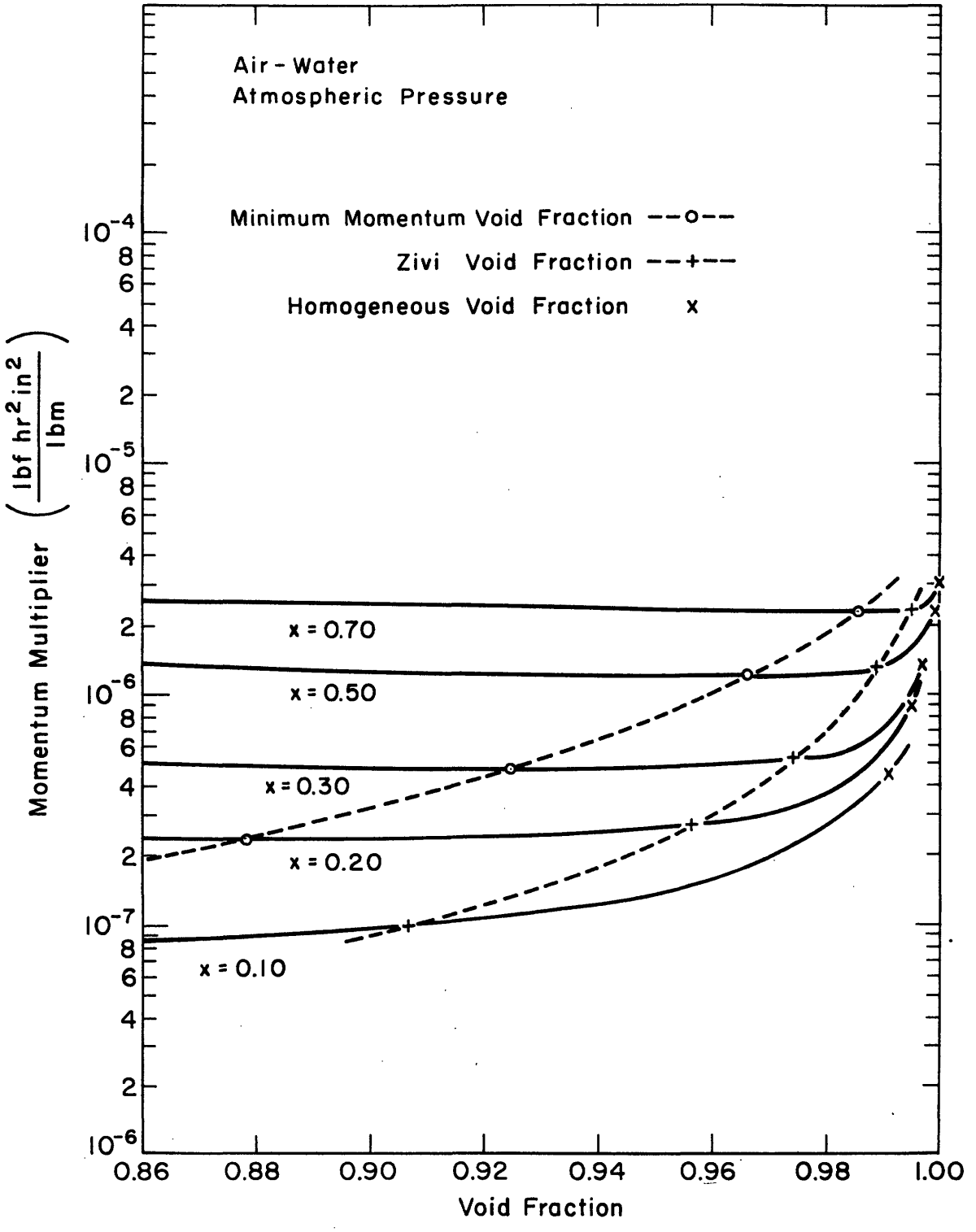

FIGURE 19. EFFECT OF VOID FRACTION ON SLIP MODEL MOMENTUM MULTIPLIER

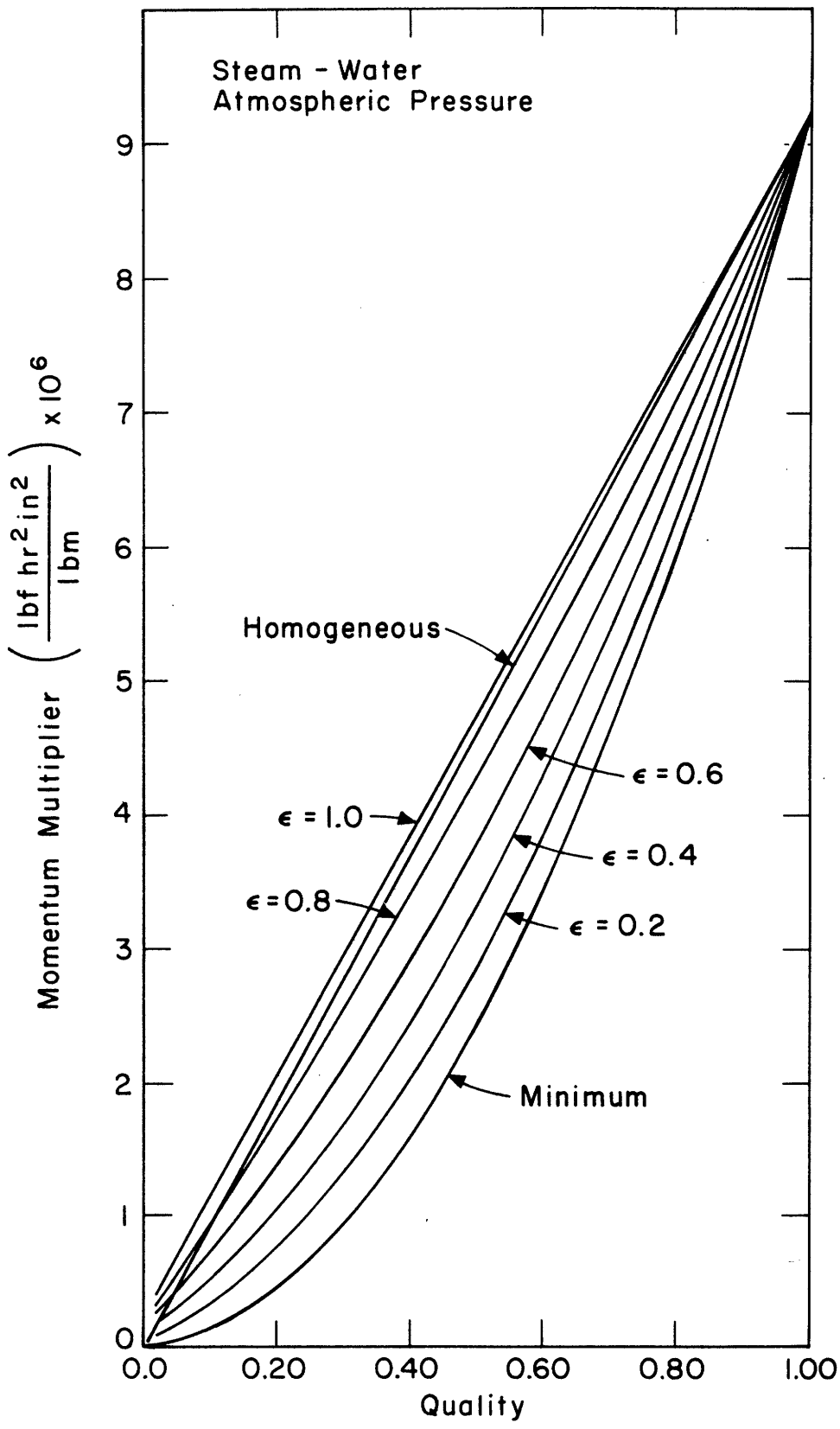

FIGURE 20. ENTRAINMENT MODEL

PAGES (S) MISSING FROM ORIGINAL

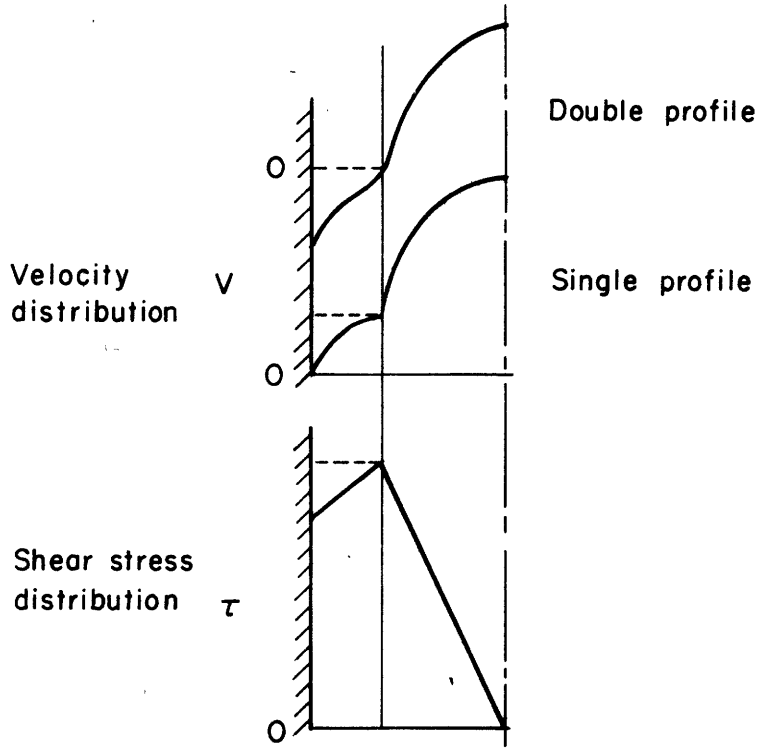

FIGURE 21. ANDERSON AND MANTZOURANIS MODEL

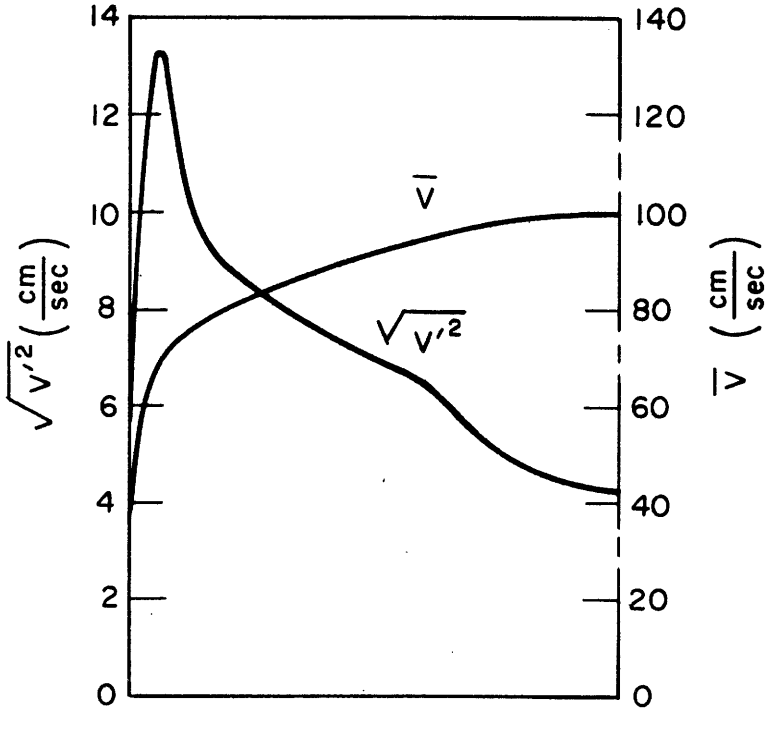

FIGURE 22. REICHARDT'S HOT-WIRE DATA

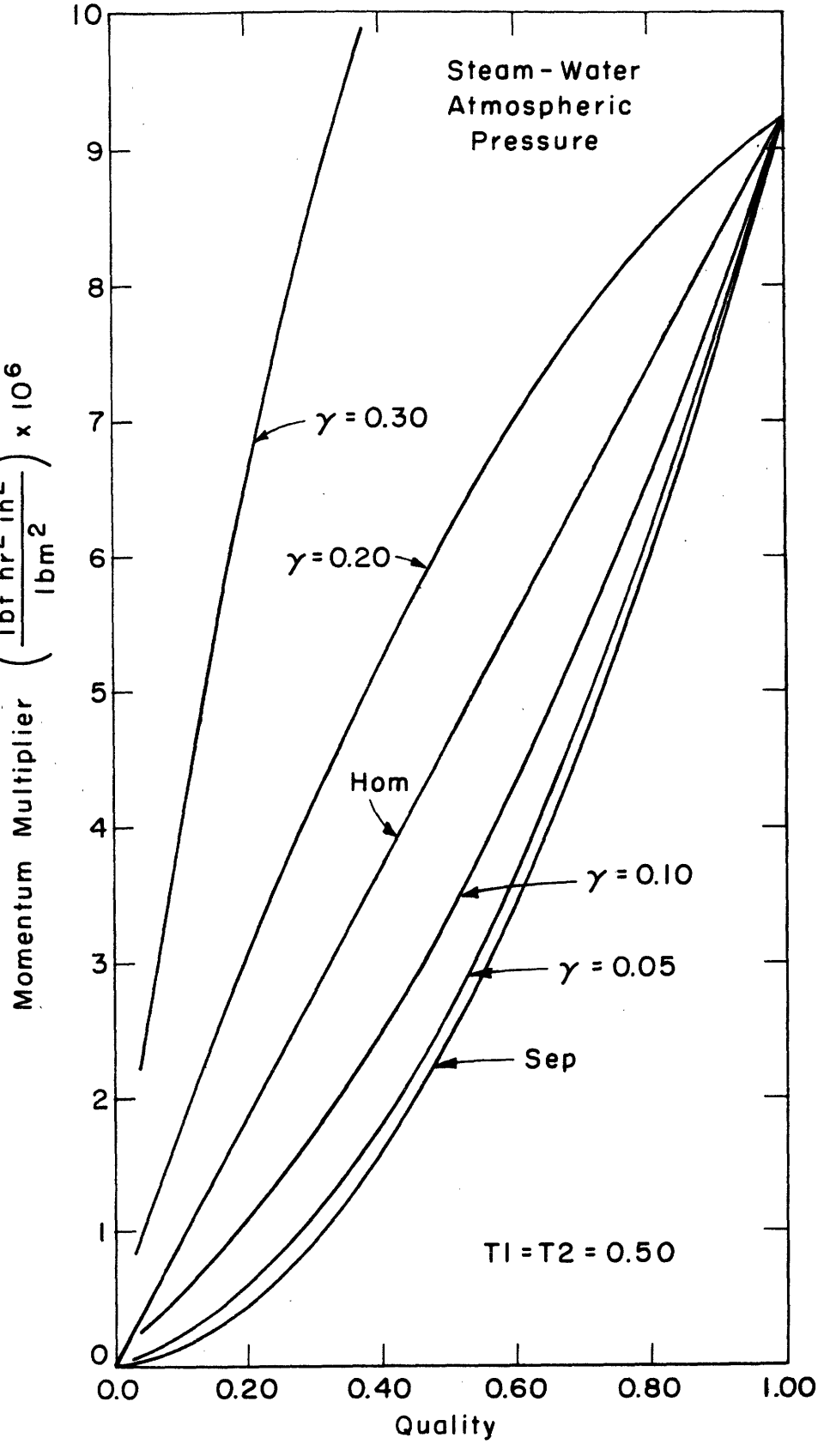

FIGURE 23. FLUCTUATING MODEL

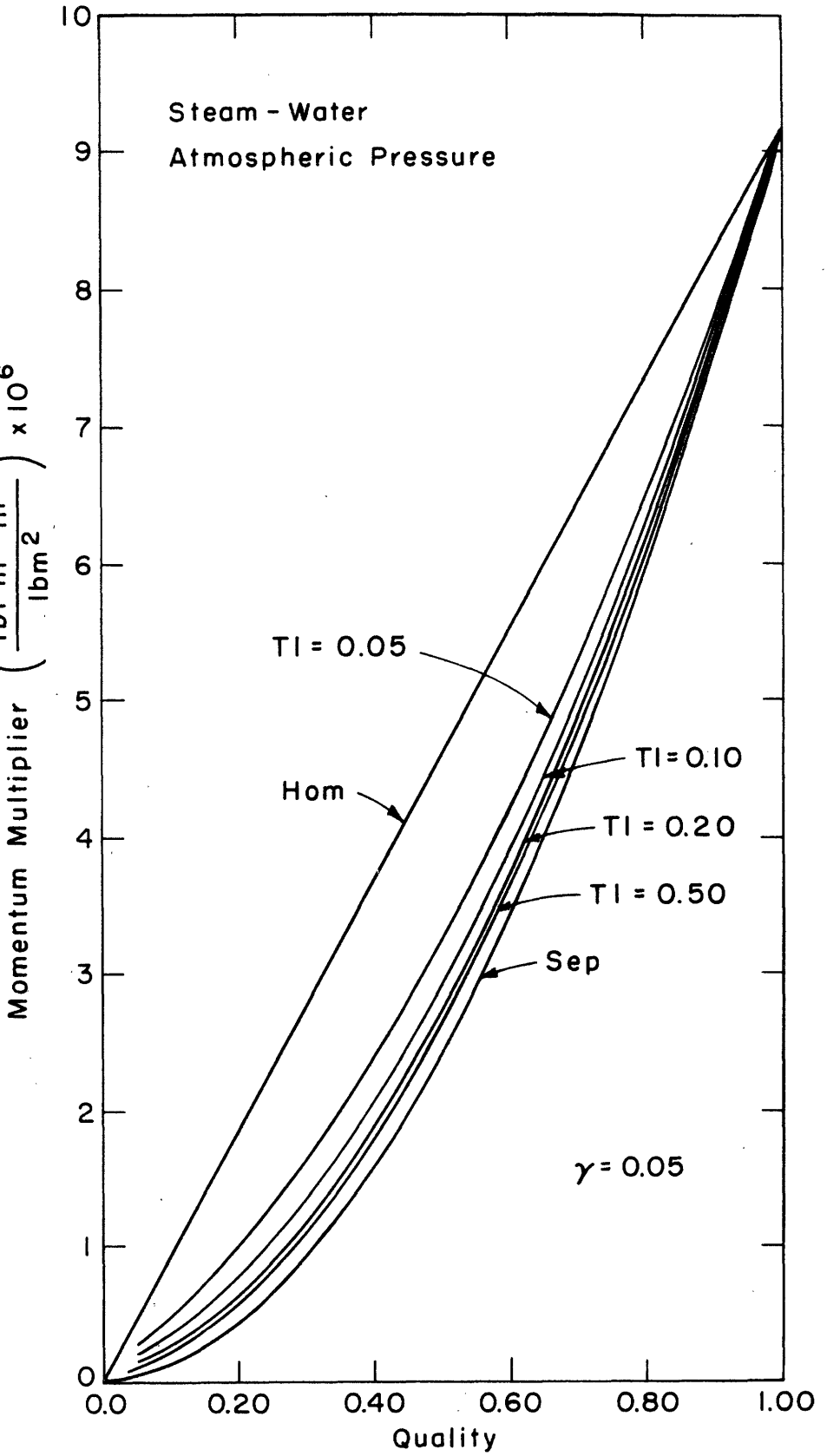

FIGURE 24. FLUCTUATING MODEL

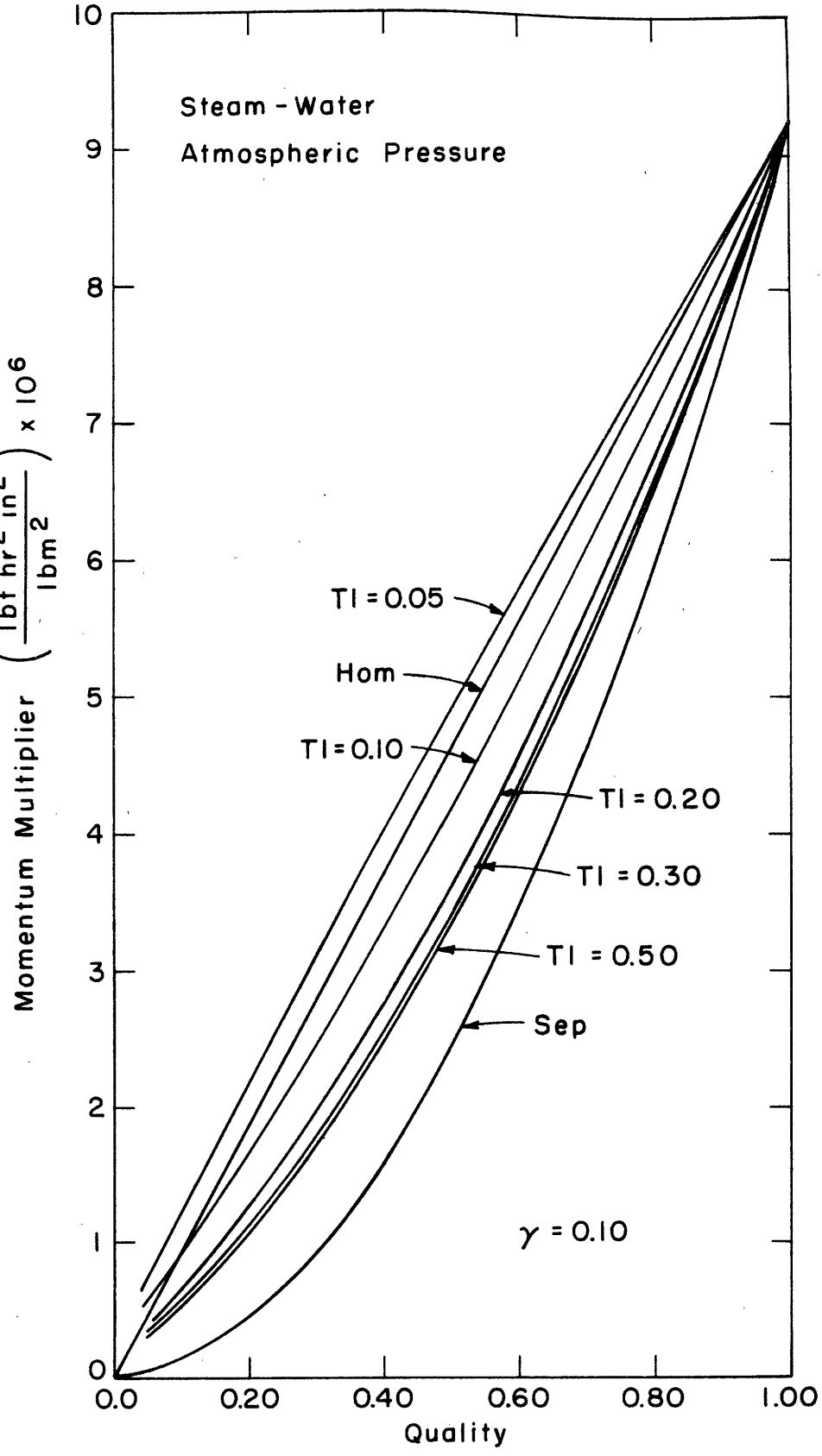

FIGURE 25. FLUCTUATING MODEL

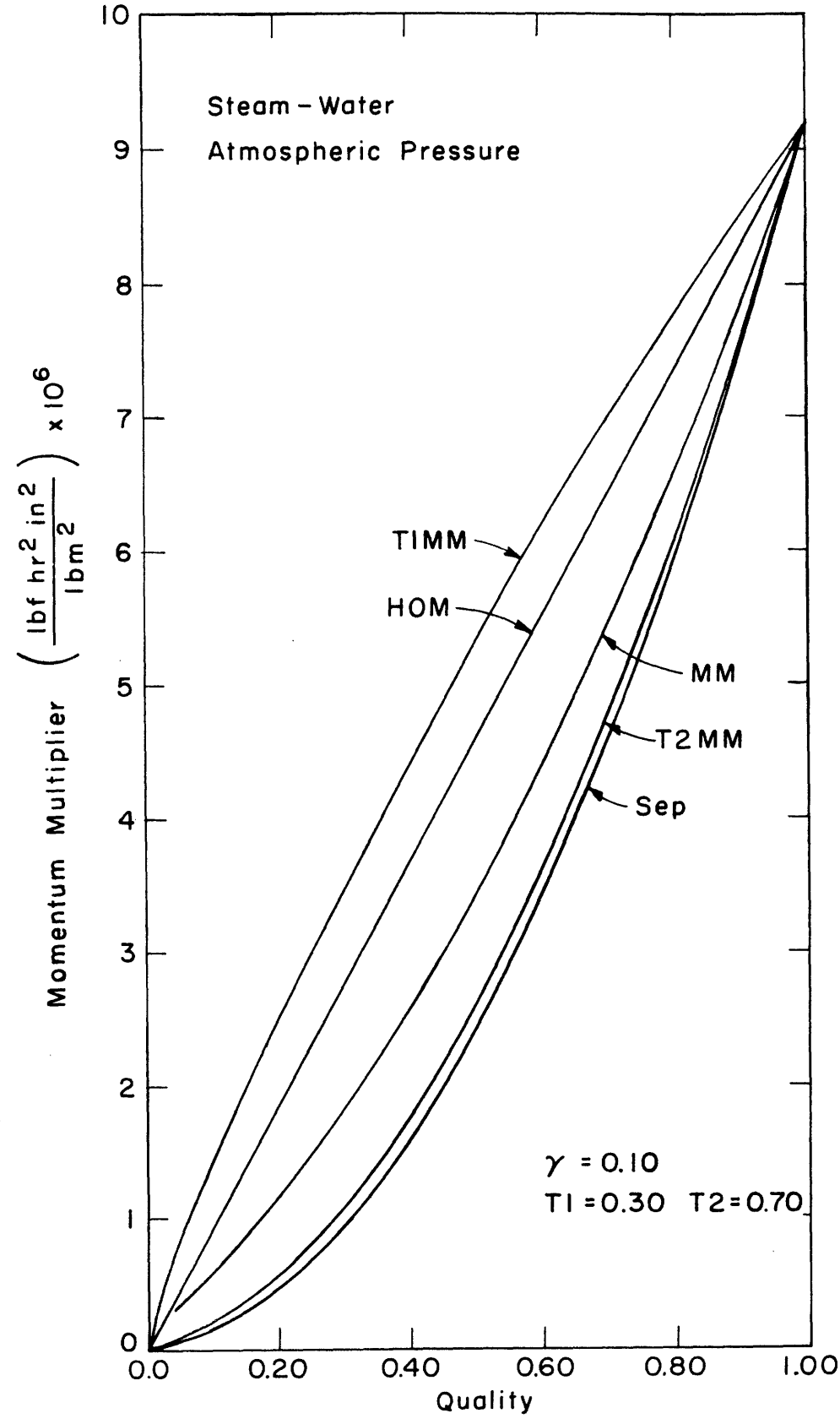

FIGURE 26. FLUCTUATING MODEL

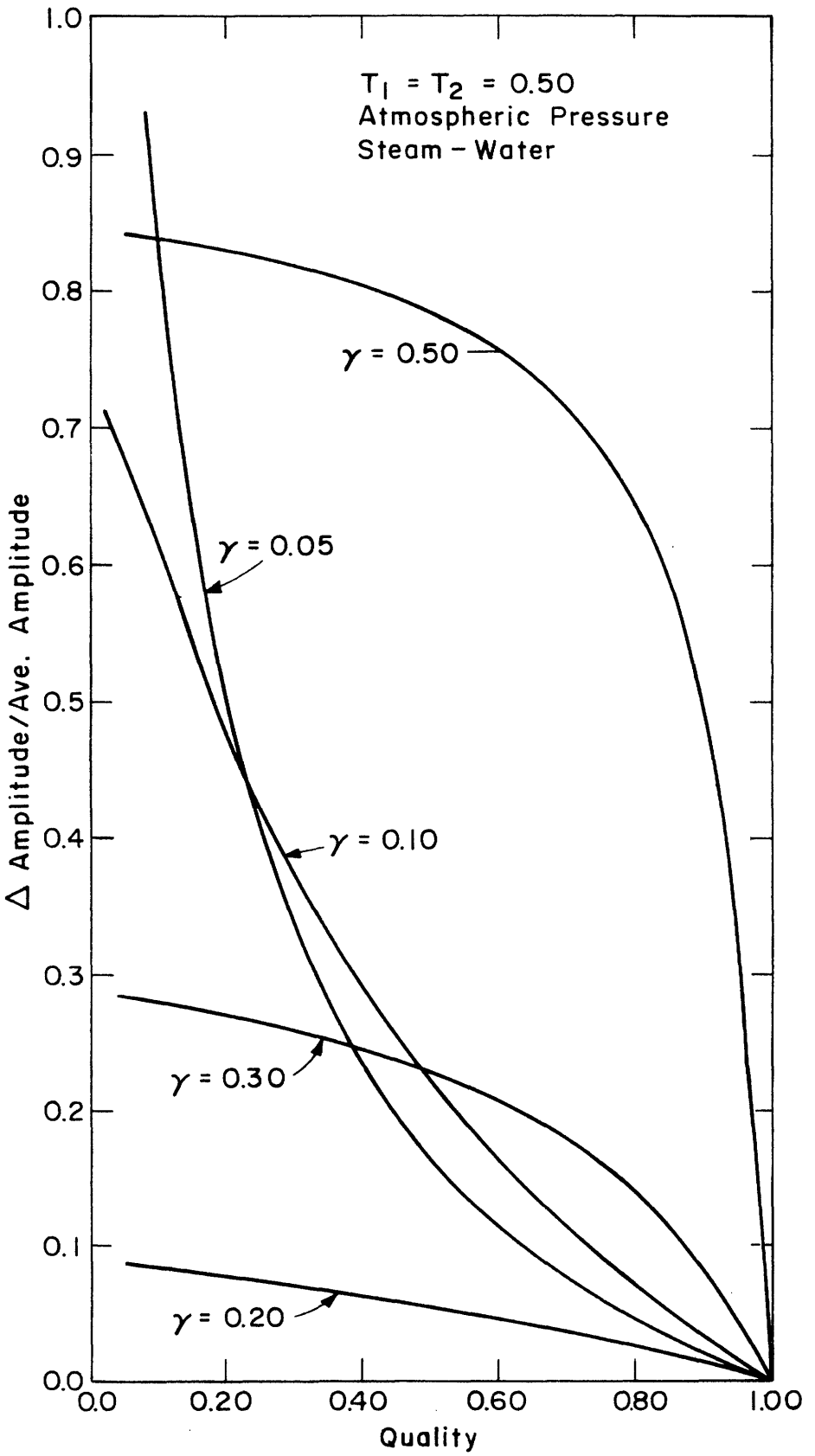

FIGURE 27. FLUCTUATION MODEL

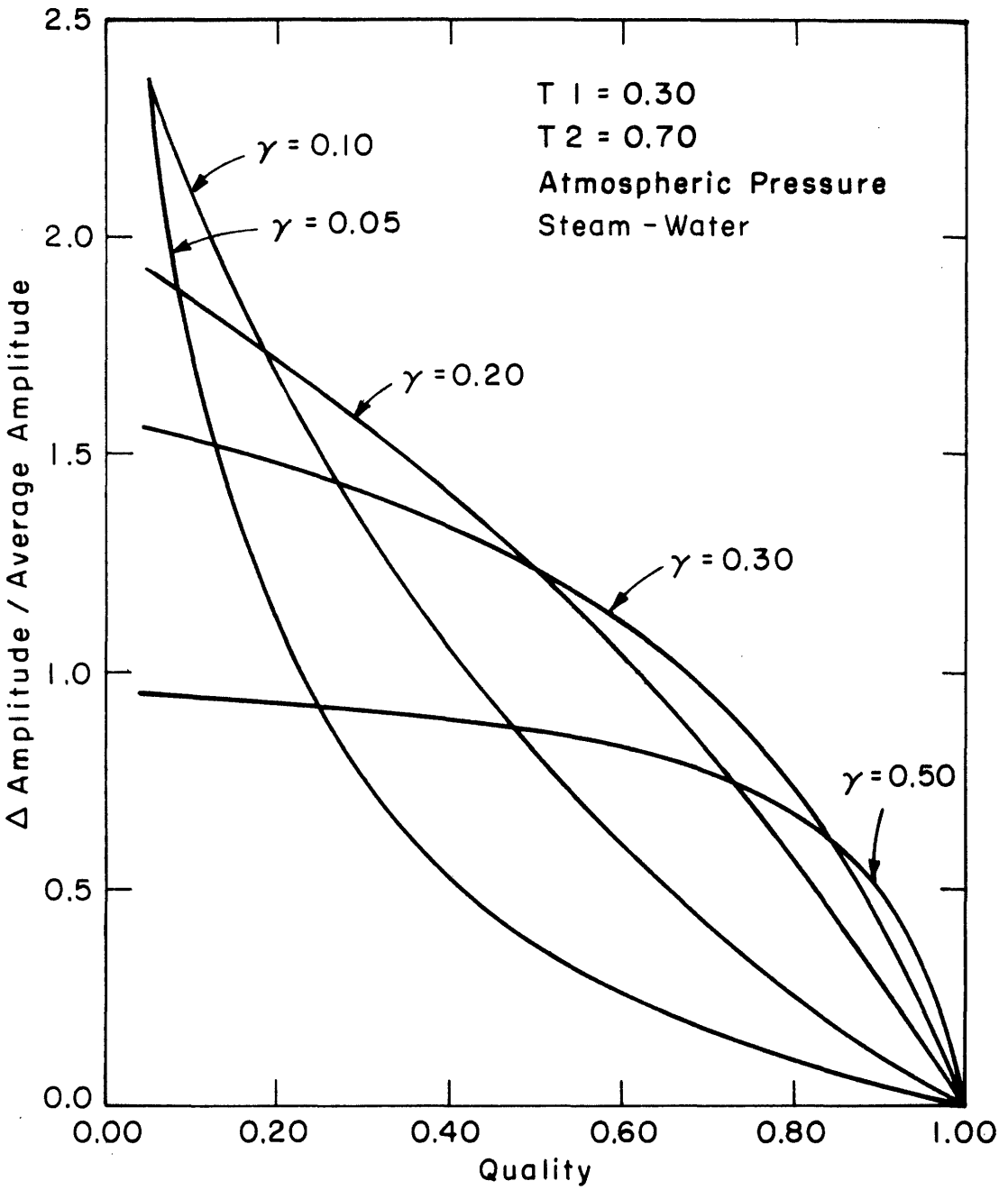

FIGURE 28. FLUCTUATION MODEL

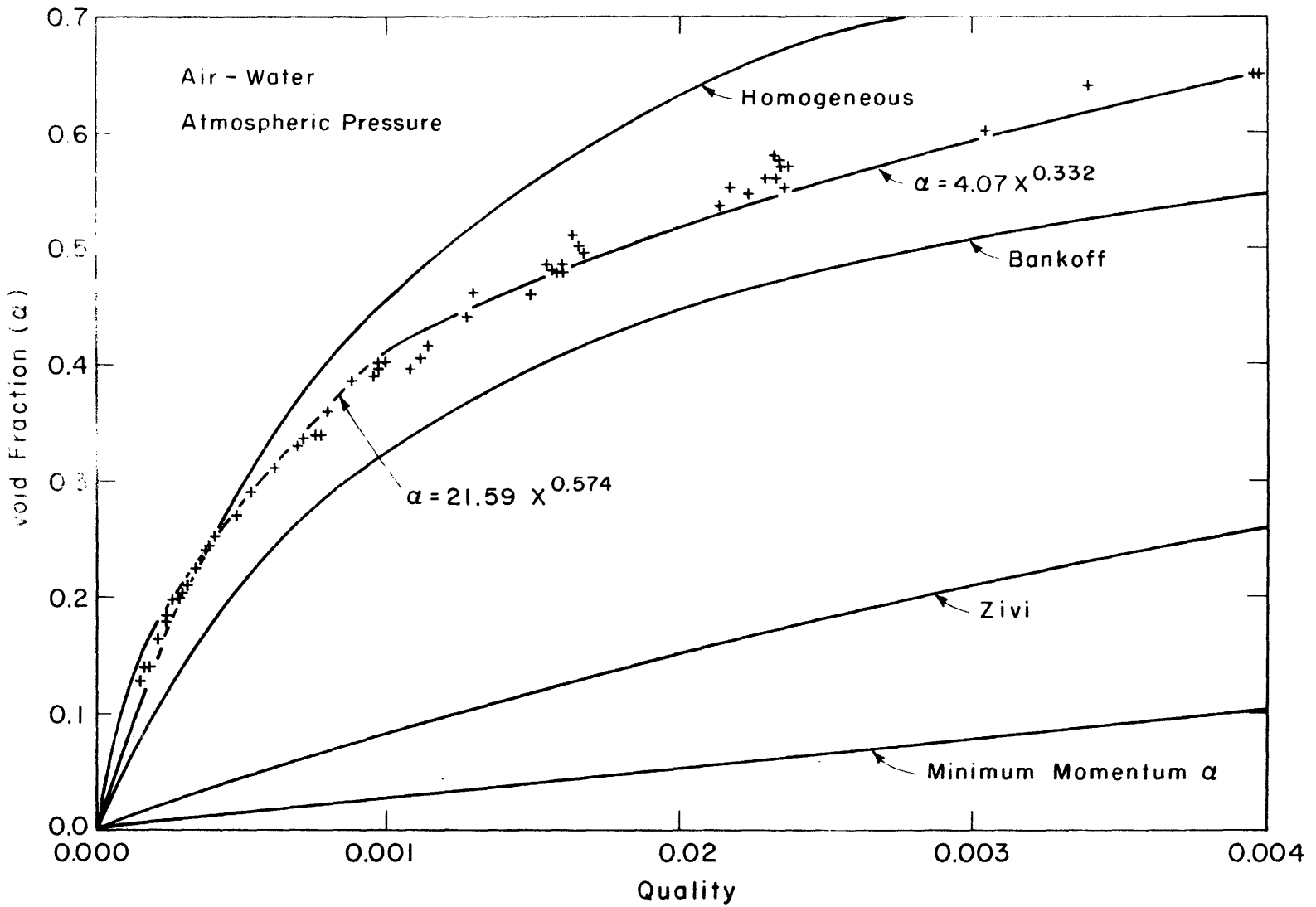

FIGURE 29. ROSE'S VOID FRACTION DATA

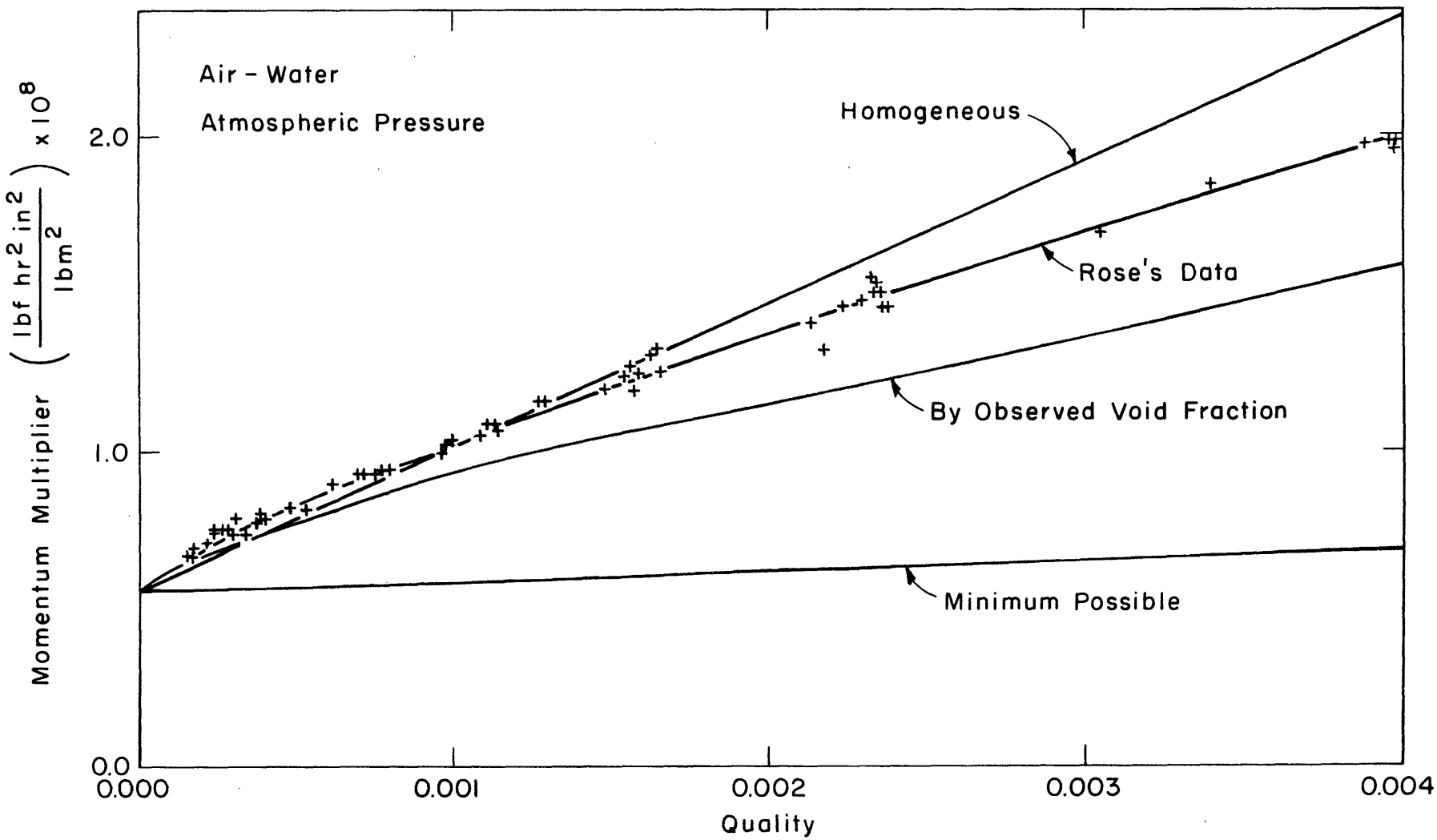

FIGURE 30. ROSE'S MOMENTUM FLUX DATA

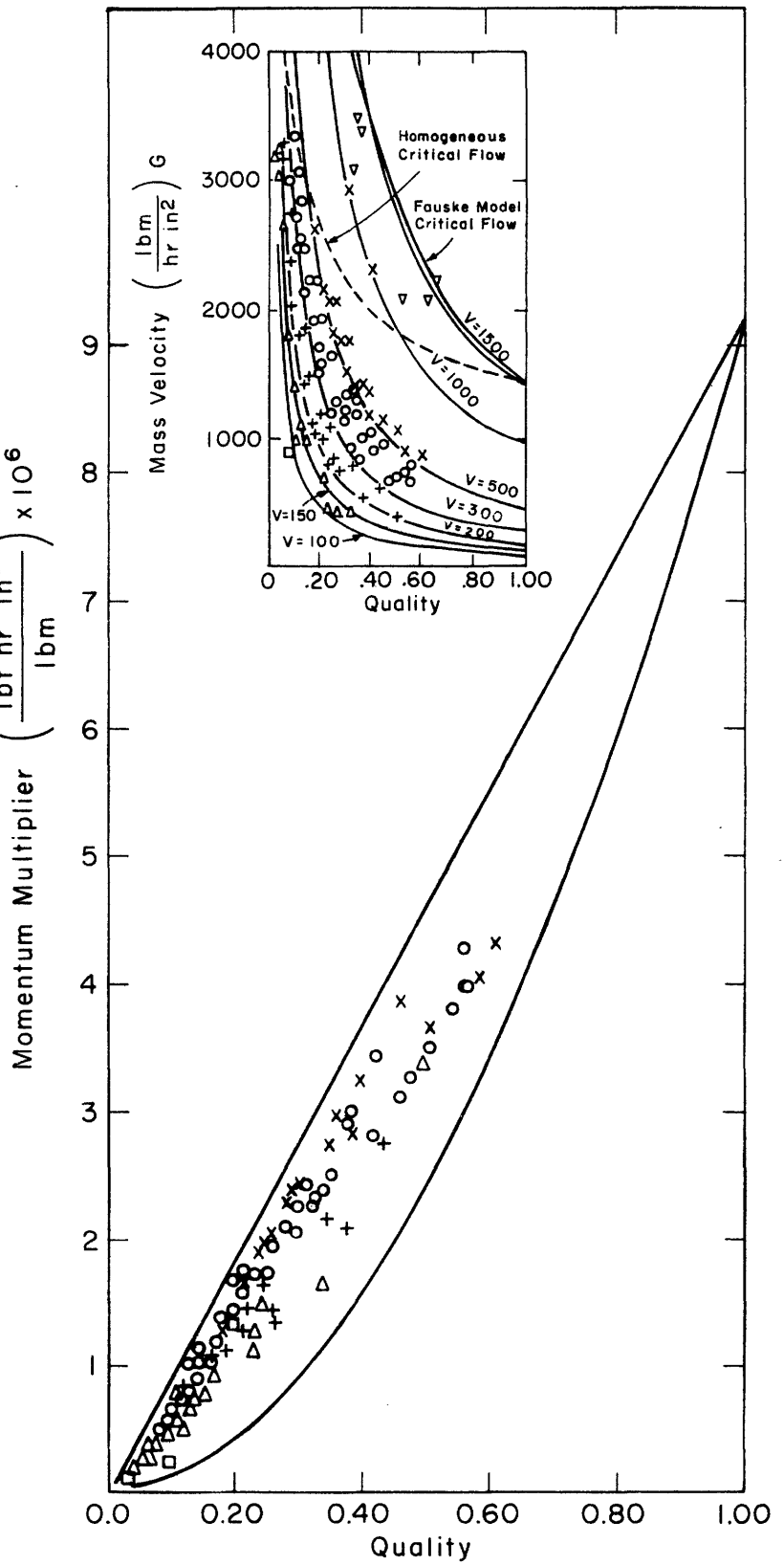

FIGURE 31. ATMOSPHERIC PRESSURE ONE INCH PIPE

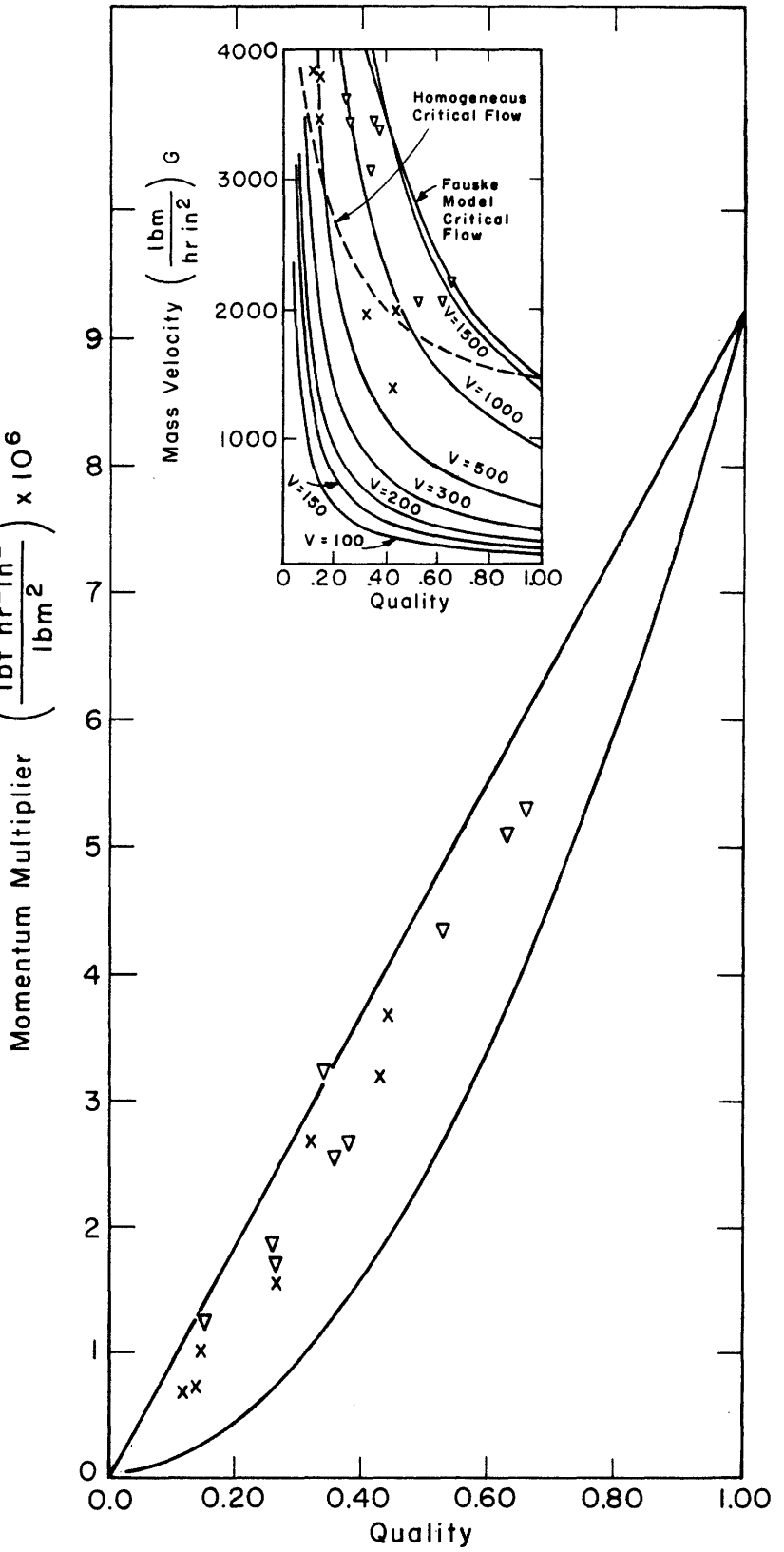

FIGURE 32. ATMOSPHERIC PRESSURE ONE-HALF INCH PIPE

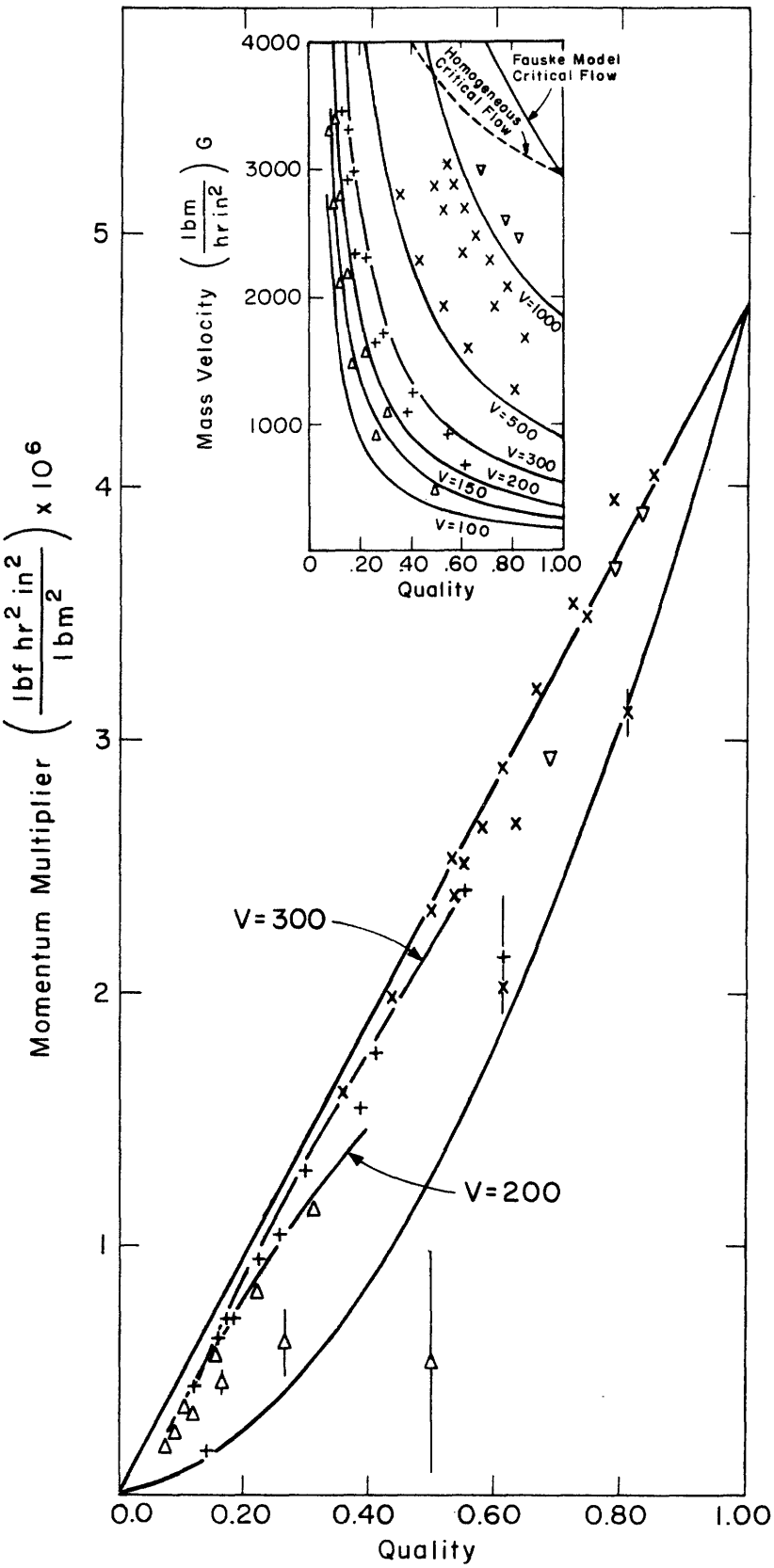

FIGURE 33. 30 PSIA ONE INCH PIPE

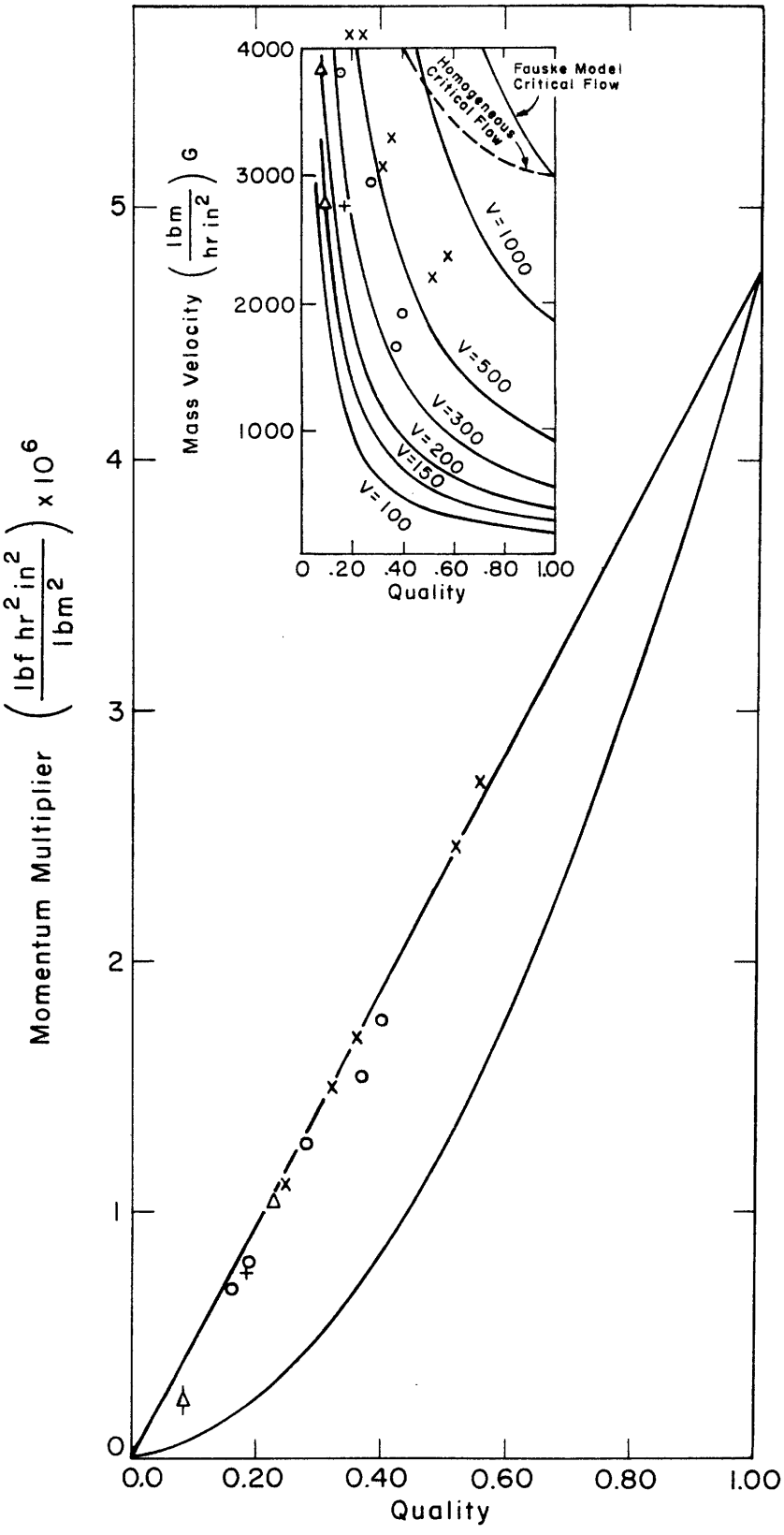

FIGURE 34. 30 PSIA ONE-HALF INCH PIPE

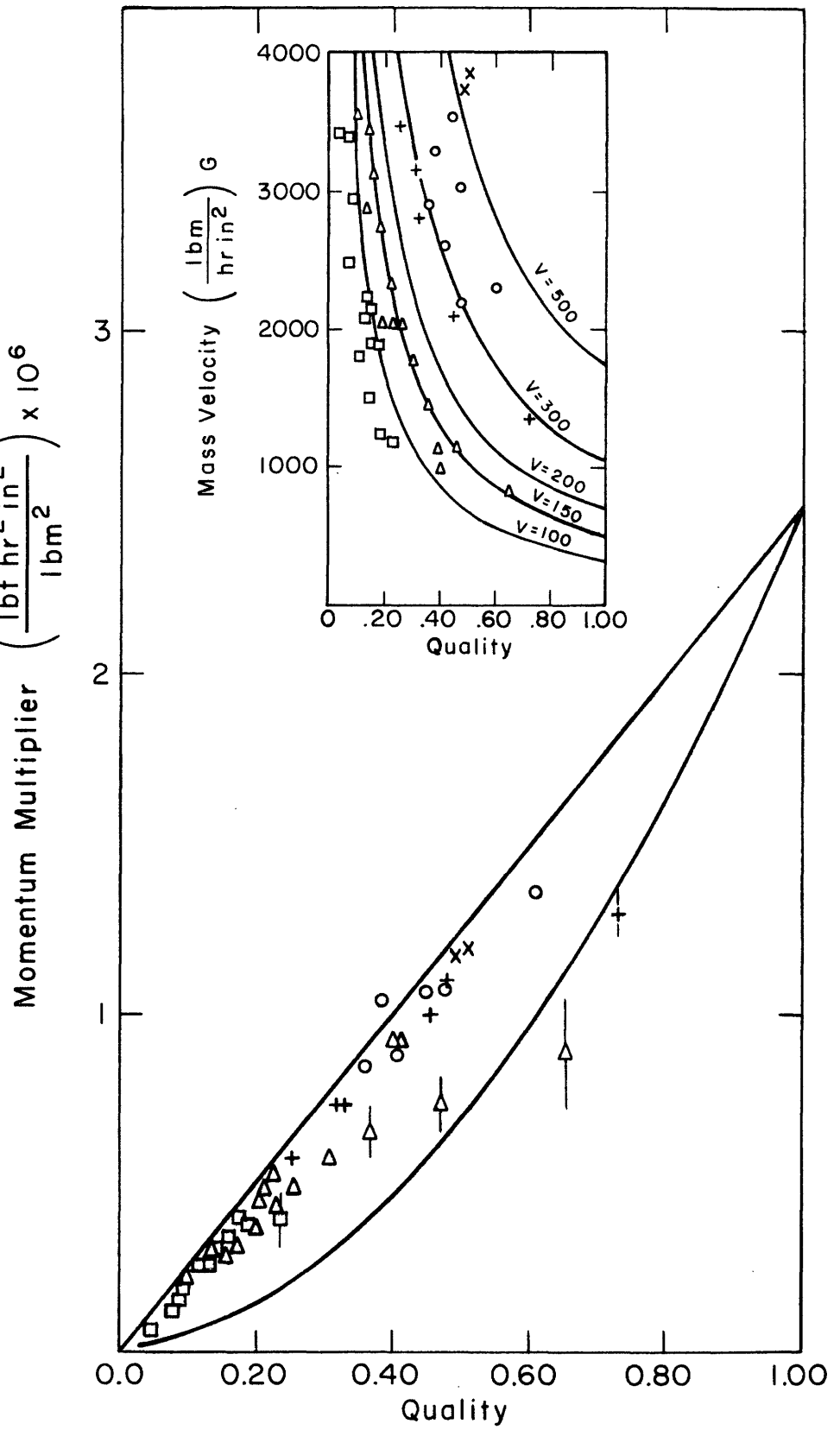

FIGURE 35. 60 PSIA ONE INCH PIPE

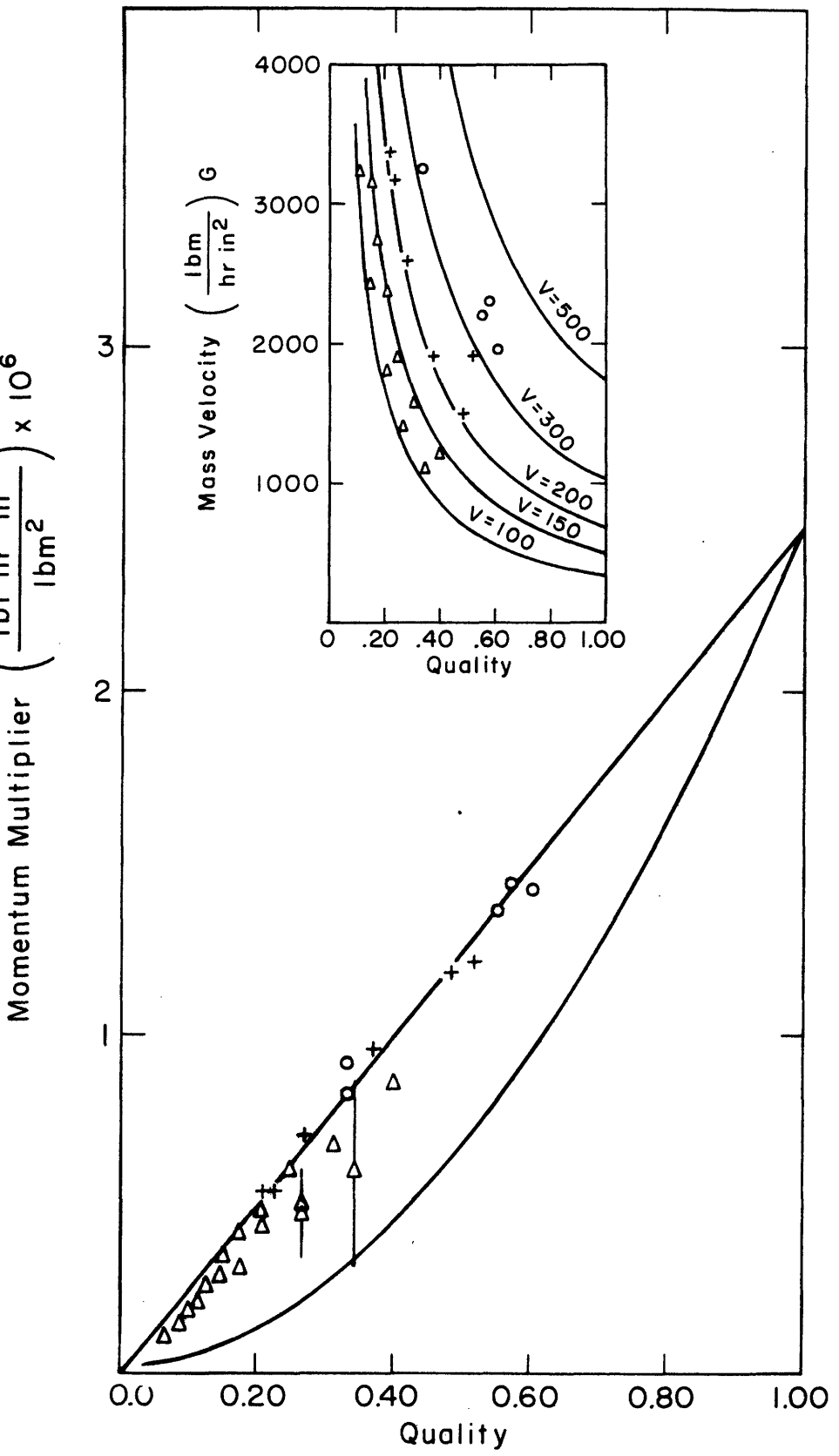

FIGURE 36. 60PSIA ONE-HALF INCH PIPE

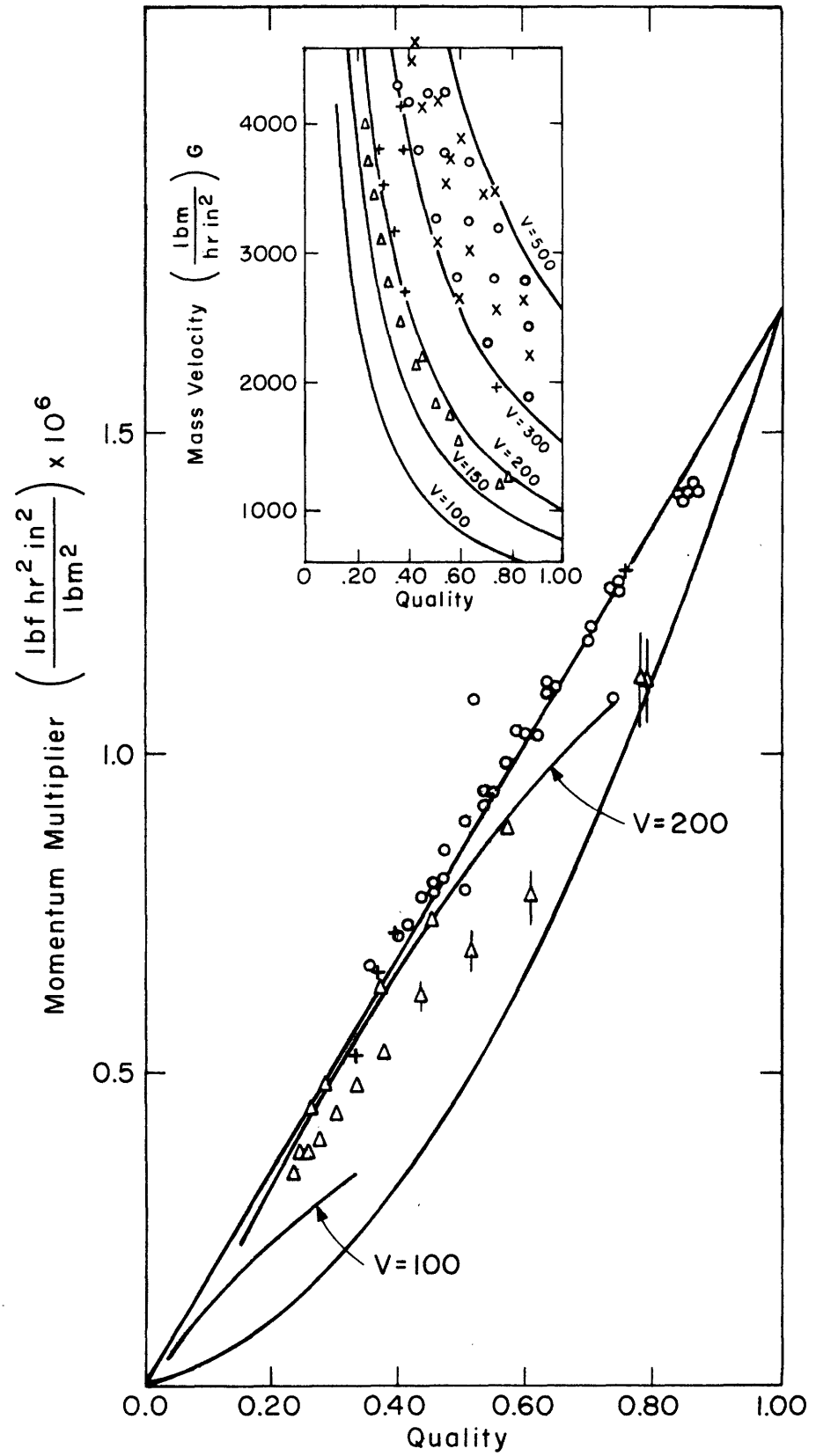

FIGURE 37. 90 PSIA ONE INCH PIPE

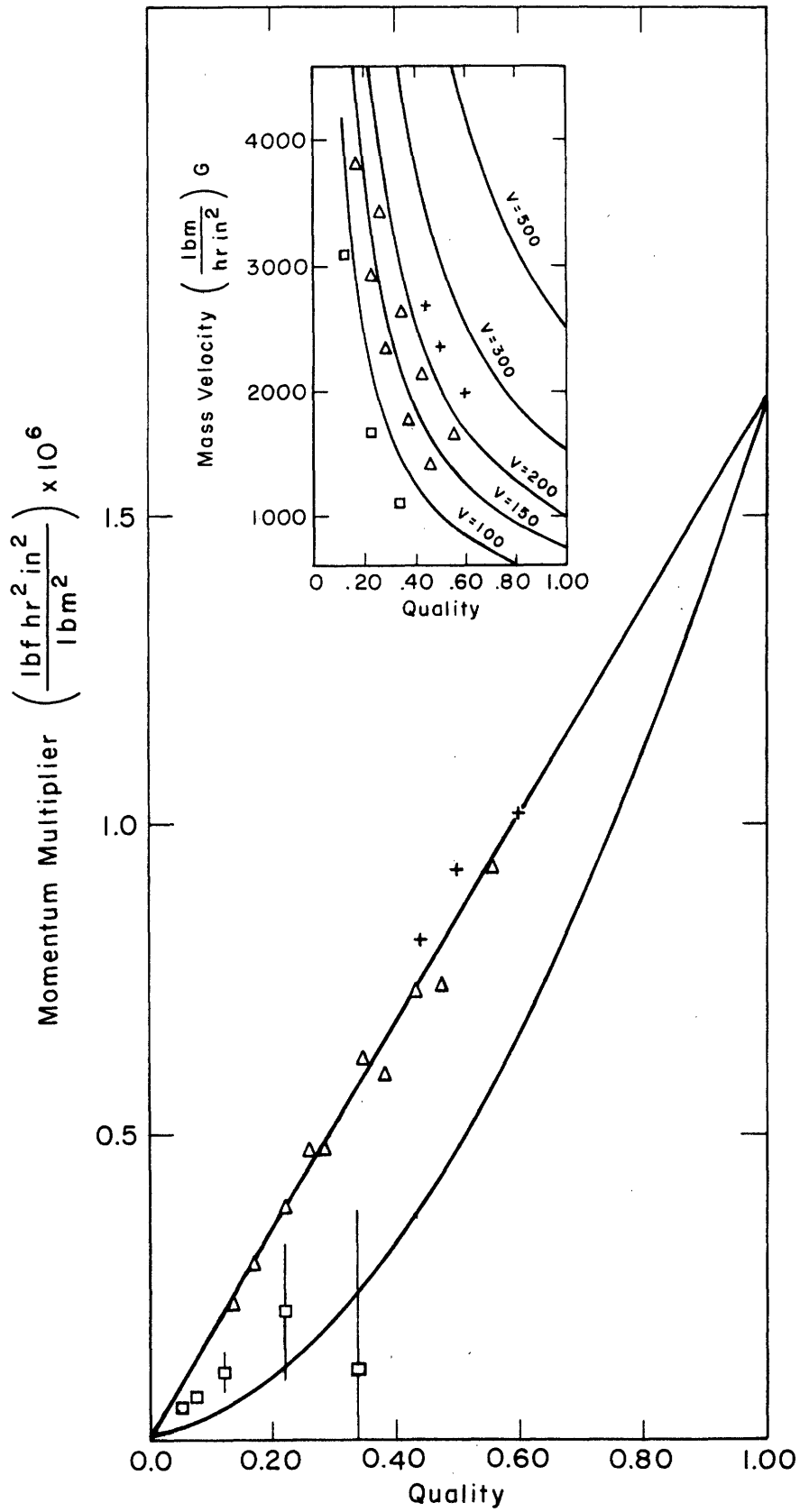

FIGURE 38. 90 PSIA ONE-HALF INCH PIPE

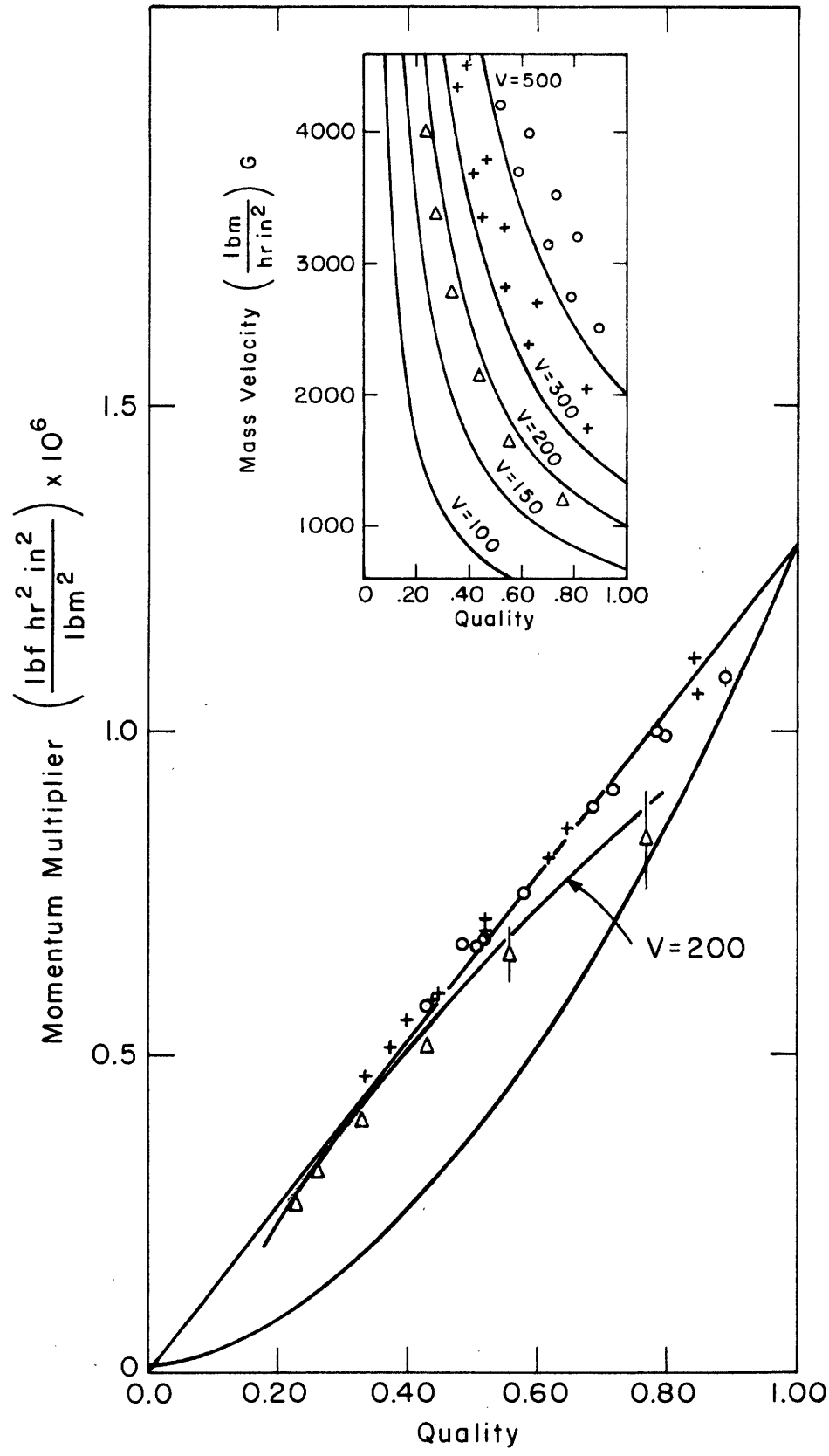

FIGURE 39. 120 PSIA ONE INCH PIPE

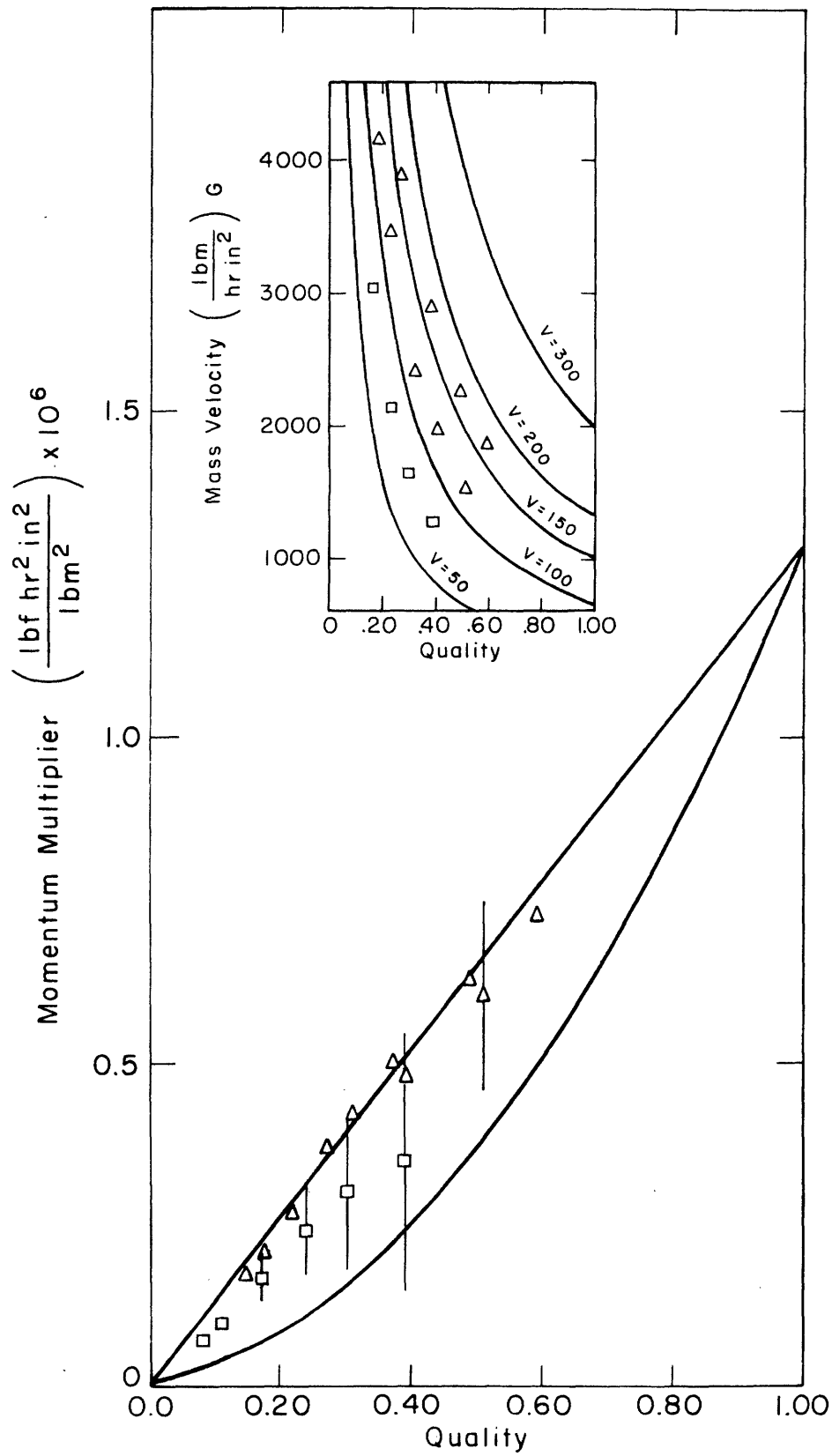

FIGURE 40. 120 PSIA ONE-HALF INCH PIPE

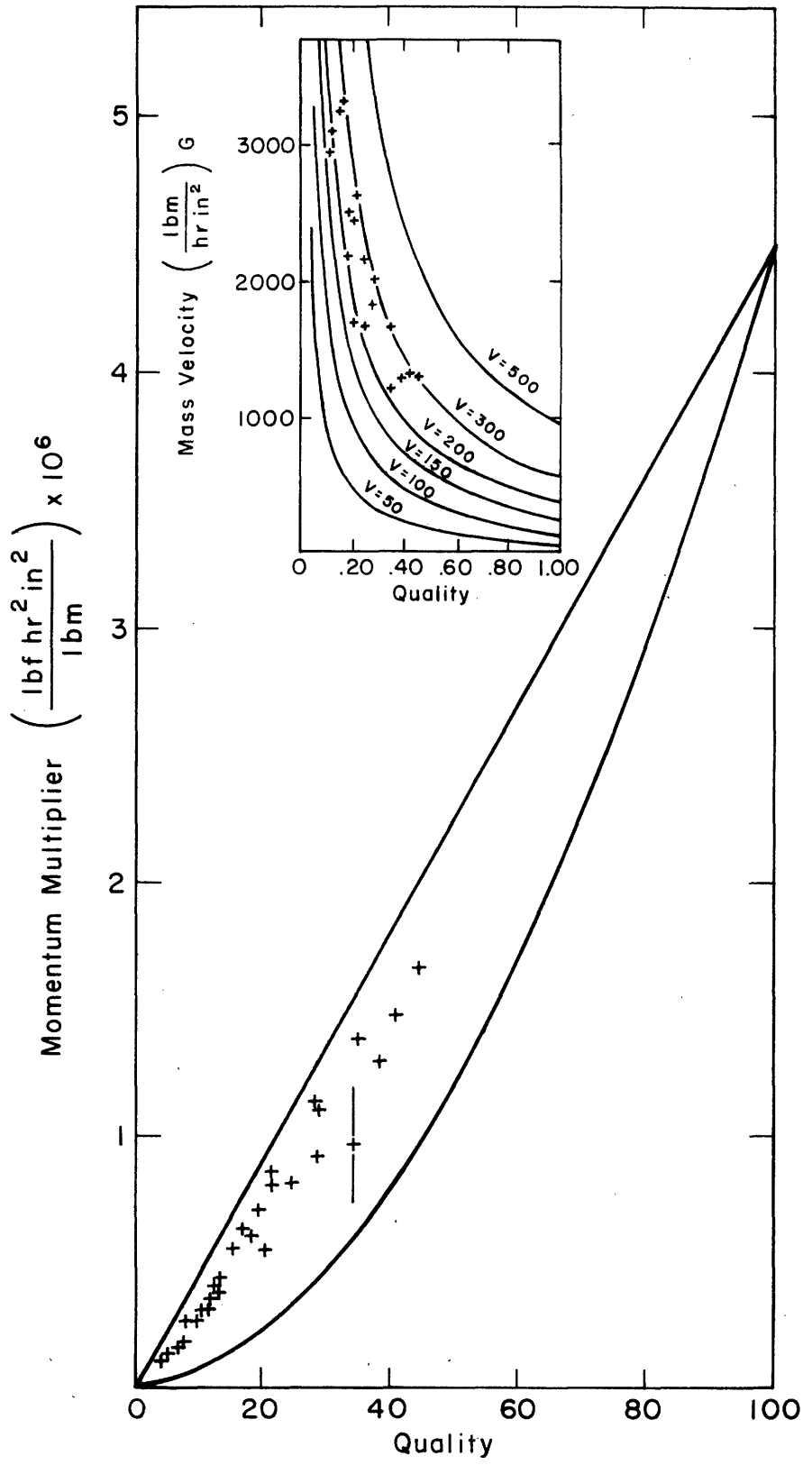

FIGURE 41. AIR – WATER 65°F

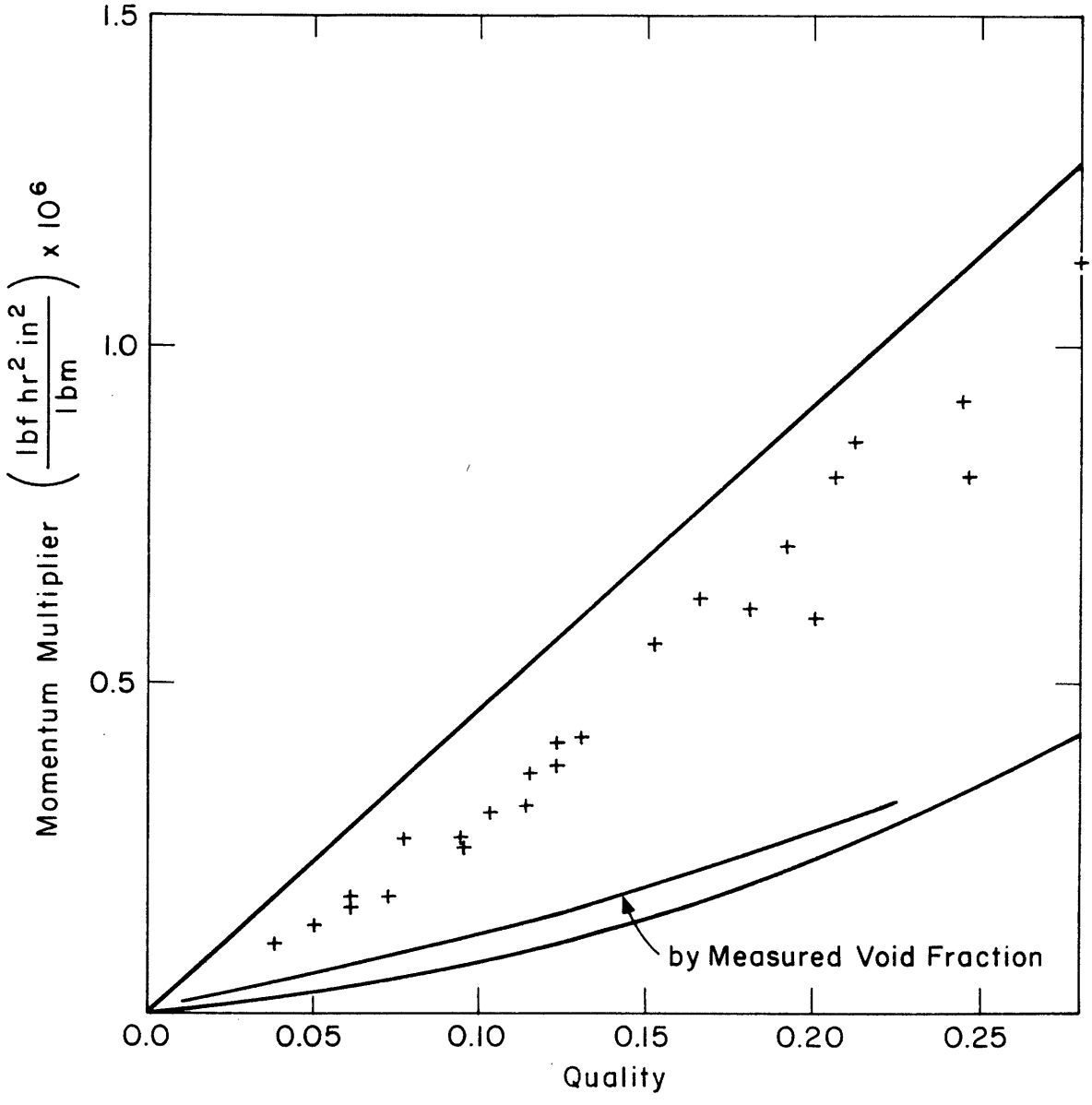

FIGURE 42. AIR – WATER 65 °F

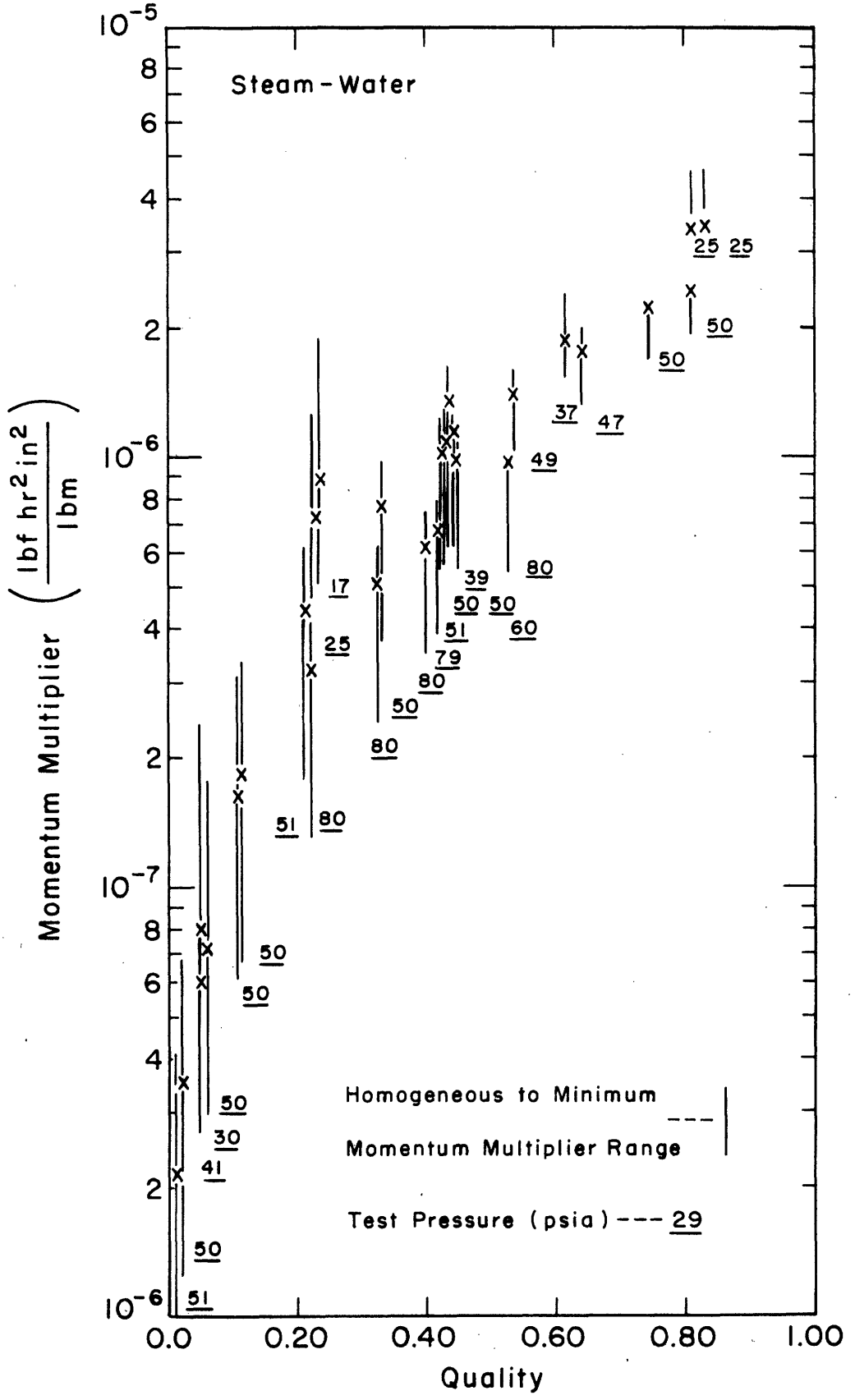

FIGURE 43. DATA OF VANCE

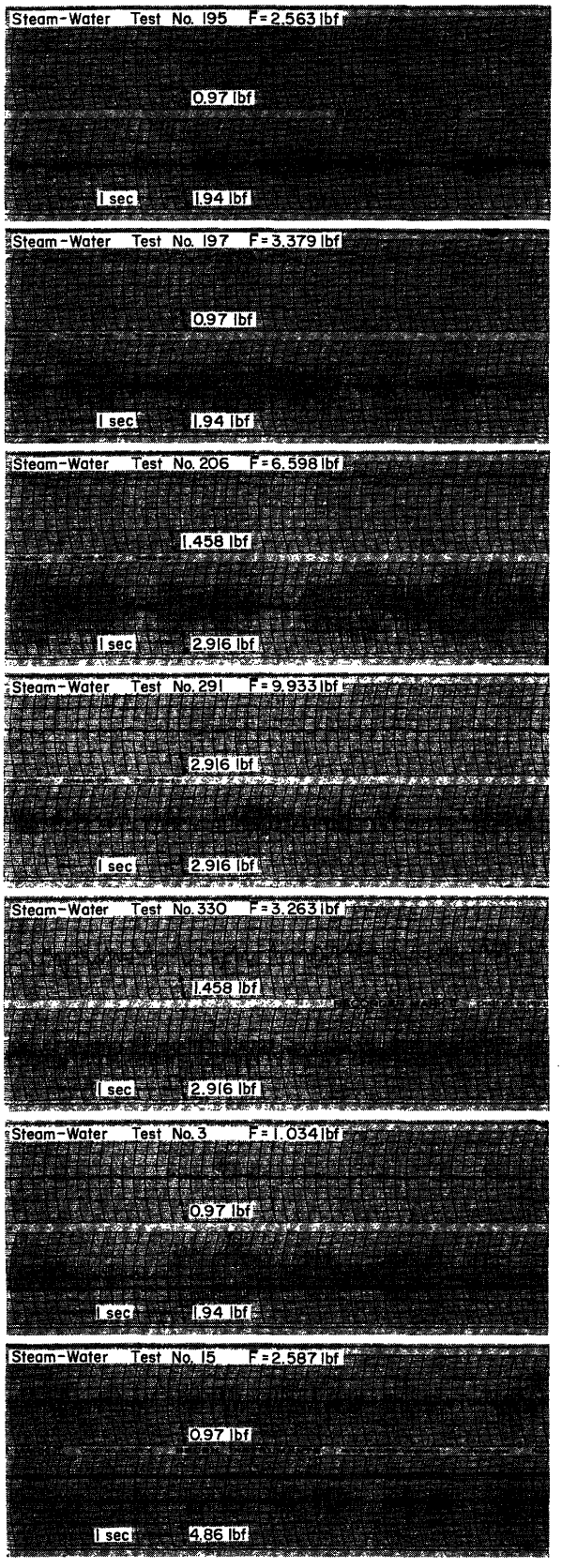

FIGURE 44 BRUSH RECORDINGS

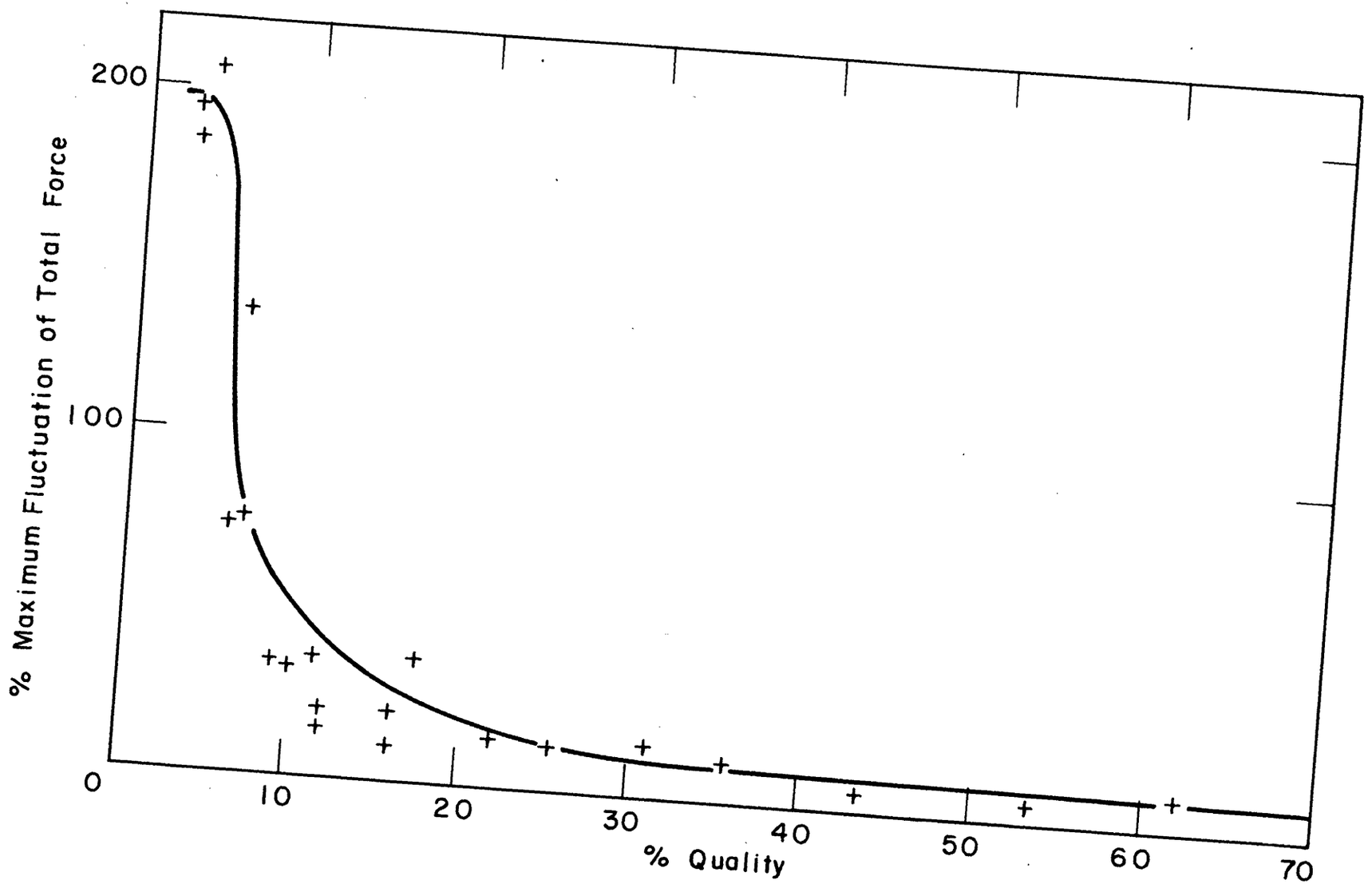

FIGURE 45. FLUCTUATION MAGNITUDE

Steam-Water, Atmospheric Pressure, One Inch Pipe

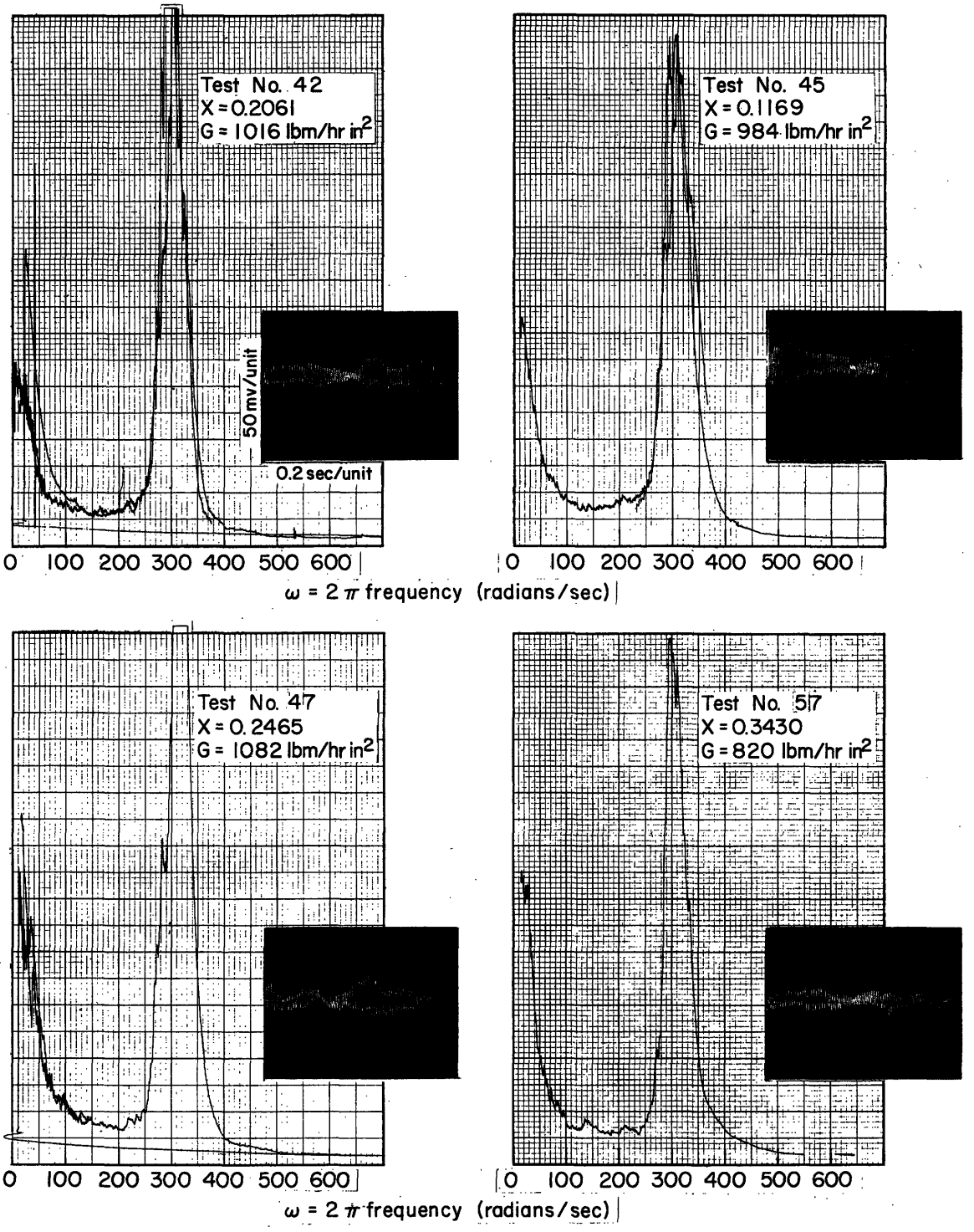

FIGURE 46. MOMENTUM FLUX SPECTRAL DENSITY

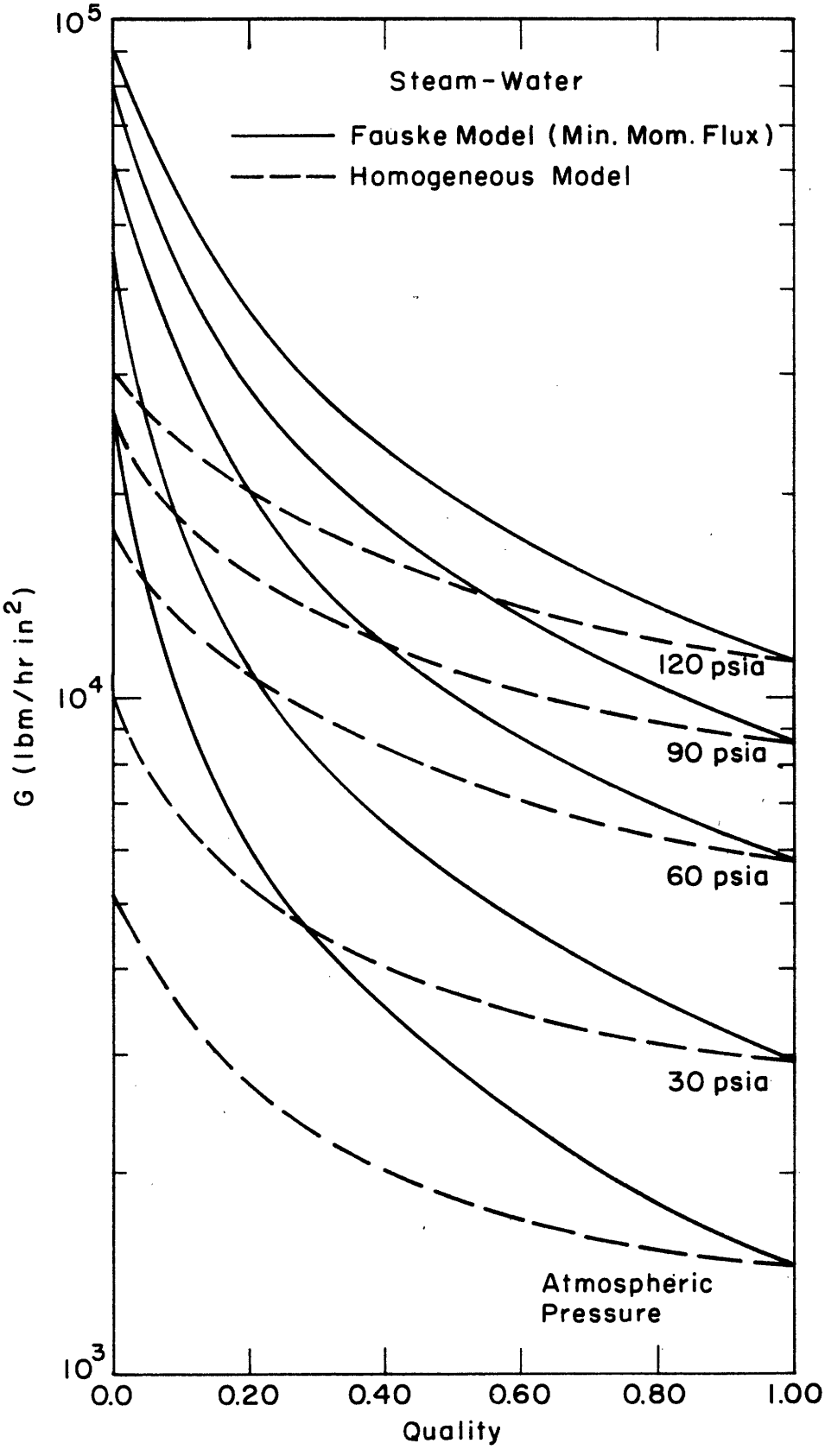

FIGURE 47. CRITICAL FLOW